Clemson University
TigerPrints

All Dissertations | Dissertations

12-2014

The Development and Characterization of Tannic Acid Cross-linked Collagen Scaffolds for the Prevention of Breast Cancer Recurrence in Lumpectomy Patients

Beau Inskeep
Clemson University, inskeepbd@gmail.com

Follow this and additional works at: https://tigerprints.clemson.edu/all_dissertations

 Part of the Engineering Commons

Recommended Citation
Inskeep, Beau, "The Development and Characterization of Tannic Acid Cross-linked Collagen Scaffolds for the Prevention of Breast Cancer Recurrence in Lumpectomy Patients" (2014). *All Dissertations*. 1459.
https://tigerprints.clemson.edu/all_dissertations/1459

This Dissertation is brought to you for free and open access by the Dissertations at TigerPrints. It has been accepted for inclusion in All Dissertations by an authorized administrator of TigerPrints. For more information, please contact kokeefe@clemson.edu.

THE DEVELOPMENT AND CHARACTERIZATION OF TANNIC ACID CROSS-LINKED COLLAGEN SCAFFOLDS FOR THE PREVENTION OF BREAST CANCER RECURRENCE IN LUMPECTOMY PATIENTS

A Dissertation
Presented to
the Graduate School of
Clemson University

In Partial Fulfillment
of the Requirements for the Degree
Doctor of Science
Bioengineering

---

by
Beau D. Inskeep
December 2014

Accepted by:
Dr. Karen J.L. Burg, Committee Chair
Dr. Brian Booth
Dr. Ken Webb
Dr. Jeong Soo Lee

ABSTRACT

Breast cancer is the second most common cancer amongst women, second only to lung cancer. In 2014, it was estimated that there were approximately 295,000 new cases of breast cancer diagnosed in women, with approximately 40,000 deaths caused by breast cancer in the United States. It has been reported that a woman has a 12% chance of developing breast cancer in her lifetime and a 3% chance of dying from breast cancer. There are several treatment options available for breast cancer, including chemotherapy, radiation therapy, as well as two different forms of surgery, mastectomy and lumpectomy. However, none of these treatment options is perfect and there is even a chance of cancer recurrence after a patient undergoes one or more of these treatments.

The long-term goal, beyond the scope of this project, is to significantly reduce the chances of cancer recurrence after a patient has undergone a lumpectomy. Currently, the chance of recurrence for a patient who undergoes a lumpectomy is around 10%. Furthermore, there is not currently an option for breast reconstruction for a lumpectomy patient. The proposed research will explore a possible approach to reducing the cancer recurrence rate as well as filling the void within the breast that was created by the lumpectomy with the patient's own tissues. The approach will include the use of tannic acid (TA) as a novel cross-linking agent for collagen scaffolds that will be used to encourage the attachment and growth of the patient's own cells, resulting in the regeneration of tissue to fill the void. As the cells remodel the scaffold, the tannic acid will be released into the surrounding tissue. In addition to tannic acid's cross-linking abilities, tannic acid has also been shown to have anti-cancer properties which will be

used to neutralize any cancer cells that may still be present within the breast. This will effectively reduce the chances of recurrence for the patient.

The focus for this research was on the evaluation of an *in vitro* model of a lumpectomy site which will used to test the efficacy of collagen beads that have been cross-linked with tannic acid. Beads cross-linked with TA concentrations of 0.1%, 1.0% and 10.0% were evaluated during the course of these studies. These beads were first evaluated using a 2D lumpectomy model and the results showed that the 1.0% and 10.0% TA beads were able to cause a higher incidence of apoptosis in cancer cells compared to preadipocytes. The 0.1% TA beads were able to support preadipocyte cell attachment and growth throughout the duration of the studies. The 1.0% TA beads were initially able to support cell growth but after 72 hrs, the level of viable cells greatly decreased.

The studies then progressed to 3D cell culture techniques using collagen/ agarose gels with cancerous cells embedded within. The gels were then exposed to the different bead types. The 1.0% and 10.0% beads were able to induce a higher rate of apoptosis in the embedded cancerous cells when compared to the control groups. The 0.1% TA beads were able to function as a viable scaffold for the duration of the 7 day study while the 1.0% TA beads were initially able to allow preadipocyte cell attachment and growth but after 4 days, the number of viable preadipocyte cells attached to the beads greatly decreased. This study was then repeated using primary cells and the same results were seen.

The results of these studies showed that the ideal TA cross-linking concentration was not found. The 0.1% TA beads do not have a high enough concentration to induce apoptosis of cancerous cells while the 1.0% TA beads was too high of a concentration to

allow for proper preadipocyte attachment and proliferation. Further studies of concentrations between these two end points is needed.

DEDICATION

I dedicate this dissertation to my parents, John and Deb, as well as my sisters, Jennifer and Jamie. You have been a constant source of support through the entire graduate school experience. I would also like to dedicate this to all my friends, both new and old, who stood by my side during these years. You celebrated with me on my good days and helped me through my bad.

ACKNOWLEDGEMENTS

I would like to thank my advisor, Dr. Karen J.L. Burg, for her constant guidance and support throughout my entire graduate school experience. She constantly proved me wrong when I doubted my own abilities and helped me develop both professionally as a research assistant and personally as a mentor and friend. I would also like to thank my committee members, Dr. Jeong Soo Lee, Dr. Ken Webb, and Dr. Brian Booth, for providing their time and support with my research project.

I would also like to acknowledge the support of the faculty and staff within the bioengineering department that provided assistance and support during my project. I would like to thank Linda Jenkins for her assistance and guidance while performing histology.

I would have not been able to complete my research without the support of my fellow members of the IBIOE lab, particularly Dr. Cheryl Gomillion, Dr. Cheryl Cass, Dr. Duong Nguyen, and Jon Shaul. They provided me with much needed guidance as well as friendship.

This project was funded in part by Avon Foundation for Women grant 02-2011-085.

TABLE OF CONTENTS

Page

Table of Contents (Continued)

Page

Table of Contents (Continued)

Page

LIST OF TABLES

Table Page

LIST OF FIGURES

List of Figures (Continued)

Figure Page

List of Figures (Continued)

Figure Page

List of Figures (Continued)

Figure Page

PREFACE

There are several possible complications associated with a lumpectomy procedure including a lack of reconstructive options and an increased risk of recurrence, approximately 10% over 10 years. Current research is being done on how to reduce this recurrence rate and provide a better outcome for lumpectomy patients. Previous work in our lab focused on the development of a collagen scaffold with anticancer properties through the incorporation of tannic acid, a naturally occurring substance that is able to crosslink collagen. Previous studies showed promising results in that cancerous cells were negatively affected by these scaffolds while preadipocyte cells were able to survive.

The overall goal of this project was to develop these scaffolds further by forming injectable bead scaffolds that could be used as a reconstructive option for lumpectomy patients. The scaffold would provide a viable point of attachment and proliferation for preadipocytes, thus allowing the regrowth of the lost tissue from the lumpectomy procedure. As the preadipocyte cells proliferate and remodel the bead scaffolds, the incorporated tannic acid will be released and cause any remaining cancerous cells to undergo apoptosis, thus reducing the rate of recurrence.

To accomplish this overall goal, 4 aims were identified to be explored:

1) To examine the effect of collagen beads cross-linked with varying amounts of tannic acid on cancerous cells in a 2D lumpectomy model
2) To evaluate the effectiveness of the different bead types to function as scaffolds as well as investigate the effect cell growth and attachment on the beads has on the release kinetics of the tannic acid from the beads within the same 2D lumpectomy model

3) To evaluate the effectiveness of the different bead types on cancerous cells as well as their ability to function as a scaffold in a 3D lumpectomy model
4) To evaluate the effectiveness of the different bead types when seeded with primary cells in the same 3D lumpectomy model

Aim 1 and 2 studies, as detailed in chapter 4, explore the basic functionality of the beads to provide the two key characteristics needed for the overall goal of this project, provide a viable scaffold and to selectively cause apoptosis of cancerous cells. This was done through the use of transwell inserts in that cancerous or non-cancerous cells were seeded on the bottom of 12-well plates. The transwell insert was placed in to the well in which the tannic acid cross-linked collagen beads were placed. For aim 1, the beads were no seeded with preadipocytes whereas for aim 2, they were. The transwell insert allowed for the diffusion of any released tannic acid from the beads into the surrounding medium and interact with the cells that were attached to the bottom of the well. Medium samples were collected and a modified F-C assay protocol was developed to quantify the amount of tannic acid released in to the medium. Glucose and lactate levels were also measured from the medium samples to better understand the metabolic activity of the cells and seeded beads underwent Live/ Dead analysis to examine the viability of the cells attached to them. Finally, the TUNEL assay was performed on the cells growing on the bottom of the wells to evaluate the apoptotic activity of them.

The studies performed to evaluate aim 3, as detailed in chapter 5, examine if the results of the 2D studies translate to a 3D environment. This was necessary because it is well documented that cells in 2D culture do not react the same way in a 3D environment. This 3D study was intended to provide a better understanding of how the

cells will react in vivo. This was done using collagen agarose gels in which cancerous cells, transfected with red fluorescence protein, were embedded. Wells were molded into the middle of these gels using a developed modified well plate lid system. Collagen beads cross-linked with different amounts of tannic acid were seeded with preadipocytes and placed into the molded wells. The gels were then sectioned and imaged using fluorescent microscopy to evaluate the effect the beads had on the embedded cancerous cells. The beads underwent Live/ Dead analysis to determine the viability of the preadipocyte cells growing on them. Medium samples were also collected and underwent the F-C assay to quantify the level of tannic acid released from the beads.

Aim 4, as described in chapter 6, was done to provide a better 3D model to simulate what may be seen in vivo. This was done through the isolation and use of primary human preadipocyte cells, collected from human breast fat tissue. These cells were used in place of the preadipocyte cell line used in aim 3 to examine how primary cells would react to the same tannic acid cross-linked beads. Besides the substitution of the primary preadipocyte cells for the preadipocyte cell line, the same procedure and evaluation technique of aim 3 was used for aim 4.

CHAPTER 1

INTRODUCTION

Overview and Statistics

Breast cancer is prevalent amongst women, second in prevalence only to skin cancer; the chance of a woman developing breast cancer in her life time is approximately 12% [1]. It was estimated that in 2014 there would be approximately 295,000 new cases and 40,000 deaths caused by breast cancer in the United States [1]. The chance of breast cancer death in women is approximately 3%, second only to lung cancer. It is important to note that not all cancer deaths are from the cancer itself but also can be initiated or facilitated by the treatment for breast cancer, such as radiation therapy. However, this rate has been decreasing since 1990; the decrease is attributed to better detection and treatment methods and technology [1].

Breast Anatomy and Development

To better understand the development of breast cancer, it is important to first understand the anatomy of the breast and the structures and functions of the tissues therein (Figure 1.1). The breast structure is located on top of the pectoralis muscle, which sits on top of the rib cage [2]. Each breast contains 15 to 20 lobes which are further subdivided into 20 to 40 lobules. It is inside these lobules that the mammary glands responsible for producing milk are found [3]. These lobules are connected together through ducts; the milk is collected in the ducts and then flows out through the nipple. The space between these structures is filled with fat and fibrous tissue, the ratio of which defines breast density. A high concentration of lymphatic vessels and lymph nodes is found throughout breast tissue; these structures facilitate the flow of lymph,

which comprises white blood vessels called lymphocytes and a fluid from the intestines called chyle, which contains proteins and fats [4]. The lymph flows to the nearby lymph nodes located in the underarm, above the collar bone, and behind the breast bone [3]. Blood vessels are also present to carry blood around the tissues to provide nutrients for the cells. The size and shape of the breast is determined by the skin envelope and the adipose tissue surrounding the connective and glandular tissues [5]. The firmness of the breast mound is dependent on the number of adipose lobules located within the breast, with higher adipose content resulting in a softer breast mound [5]. The deep fascia and a thin layer of loose connective tissue is located between the breast and the pectoralis muscle, the connective tissue allowing the breast to move freely over the deep fascia. The breast is attached to the skin through suspensory ligaments, also termed Cooper's Ligaments, which provide additional support and also contribute to the shape of the breast mound [5].

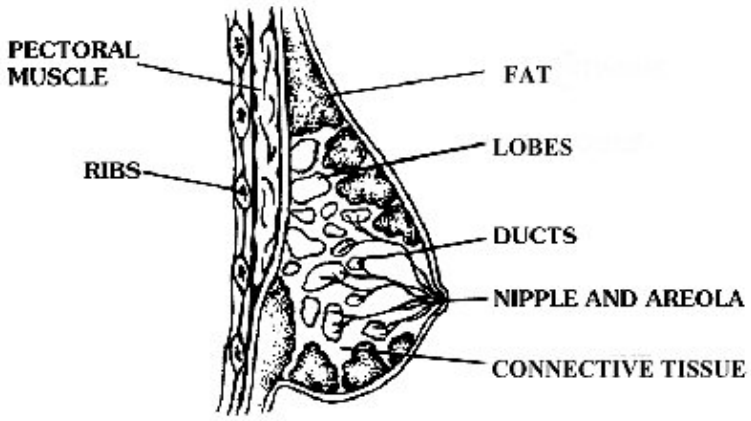

Figure 1.1: *Anatomy of the Female Breast [6]*

Several changes occur in the breast as a women goes through puberty and menopause. During puberty, hormones released by the ovaries and pituitary gland cause the tissue to grow and the ducts to expand to form mature ductal structures [5]. While the structures are fully formed, they do not become fully active until pregnancy when the lobules grow and start producing milk. During menopause, when hormones are no longer being produced by the ovaries, the lobule count in the breast decreases and those that remain shrink in size. This change leads to a lower breast density, since the ratio of dense, fibrous tissue to adipose tissue decreases. For this reason, a woman's breast is typically more dense before menopause than it is after [5].

Breast Cancer Types and Progression

There are two main categories of breast cancer, which are defined by the origin of the cancer. The two types include ductal carcinomas, which originate from the ducts responsible for milk transport, and lobular carcinomas, which originate from the lobules that supply the ducts with the milk [7]. There are several possible causes for breast cancer and each can contribute to the formation of cancerous tissue. The primary causes are believed to be from genetic and/ or hormonal factors [8]. However, there are also contributing factors such as age, family history, reproductive and menstrual history, as well as breast density [8]. Prognosis for breast cancer depends on the stage of the cancer at detection as well as the location and type of cancer [8].

Breast cancer progresses through stages as it spreads through the breast and into other parts of the body. Stage zero breast cancer is characterized in one of two ways, as either a ductal carcinoma *in situ* or a lobular carcinoma *in situ*. Both

carcinomas have abnormal cells within either the lining of a breast duct or within the lobules of a breast. The abnormal cells have not spread to other tissues of the breast [3]. Stage one breast cancer is the most common form of breast cancer in women in the United States and is characterized as a tumor less than 2 centimeters in diameter that has not spread to the auxiliary lymph nodes in the arm pit [2]. Stage two breast cancer is characterized as a tumor greater than 2 centimeters, cells of which have not spread to the axillary lymph nodes, as a tumor less than 2 centimeters, cells of which have spread to the axillary lymph nodes, or as an absence of primary tumor, with cancerous cells detected in the axillary lymph nodes [3]. Stage three breast cancer is characterized by spread of cancerous cells to the axillary lymph nodes or spread to lymph nodes near the breastbone. The cancer may have even spread as far as the skin of the chest wall or the skin of the breast [3]. By stage three, the cancer can be classified as either operable or inoperable, depending on the extent to which the cancer has spread [3]. Stage four breast cancer has spread outside the breast to other organs of the body, typically bones, lungs, liver, or the brain [3].

Breast Cancer Risk Factors

There are several risk factors associated with the development of breast cancer. The foremost of these factors is breast density, defined as the ratio of the volume of dense tissue in the breast to the total volume of the breast [9]. Dense tissues within the breast are defined as tissues that are not adipose tissue, such as the glands, ducts, and lobules. Several studies have shown that a woman with a higher breast density is at a higher risk for developing breast cancer. Therefore, anything that risks the increase in the prevalence of dense tissues within the breast is a risk factor that may increase the

likelihood of breast cancer development [10]. Some examples of what may cause an increase in breast density include hormone supplements for hormone replacement therapy, decreased body mass index, and parity. These factors, as well as others, will be discussed further. The effect of diet, alcohol consumption, and exercise on breast density has also been explored because of the effect these factors have on overall body fat content [11]. However, little evidence was shown to suggest any strong correlation between any of these factors and the density of the breast [12]. The most conclusive correlation found was that a high alcohol intake is associated with increased breast density [11]. It was also noted that a higher intake of white wine in postmenopausal women was associated with an increase in breast density while red wine had the opposite effect. There was no relationship between type of alcoholic drink and breast density of premenopausal women noted [11].

A breast can be assigned to one of three different categories: N, P, or D, with N being the least dense and D being the densest. P and D are further divided into four sub-categories, one through four [13]. Table 1.1 summarizes how the different density categories are defined.

A common measure, suggestive of breast density, is body mass index (BMI) or weight. Several studies have shown an inverse correlation between a woman's BMI and her breast density [14]. This becomes apparent since BMI is a proxy for body fat percentage based on height and weight. Therefore, a higher BMI correlates with a higher percent of body fat in the individual, which can also be associated to a higher fat content in the breasts. A higher volume of adipose tissue in the breasts results in a lower breast density score. Therefore, it is more likely that underweight women and those with a lower BMI and fat percentage may have a higher risk of developing breast cancer [13].

However, this is not always true and it has been acknowledged that women of the same height and weight, with the same BMI, may have very different body compositions and, therefore, very different percentages of fat within the breasts. Risk of breast cancer is best assessed on a patient-by-patient basis.

Table 1.1: *Breast Density Scoring Guide [13]*

Density Score	Density Value
N	Fatty breast with <10% dense breast tissue
P1	10-25% Extent of ductal prominence*
P2	26-50% Extent of ductal prominence
P3	51-75% Extent of ductal prominence
P4	>75% Extent of ductal prominence
D1	10-25% Extent of dysplasia**
D2	26-50% Extent of dysplasia
D3	51-75% Extent of dysplasia
D4	>75% Extent of dysplasia

*Ductal Prominence: Prevalence of ductal tissue
**Dysplasia: Abnormal cellular proliferation

Another method used to estimate body composition is to calculate the patient's body surface area (BSA). BSA, like BMI, is calculated using only the height and weight of an individual and a simplified formula. The formula was developed by Du Bois and Du Bois after performing a correlational study between castings of different body segments and geometric measurements of those segments [17]. It has become a common

practice for some adult-focused oncologists to use BSA instead of BMI to determine patient dosing [17]. However, it has been shown that calculations relying on BSA may cause under dosing of obese women, due to the difference of physiological changes seen in obese patients compared to those of average weight [17]. This difference is due to disproportionate changes in weight and height, where weight increases with little change in height [18]. Studies have been conducted to modify the original BSA equation to better model all body types, but there is yet to be a consistently used equation other than the original Du Bois equation [19]. The high variability of the human body mandates the need for patients to be assessed individually.

Height has also been investigated as a possible indicator for a woman's risk of developing breast cancer. The connection between height and breast density has not been studied as extensively as other risk factors, but some studies have shown a strong correlation [15]. These studies concluded that taller women typically have more dense breasts and, therefore, may be at a higher risk for developing breast cancer. While a conclusive explanation for this correlation has not been accepted, some hypotheses have been suggested. Several factors, such as hormones, nutrition, and genetic disposition, influence the height of women. One hypothesis involves the hormones activated during normal development in puberty, when women reach their maximum height. The hormone estrogen is very active during this time and is responsible for signaling several developmental changes, including height and breast development. It has been suggested that the activity of estrogen during this time causes an increase in height and also causes the development of denser tissues within the breast [15].

Hormones have been strongly correlated to breast density, since hormones like estrogen and progesterone are responsible for the development of mature lobules,

ducts, and glands. The development of these structures causes an increase in dense tissue volume, which increases the density of the breast. One key event that occurs in a woman's lifetime is menopause, where the level of estrogen produced in the body severely decreases. As such, menopause causes a shift in the density of the breast as estrogen levels drop and cause structures in the breast to decrease in size [13]. Therefore, younger women who have not gone through menopause are at a higher risk than those who have gone through that phase. During menopause, some women counteract the related symptoms by use of hormone replacement therapy (HRT), where estrogen is introduced back into the body, usually with tablet supplements [20]. Studies have shown that women undergoing HRT have higher breast densities compared to those women who are not following a HRT regimen and are at a higher risk for developing breast cancer [13, 16, 21]. This point is also intuitive since the therapy provides the body with estrogen and keeps levels closer to pre-menopausal physiologic levels. HRT results in a continuance of the mature structures within the breast and few density changes are seen as compared to the density of the breasts prior to the onset of menopause.

The link between the use of oral contraceptives and the risk of breast cancer has also been explored, because oral contraceptives also increase the levels of estrogen. A study was performed in 2002 in Norway and Sweden, where 103,027 premenopausal women were given a survey about their use of oral contraceptives. This data was then compared to the incidence of breast cancer amongst these women in order to elucidate possible significant trends [22]. What was shown was that the risk of breast cancer increased for those women that were current/ recent users of oral contraceptives, and the increased risk of breast cancer was seen as far as 10 to 15 years after cessation of

use [22]. Another study was performed in 2009 by L. Rosenberg and associates that confirmed these results, using similar methodology; 2618 women were interviewed and their use of contraceptives assessed [23]. Yet another study performed in 2010 by D. Hunter and associates confirmed these results, showing that the use of contraceptives does provide an excessive risk of breast cancer, specifically for those individuals using triphasic preparations of levonogestrel [24]. This study also used the same type of methodology as the Norway-Sweden study; a survey was administered to 116,608 female nurses between the ages of 25 and 42 and those diagnosed with breast cancer were noted [24].

However, there are individuals who contend that contraceptives can be used to reduce the risk of developing breast cancer. A study was performed by D.V. Spicer and M.C. Pike, in which they developed a new kind of contraceptive [25]. Their work stemmed from the observation that there is a decrease in the rate of incidence of breast cancer in postmenopausal women. It was hypothesized that this was due to the fact that the levels of estrogen and progesterone are greatly reduced after menopause and, therefore, are not present to encourage cell proliferation in the breast [25]. A decrease in cell proliferation suggests a decrease in the number of genetic mutations that arise from errors that occur during cell proliferation. With fewer mutations, the liklihood of breast cancer development would be reduced [25]. Contraceptives were developed in the 1970's called Gonadotropin-releasing hormone agonists (GnRHAs) that, when administered chronically, prevented ovulation by drastically reducing the amount of estrogen and progesterone released by the ovaries. However, GnRHAs also caused severe fluctuations in serum levels of estrogen, causing some women to lose bone mineral density and develop osteoporosis [25]. Spicer and Pike performed a study in

which the use of GnRHAs caused premenopausal women to have postmenopausal hormone levels [25]. To prevent fluctuations in serum levels of estrogen, synthetic estrogen was administered at low levels and prevented the unwanted side effects [25]. In this manner, contraceptives may be used to also combat the risk of developing breast cancer.

Another commonly explored risk factor associated with breast density is the number of live births the woman has had. According to studies, the density of the breasts may be inversely correlated to the number of live births. Therefore, women who have had one or more children are more likely to have less dense breasts than those women who have had none [10]. This finding can be attributed to hormonal affects that occur during pregnancy, but the exact mechanisms are not yet fully understood.

Breast Cancer Diagnosis and Treatments

Breast cancer can only be fully diagnosed by way of biopsy where, once a questionable lump is located, an incision is made and a small portion of the mass is removed. The biopsied tissue sample is then examined for the presence of breast cancer markers and the patient is subsequently diagnosed. Once diagnosed, several breast cancer treatment options are available. Treatment must be determined on a patient-by-patient basis, since specific cases of breast cancer have distinct differences. The treatment option is chosen based on stage of the cancer, size of the tumor, health condition of the patient, and several other factors. Also, different treatment options can be used in combination to maximize the desired outcome.

Radiation therapy is a treatment option involving the application of radiation to kill cancer cells and prevent their spread. The radiation can be in the form of high power x-

rays or in the form of a radioactive substance. The use of x-rays, or other high energy radiation waves, outside the body is called external radiation therapy. Internal radiation therapy entails radioactive substances that are introduced directly into the body either in or near the cancer location [3]. However, there are limitations for radiation therapy and when it can be used. Radiation therapy can only be used once per breast, with very few exceptions. Also, if a woman is pregnant, radiation therapy will not be given since the radiation can harm the fetus [2]. Radiation therapy can be applied to a breast that has a breast implant, saline or silicone. However, the procedure will have additional complications that must be taken into consideration since the radiation may react with the implant material, resulting in a hardened implant and poor cosmetic effect [2].

Another common treatment option is hormone therapy, which leverages the dependence of cancer cells on hormones, particularly estrogen. The focus of hormone therapy is to prevent breast cancer cells from receiving stimulation from estrogen, or other hormones that promote the growth of the cancer, and to cause apoptosis of the cells [26]. Cancer cell apoptosis may be achieved by blocking the receptors of the hormones or destroying the glands that produce the hormone [26]. The most common hormone therapeutic is tamoxifen, which blocks estrogen receptors of so-called “estrogen receptor-positive” cancerous cells. Another type of hormone therapy is designed to suppress the production of hormones in the body. This hormone treatment involves two different types of drugs, the use of which depends on the menopausal status of the patient. In postmenopausal women, aromatase inhibitors are prescribed, while luteinizing hormone-releasing hormone agonists are prescribed for premenopausal women [26].

Chemotherapy is yet another option available for cancer patients. Much like targeted therapy, chemotherapy is also based on the ability to identify the differences between cancer cells and normal cells. Chemotherapy involves drugs that are either administered intravenously or orally and which travel through the blood stream to reach cancer cells throughout the body [3]. The drugs can also be administered by injection into a specific organ, body cavity, or cerebrospinal fluid to affect cancer cells found within a specific region of the body [3]. The time at which the therapy is administered can be altered to coincide with the timing of a surgical procedure. Neoadjuvant chemotherapy is given prior to any surgical procedure in order to reduce the size of the tumor and, therefore, reduce the trauma caused by the surgical procedure [27]. Adjuvant chemotherapy is given after the initial surgery to eliminate cancer cells that may have been missed and are located in the surgical margins or have metastasized to another location, other than the primary tumor site [27]. Salvage therapy is given after the cancer has recurred or is still progressing after a prior round of chemotherapy [27]. The final form of chemotherapy is called consolidation therapy, which is applied after the cancer has gone into remission. The purpose of this therapy is to eliminate any remaining cancer cells that may have been missed during the previous chemotherapy session [27].

Targeted therapy is a method used to improve the treatment of the patient, where specific characteristics of cancer cells are used to identify and attack the cancer cells while leaving normal cells unharmed. These target characteristics can range from the presence of certain active receptors to cancer-specific gene mutations [28]. The target characteristics are essential for the survival of the cancerous cell. Therefore, the targeting agents inhibit the target characteristic, thus disrupting the cancerous cell's

ability to survive and leading to the death of the cell [28]. For example, tyrosine kinase inhibitors (TKIs) have been developed to target receptors specific to cancer, e.g., human epidermal growth factor receptor – 2 (EGFR2) and epidermal growth factor receptor (EGFR). These inhibitors bind to the adenosine triphosphate (ATP)-binding pocket of the receptors, which prevents the activation of the receptors. This disruption causes blocking of downstream signal cascades responsible for gene transcription, cell proliferation and apoptosis [28]. This example describes only one type of targeting; there are several additional types of targeting agents that identify other characteristics of cancer cells.

Breast Cancer Surgical Options

In addition to the therapies described above, surgical options are also available for certain breast cancer patients that are determined able to undergo the procedure. There are two main surgical procedures, mastectomy and lumpectomy. The progression of the breast cancer is the main determinant of which procedure is used. If the cancer has spread beyond the tumor mass formation, then a mastectomy, or removal of the entire breast, is recommended. If the cancer has not progressed outside the initial tumor mass, then a lumpectomy, or removal of just the cancerous mass, can be performed followed by application of an adjuvant therapy, most often radiation therapy [29].

Besides progression of the cancer, some other indications that incline a patient to opt for a mastectomy include pregnancy, resistance to radiation therapy, anticipated poor cosmetic outcome, and patient preference which can be influenced by factors like family history or belonging to a high risk group [29]. A lumpectomy typically requires a patient to undergo radiation therapy after the surgery to ensure that any cancer cells that

may have been missed and not excised are destroyed. If the patient is unable to undergo radiation treatment, then the patient is more likely to undergo a mastectomy in order to maximize the odds that the cancer is abated.

During a mastectomy, the interior of the breast mound, i.e. the nipple, the areola, and the site of the biopsy incision, is removed, as well as a wide margin of tissue around the incision [29]. Prior to surgery, the extent of the axilla tissue that must be removed in order to remove the cancerous tissue is determined. Cancer cells most easily spread through the lymphatic system; so, the progression of the cancer can be determined by examining the lymph nodes around the cancerous breast [29]. Because of the ease of travel through the lymphatic system, it has become common practice to remove some of the surrounding lymphatic vessels and nodes. If too much lymphatic tissue is removed, serious implications, such as severe edema, can occur and may persist for the life of the patient. Figure 1.2 depicts the different levels of lymphatic vessel dissection. A higher level of dissection results in the removal of lymph nodes in a larger radius away from the cancer locus.

One means of decreasing the amount of lymphatic tissue dissected is by using the sentinel lymph node. The sentinel lymph node is the node in the axilla that is closest in proximity to the tumor mass [29]. The sentinel node is found by injecting a dye around the cancerous tumor and, after a certain amount of time, examining the axilla with blunt dissection until a node colored with the dye is discovered. The lymphatic tract is followed to ensure that the node is the first node with the coloration and consequently determined to be the sentinel node [29]. Once located, the sentinel node is excised and examined for cancerous cells.

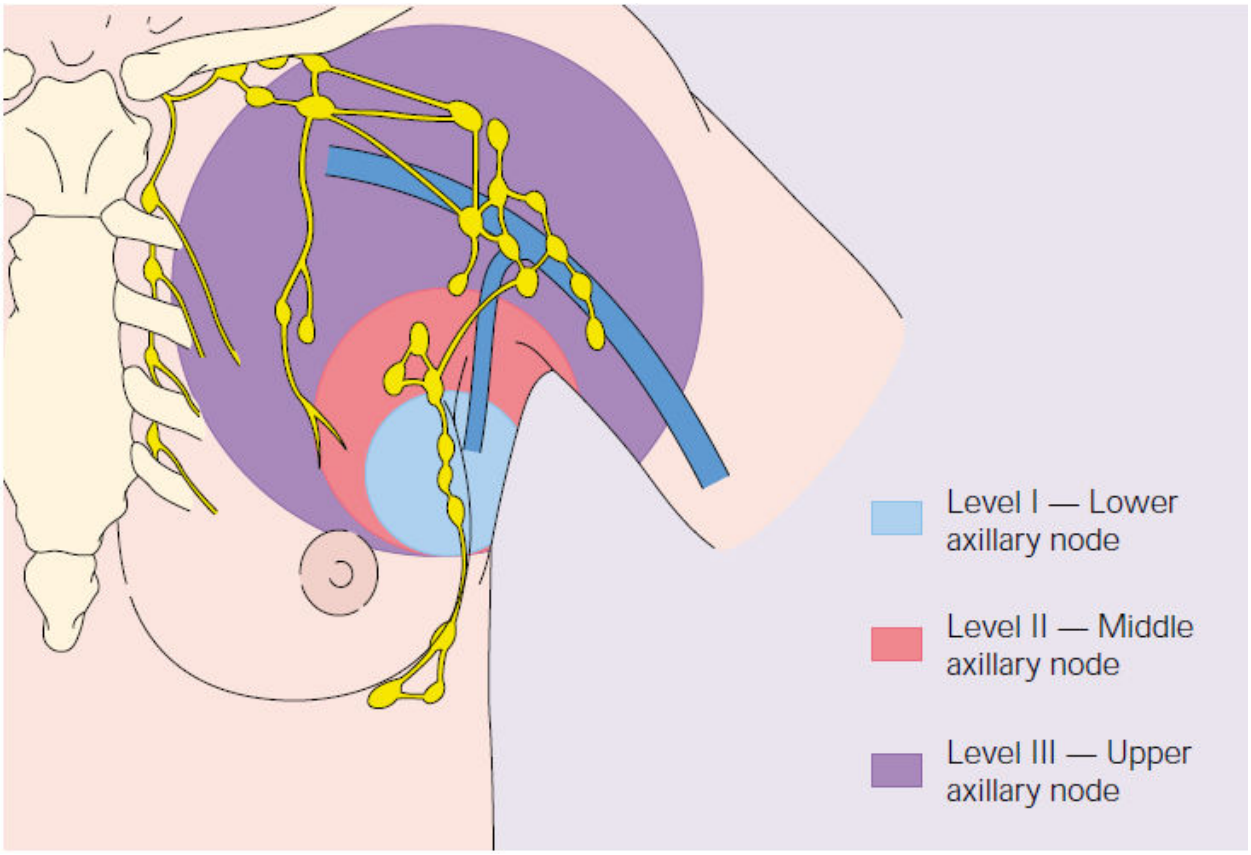

Figure 1.2: *Lymphatic Vessel Dissections [29]*

If the node is positive for cancer, then the remaining axilla is excised to ensure that a vast majority of the cancerous cells have been removed. Another similar method uses gamma probe mapping where, instead of injecting a visual dye, a radioactive dye is used and then tracked through the body to the sentinel node [29].

The second form of breast cancer surgery, a lumpectomy, is termed breast-conserving surgery because only a small portion of the breast is removed and not the total breast mound [29]. This type of surgical treatment can only be performed when the tumor is small, and there are no extensive intraductal components (EIC) present [29]. EIC is characterized by the prominence of carcinoma within the normal tissue in addition to the primary tumor [29]. When a patient is EIC positive, a larger portion of the tissue

surrounding the tumor must be removed. The tissue margins of the incision are then tested for the presence of cancer. If cancer is present in these margins, then a mastectomy is considered [29]. For patients who either show no signs of EIC or have margins that are EIC- negative, a follow up of radiation therapy is sufficient [29]. There are no cosmetic surgical procedures available for the reconstruction of a breast following lumpectomy.

Following a mastectomy, patients are given the option of undergoing breast reconstruction surgery. Breast reconstruction can be performed using a variety of implants, including artificial implants or tissue transplants. The type of reconstruction procedure is determined first by the physical limitations of the patient and then by preference. An option that has grown in popularity is having breast reconstruction immediately following mastectomy [30]. Previously, it was thought that reconstruction should be delayed to prevent any possible interference with an adjuvant therapy. However, there are many benefits to immediate reconstruction, such as having only one surgery and hospital stay and better aesthetic results [30]. According to a study by S.K. Al-Ghazal and associates, there is also significant psychological impact for those that delay breast reconstruction. The study included 121 patients that had undergone different types of breast reconstruction and were assessed for anxiety, depression, body image, self-esteem, sexuality, and satisfaction [31]. The results of this assessment showed that 95% of patients that had undergone immediate reconstruction preferred this technique, while 76% of the patients that had delayed reconstruction would have preferred immediate reconstruction [31]. It was also shown that anxiety and depression were decreased, while body image, self-esteem, and sexual feelings of attractiveness and satisfaction were significantly superior in the patients that had immediate

reconstruction compared to those that had delayed reconstruction [31]. There are still some risks involved with this combination surgery, such as extended surgical time and an increase in the complexity of the procedure [30]. The risk and rewards of undergoing such a procedure are evaluated on a patient-to-patient basis, in order to decide whether or not it is the right option for that particular person.

Breast Reconstruction

There are two primary types of tissue implants for breast reconstruction, synthetic and autologous. Generally, synthetic implants are simpler and require less surgical time but the results are not as aesthetically satisfactory [30]. The simplest reconstruction with a synthetic involves the silicone breast implant. This implant is a simple silicone gel- or saline-filled silicone bag that is implanted in the submuscular position beneath the removed breast mound. Historically, the bag was implanted subcutaneously in the void of the mastectomy flap, but this positioning caused several complications and resulted in a very poor aesthetic result [30]. A complication with breast implants is capsular contracture around the implant. The occurrence of contraction can be greatly reduced by choosing saline-filled implants rather than silicone gel implants; studies showed the incidence of capsular contracture was reduced from 60% to 30% with use of saline implants [30]. This decrease may be influenced by the silicone gel undergoing a reaction to irradiation following the reconstruction [30]. Capsular contraction is also reduced by the use of textured surfaces on the implant. By applying a textured surface, there is an increase in tissue adherence and a reduction in the risk of abnormal placement [30]. The use of textured surfaces resulted in a reduction of the incidence of capsule formation, to around 10% or less [30].

Another form of synthetic reconstruction uses a breast implant but includes another surgical implant, a tissue expander, which is implanted prior to implantation of the permanent implant [30]. Accordingly, a tissue expander is implanted in the submuscular position underneath the removed breast mound. The expander is then progressively inflated with saline over the course of several weeks [30]. The contralateral breast is used as a measure of the appropriate breast volume. Typically, the expander is inflated gradually over several weeks, with postoperative saline injections through a remote port, to approximately 150 – 200% of the desired breast volume. This procedure is conducted to account for tissue contraction after removal of the expander implant as well as reproduce the natural sagging, or ptosis, of the breast [30]. Once the desired volume has been reached, the expander is deflated and surgically removed and the permanent breast implant is placed in the void created by the expander [30]. There has also been some preliminary work to create an absorbable tissue expander that would not require an additional surgical procedure for removal of the device [32]. The underlying concept is to avoid disruption of newly repaired tissues within the breast after the initial surgery and allow the breast to heal without interruption [32]. As the expander absorbs, different signaling factors would be released that would encourage new tissue growth, filling the void [32]. The use of traditional non-absorbable tissue expanders is most often recommended for patients with small breast volume and those who are unfit or unwilling to undergo major reconstruction surgical procedures [30]. The advantages to the expander-implant method are the simplicity of the procedure and shorter periods of time spent in the operating room and recovering in the hospital. Some of the drawbacks include a lack of natural consistency, projection in the nipple area, and adverse capsular contracture [30].

Another type of synthetic breast implant was developed that incorporates an expander into the permanent implant. This implant reduces the number of surgeries needed for the reconstruction process, but is still able to produce the natural ptosis to recreate the proper aesthetic result [30]. These implants have an inner pocket of saline surrounded by silicone gel. The saline pocket is used to adjust the volume of the breast while the silicone gel surrounding the pocket is used to create a more natural feel to the breast. The complications, however, are similar to those seen with the previous synthetic implants [30].

Autologous breast reconstruction, the use of the patient's own tissue, is more complex, requiring more extensive surgery and a longer recovery time, but the results are much more natural and aesthetically pleasing than those of synthetic implants [5, 33]. There are two primary tissue retrieval sites, the abdomen and the back [5]. On the abdomen, the transverse rectus abdominis musculocutaneous (TRAM) flap is surgically excised, often times with the blood supply network intact, and is then molded into the breast mound. This procedure uses the natural fatty tissue as well as the abdominal wall skin to produce a more natural breast [5, 34]. The procedure includes abdominoplasty, or a tummy tuck, resulting from the removal of the TRAM flap. However, use of the TRAM flap requires that an additional surgery be performed to reconstruct the nipple-areola and to improve the shape of the reconstructed breast mound [5]. Also, a weakening of the abdomen as well as contour abnormalities of the abdomen can occur after this procedure [5]. The latissimus dorsi, LD, flap is located on the back. The reconstruction using this muscle flap is similar in concept to that of the TRAM flap procedure but is less involved [5, 34]. However, the results compared to the

TRAM flap procedure are inferior due to muscle tissue atrophy. Also, a common problem is inconsistent volume at the donor site on the back [5].

Breast Tissue Engineering

Breast tissue engineering is another option, beyond that of implants or autologous reconstruction, which is being explored in research. In general, tissue engineering is the application of engineering practices, the use of science and math in the design of new technologies, with end goal of replacing or enhancing the function of a biological tissue. This is accomplished by combining cells, biomaterials, and biochemical signals in an attempt to produce a functional tissue or whole organ [35]. Below is a figure that illustrates the general concepts of the tissue engineering process. Currently, breast tissue engineering has not been translated from the laboratory to the clinic due to several existing challenges related to cell culture, scaffold type, and animal model selection.

Cell Culture

The challenges of cell culture arise primarily from the cell type being cultured. The breast is composed of adipose tissue and dense tissues (blood vessels, glands, ducts, etc.); however, the focus of current breast tissue engineering research is on generating adipose tissue for tissue bulking and to provide filler material. Adipose tissue culture is quite challenging. Tissue engineering requires that the cells being cultured be

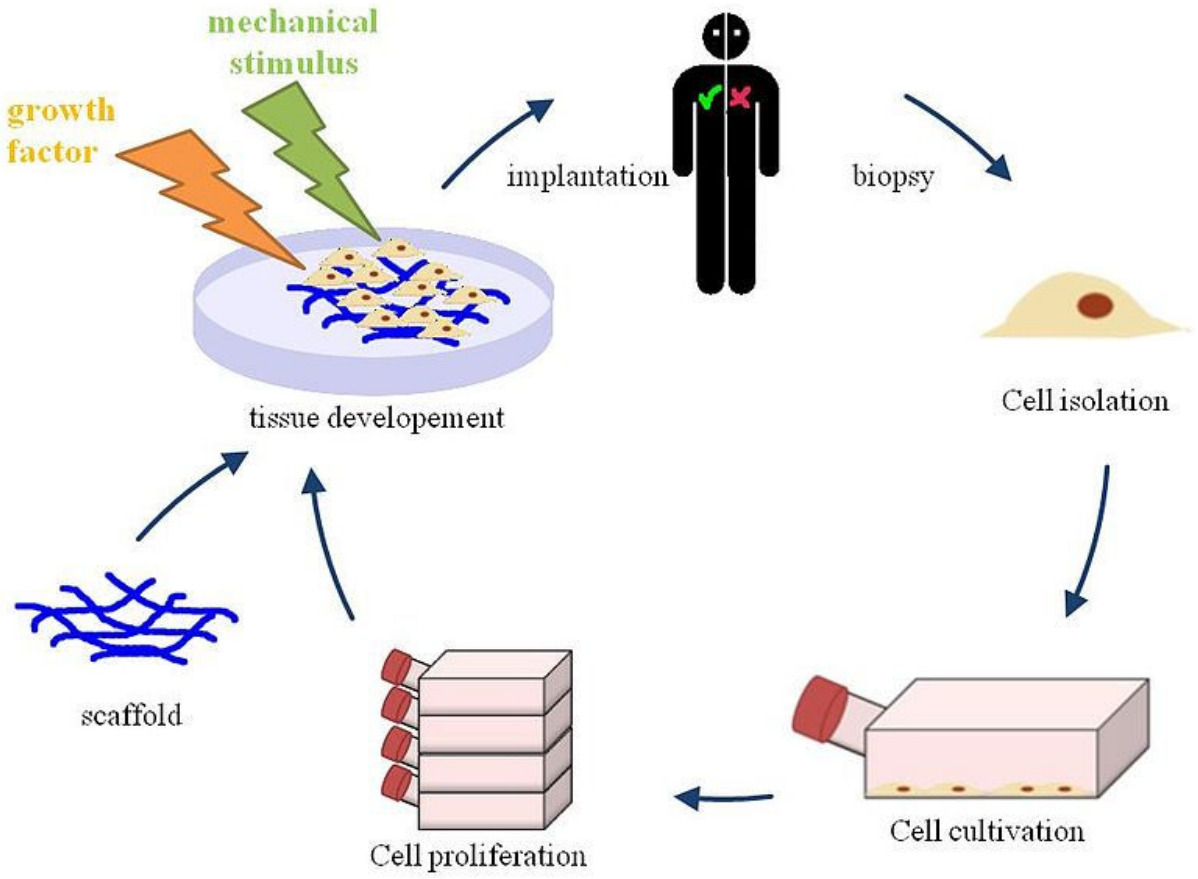

Figure 1.3: *The Tissue Engineering Process [35]*

able to withstand laboratory procedures like pipetting and centrifugation. Mature adipocytes, the cells that make up adipose tissue, are extremely sensitive to basic culture techniques [5, 36]. Approximately 80% - 90% of the cytoplasm of an adipocyte is lipid and, therefore, an adipocyte may not readily withstand the forces exerted on it during aspiration. This sensitivity results in approximately 90% of adipocytes being damaged and unable to proliferate or survive [5, 36]. In addition to being structurally weak, adipocytes are terminally differentiated cells that are unable to expand and proliferate to viable, clinically relevant tissue engineering numbers [5, 36]. To minimize

these challenges, preadipocytes, i.e. precursor cells that differentiate into mature adipocytes once introduced to the correct conditions, are often used [37]. Preadipocytes have the mechanical strength necessary to withstand the conditions of the processes required for tissue engineering, and they can readily proliferate to viable numbers that are usable for tissue engineering applications [5, 38, 39, 40]. It has now become common practice to use preadipocytes for adipose tissue engineering.

There are multiple sites in the human body where adipocytes, preadipocytes, and other cell types for adipose tissue engineering can be harvested. While varying degrees of success have been reported for these different cell types, the most common types are stem cells, which include human bone-marrow-derived mesenchymal stem cells (hBMSCs), human adipose-derived mesenchymal stem cells (hASCs), and human pluripotent cells [41]. Mesenchymal stem cells are self-renewing, and are able to differentiate into the major specialized cell types that serve to maintain the integrity and repair the tissues in which they are found [42, 43]. Both types of mesenchymal stem cells, mentioned previously, have the ability to differentiate into adipocytes when introduced to adipogenic differentiation medium [44 - 50] and also have several common receptors and cellular markers [41]. The biggest difference between the two mesenchymal stem cell types is the location from which they are harvested. The hBMSCs are harvested from the bone marrow, through a relatively painful procedure, which lessens the clinical relevance of harvesting large quantities for tissue engineering [41, 51]. In contrast, hASCs are found in large quantities within adipose tissue which can be harvested in large volume during procedures like biopsies and liposuction [41, 52]. Approximately 400,000 liposuctions are performed a year; as a result of these procedures, 100 mL to 3,000 mL of tissue is collected and normally discarded [53, 54].

However, since the discovery of hASCs, this collected tissue has been shown to have great potential as a source of mesenchymal stem cells and may replace hBMSCs as the primary source [41]. The newest cell source comprises human pluripotent cells, particularly human embryonic stem cells, hESCs. These hESCs are harvested from the inner cell mass of a 3-5-days-old embryo, also termed a blastocyst [55, 56]. Study of these cells show that they are also able to readily differentiate into adipocytes and can remain unspecialized when they are cultured with leukemia inhibitory factor (LIF) [41, 55]. One study involved the transduction of hESCs with *Oct-4* short hairpin ribonucleic acid (shRNA). *Oct-4* is a transcription factor that is used to help maintain hESCs in their undifferentiated, pluripotent state. The transduction of the shRNA associated with *Oct-4* resulted in the silencing of *Oct-4* transcription factor, which led to an increased rate of spontaneous differentiation of the hESCs toward an adipogenic phenotype [57]. The use of pluripotent stem cells for the generation of native adipose tissue formation has great promise, and the use of human cells for adipose tissue engineering is becoming more feasible as the field progresses [41].

Preadipocytes differentiate into mature adipocytes under the correct conditions, but the optimal conditions for adipocyte differentiation are not yet fully known. One factor under investigation is the effect of three-dimensional cell culture on differentiation. Cells grow and proliferate to form a single confluent layer on the bottom of a culture flask. While typical for cell culture, this is not how cells grow in the body under normal physiological conditions. Therefore, to better mimic the *in vivo* setting, three-dimensional cell culture is being more frequently used for experimental investigation [58, 59, 60]. However, tested stimuli that cause differentiation in a two-dimensional set up may not have the same effect in a three-dimensional set up [61, 62]. A study performed

by Stacey and coworkers showed that preadipocytes grown in three-dimensional culture conditions and exposed to the same differentiation stimuli as preadipocytes grown in two-dimensional culture conditions produced mature adipocytes that functioned much more closely to those found within the human body [61]. Functionality was determined by measuring the production of biochemicals from the differentiated cells and comparing that to physiological levels [61]. This finding suggests that simply growing preadipocytes in three-dimensional cell culture results in differentiation into mature adipocytes that function at more relevant levels than those cultured in two dimensions [61].

Within this same study by Stacey and coworkers, different adipocyte differentiation methodologies were explored. In one methodology, differentiation medium was made, containing Dulbecco's Modified Eagle's Medium supplemented with 3% fetal bovine serum, L-glutamine, penicillin, streptomycin, biotin, pantothenate, human recombinant insulin, dexamethasone, isobutyl-methylxanthine, and indomethacin [61]. This type of adipogenic cocktail has been used extensively in research and has been shown to cause adipogenesis of preadipogenic cells. A second method of differentiation involved co-culture of preadipocytes with mature adipocytes, seeded in transwell inserts [61]. The mature adipocytes did not physically contact the preadipocytes, but the factors they produced were expelled into the surrounding medium, where the preadipocytes could recognize and uptake them [61]. In both methods, samples of the medium were taken and levels of glycerol, leptin, and adiponectin were quantified to measure adipogenic differentiation [61]. The two differentiation methodologies were applied to both the two-dimensional cultures and three-dimensional cultures. In both cultures, the preadipocytes grown in the adipocyte transwell inserts produced levels of the three substances of interest that were much more closely aligned with those seen by mature

adipocytes *in vivo*, compared to those grown in differentiation medium alone [61]. This suggests that, while the addition of differentiation medium is the more commonly used methodology to differentiate preadipocytes to adipocytes, it may not be the most effective and further exploration is needed.

Another adipose tissue engineering challenge that is being researched concerns the co-culture of preadipocytes with other cell types to produce more anatomically correct tissue constructs. In a study performed by Huss and coworkers, human mammary epithelial cells and preadipocytes were harvested from breast tissue biopsy samples. To isolate these cell types, the tissue samples were digested after the removal of connective tissues and blood vessels to prevent contamination of fibroblasts in cell culture [63]. The primary cells were co-cultured in culture flasks as well as within collagen gels, the latter providing three dimensional environments for growth. The human mammary epithelial cells grew in patches in the culture flasks and had a "cobblestone appearance", with preadipocytes growing around these epithelial patches [63]. After some time, the preadipocytes became more rounded as they accumulated lipid and grew radially around the epithelial patches [63]. Within the gels, the epithelial cells formed ductal structures as the cells lined up in rows, became interconnected, and thickened. At the end of these ductal structures, swellings resembling alveoli were noticed [63]. Clusters of cells, identified as adipocytes, were also noticed beside these ductal structures. This type of cell organization mimics the natural anatomical structures seen within the human breast [63]. This finding suggests that more anatomically accurate tissue constructs may be grown in the laboratory, when preadipocytes are exposed to other cell types that are found within the breast *in vivo*. However, there is concern for oncological implications of this type of construct, due to the introduction of

epithelial cells which are more susceptible to mutation and cancer formation compared to adipocytes alone [63].

Scaffold Type

Another important consideration of breast tissue engineering is the scaffold on which the selected cells will be grown. There are several different types of materials that can be used to form the scaffold, each with their own advantages and disadvantages. Selection of a material to use as a scaffold depends on the purpose and characteristics of the tissue that is being replaced as well as the physical characteristics and health of the patient.

Some of the very first studies performed regarding adipose tissue replacement used a method called autologous fat transplantation [5]. This methodology simply involved harvesting adipose tissue from a location on the patient and transplanting that tissue to the breast tissue void. This was done without a scaffold in place to guide the shape of the tissue replacement. The results of this type of procedure were very poor, with 50% - 70% reduction in volume due to the resorption of the grafted tissue. Resorption occurs because adipocytes are anchorage dependent and require a scaffold to survive. Additionally, the adipocytes found in the tissue graft were terminally differentiated and, therefore, could not proliferate [5]. After several failed attempts, it was determined that a scaffold is required for proper breast tissue replacement.

One of the scaffolds explored for the purpose of replacing adipose tissue was composed of poly(lactide-co-glycolide) (PLG) [64]. PLG is an absorbable polymer that is slowly degraded in the body; in theory. a PLG tissue engineering scaffold would be replaced by a tissue matrix created by proliferating cells within the scaffold. In a study

by Patrick and coworkers, PLG disks were prepared by casting a 75:25 lactide to glycolide PLG solution over sodium chloride (NaCl) crystals. After the PLG had solidified, the disks were placed in deionized (DI) water to leach the NaCl, resulting in porous PLG disks [64]. These disks were subsequently seeded with preadipocytes from 70 – 80 day-old Sprague-Dawley and Lewis rats and then embedded into the fat pads of Lewis rats [64]. Within each rat, four disks were implanted, three of which were seeded with preadipocytes and one which was an acellular control [64]. The disks were harvested 2 and 5 weeks after implantation and histologically evaluated. The histological evaluation showed that the preadipocytes had differentiated into mature adipocytes and were found throughout the thickness of the PLG disks, filling in the pores created by the leached NaCl [64]. The results of this study showed that the use of PLG as a scaffold for adipose tissue engineering was viable and allowed viable cell attachment, infiltration, and differentiation [64]. However, Patrick cited in a later paper that an issue with PLG arises when long term studies are conducted. After a period of 5 months, the PLG scaffolds assessed in his studies were completely absorbed, as was the volume of generated adipose tissue [5]. Therefore, PLG alone, in the specific form studied, may not be a viable scaffold for long term correction of adipose tissue defects.

Various polymer hydrogels, such as polyethylene glycol (PEG), have also been explored as scaffold materials for adipose tissue engineering. One advantage of these hydrogels is their ability to be modified with different peptide sequences to better tailor them for the application for which they are designed [5]. For instance, a peptide sequence can be added to the backbone of the polymer chain to make it susceptible to biodegradation by enzymes secreted by cells, e.g. the enzyme collagenase [5, 65, 66, 67]. Peptide sequences can also be added to provide binding sites for cells, including

sites that preferentially bind to specific cells, like preadipocytes, over other cell types [5]. Another advantage of a hydrogel is that cells can be added directly to the hydrogel solution, injected into the defect site, and photopolymerized, resulting in a hydrogel that is customized for the shape of the defect and already loaded with preadipocytes throughout [5]. Alginate is another naturally occurring hydrogel that is commonly used in much the same way as PEG but it must also be modified with a peptide sequence to allow cell attachment [5, 68].

Biological polymers have also become popular scaffold materials for adipose tissue engineering because of the increased biocompatibility of the materials when properly prepared. Some examples of biological polymers include collagen and hyaluronic acid [5]. Scaffolds produced from these materials typically are hydrogels or porous structures like mesh or sponges with regulated pore sizes [5]. It is important that the pores of the structure are matched to the cell needs, or the cells being grown will not be able to properly infiltrate the scaffold and differentiate [5]. It is important that the porosity of the scaffold is high enough to provide enough room for preadipocytes to differentiate into mature adipocytes [5].

Scaffolds for tissue engineering are not limited to the use of one type of material. Composite scaffolds that use two or more types of materials can be used to help combat and overcome the weaknesses and shortcomings of one material. For instance, a material that has excellent cell attachment characteristics but is not very durable can be combined with a more durable material, hopefully resulting in a scaffold that is both durable and able to support cell growth.

A study was conducted by Sin-Daw Lin and coworkers, combining different types of scaffolds and materials. In this study, gelatin sponges, polyglycolide mesh, and

monofilament polypropylene mesh were used to construct three-dimensional scaffolds that predefined shapes on which human adipose derived mesenchymal stem cells (hAD-MSCs) were grown [69]. The scaffolds were made of an outer polypropylene mesh pocket that contained gelatin sponge cubes and polyglycolide mesh [69]. Gelatin is a good scaffold for cell growth and attachment and can be molded into a desired shape. but it loses its dimensional stability over time [69]. The polyglcyolide mesh was used to increase the surface area available for cell attachment [69]. Polypropylene mesh was used because of its ability to maintain dimensional stability after being implanted into the body [69]. These scaffolds were then seeded with a high density hAD-MSC suspension in a 6-well plate coated with agar to force the cells to attach to the scaffold [69]. These scaffolds were cultured in adipogenic differentiation medium to encourage the hAD-MSCs to differentiate into mature adipocytes [69]. After 2 weeks, the scaffolds were implanted into the backs of nude mice for 2 months and then excised for analysis [69]. Analysis showed that the scaffolds contained new adipose tissue as well as neovascular structures [69]. The gelatin cubes, as well as the polyglycolide mesh, had been completely absorbed by the body but the outer polypropylene mesh remained in the predefined dimensions as before implantation [69].

Some scaffolds do more for tissue engineering purposes than simply provide a matrix on which cells will grow. Some scaffolds have an incorporated therapeutic agent such as a drug or growth factor, and are termed therapeutic scaffolds. The concept behind these scaffolds is that the therapeutic agent incorporated into the scaffold is released as the cells remodel the scaffold during cell growth and proliferation. The therapeutic agent therefore has a direct effect on the surrounding tissue where the scaffold was placed.

These therapeutic agents can affect the tissue surrounding the implanted scaffold. An example of this approach can be seen in a study conducted by Shi and coworkers, where the therapeutic agent, angiogenin, was incorporated into a scaffold [70]. Angiogenin is a drug that has been shown to promote neovascularization, so the intent of its incorporation was to help promote the growth of new vasculature throughout the scaffold [70]. This result would theoretically increase the chances for the success of an implanted tissue replacement and improve the overall outcome of the procedure. The investigators subcutaneously implanted these scaffolds into rabbits and, after 28 days, the scaffolds were excised [70]. The study showed that scaffolds with incorporated angiogenin had increased neovascularization [70].

Another therapeutic scaffold was assessed by Lee and coworkers. The agent for this therapeutic scaffold was incorporated to target cells grown on the scaffolds rather than targeting the surrounding tissue. Accordingly, transforming growth factor – beta 1 (TGF-β1) was incorporated into microspheres that were embedded into the scaffold [71]. Chondrocytes were then incubated on these scaffolds and the effect of TGF-β1 on these cells was evaluated. The results showed that the chondrocytes grown with TGF-β1 had increased production of glycosaminoglycans (GAGs) as well as an increased proliferation rate [71]. These results suggest that a scaffold using TGF-β1 would be advantageous for the growth of cartilage tissue replacements [71].

A final example of a therapeutic scaffold is one in which the agent targets and neutralizes a specific type of cell found in the surrounding tissue, such as a cancer cell. Gupta and coworkers developed and tested such a scaffold; specifically, they embedded a scaffold with nanoparticles containing emodin, an anti-cancer drug [72]. This scaffold was intended to fill the site where a cancerous tumor was removed from the breast [72].

The concept behind this scaffold was that if cells proliferated on the scaffold and remodeled it, the emodin contained within the nanoparticles would be released and would neutralize any cancerous cells in the surrounding tissue [72]. These scaffolds were implanted next to the mammary fat pads of nude mice in which cancerous cells had been injected. The results of this study showed that the size and number of the tumors next to emodin-loaded scaffolds were reduced compared to those next to scaffolds without emodin [72].

Animal Testing for Adipose Tissue Engineering

Typically, the last step for a tissue engineered implant, before it is translated to clinical trials, involves animal testing. The cellular scaffold is moved out of the cell culture dish and incubator and into an *in vivo* environment where the interaction between the implant and a living biological system can be studied. However, this too is an area of high variability since not all studies compare the same animal model, surgical techniques, or implantation sites.

There are primarily three different types of animals used in adipose tissue engineering: mouse, rat, and large animals such as pigs and cows. There are, however, several different genetic strains that can be used for each, each with distinct physiological variations that make it almost impossible to compare between studies that do not use the same genetic strain [73]. The majority of mice used in adipose tissue engineering studies are genetically modified to be immune-deficient in order to prevent rejection of implanted human cells and allow scaffold constructs to function under normal physiological conditions without attack by the host immune system [73]. However, even though the mice are genetically altered for immunodeficiency, there are several different

genetic modifications that can result in immunodeficiency [73, 74]. These varying genetic modifications can cause varying levels of different hormones throughout the host body. Hormonal differences will result in adipose tissue development differences that will likely result in different biological reactions to the same implant [73]. Laboratory rats also have several different genetic varieties, which pose the same complications as mice when attempting to compare studies [73].

Another important factor that is often overlooked by researchers is the gender of the animal [73, 74]. Biologically, males and females of the same species have different hormone levels due to differences in development as the animals mature. Similar to genetic variations, gender-induced differences in hormones cause a difference in adipose tissue development which may result in different biological reactions to the same scaffold construct [73].

One other complicating factor is the size of the actual animal in question. Small size animals include animals such as mice and rats, while larger sized animals include sheep, domestic pigs, and cows [73]. When considering mammary tissue, the larger sized animals are more physiologically relevant to humans [75]. This issue raises the question of applicability of translating animal model results to an expected human clinical trial outcome. Large animals can accommodate the same size implant as one that would be used in a human [73]. Also, the internal anatomy of larger animals, such as the domestic pig, is much more similar to the human anatomy in regards to organ size and heart rate [73, 76, 77, 78]. It was also shown that the histoarchitecture and hormonal control of the mammary glands of larger animal models is much more applicable to humans compared to those of rodents [79, 80]. Studies have shown that bovine cells as well as human cells do not outgrow in the mammary fat pads of immune

suppressed mice. This result suggests that the fat pads of rodents do not provide an environment suitable for the proper growth of human or bovine mammary epithelium [79]. It has also been shown that progesterone has a much different effect on the mammary tissue of mice when compared to larger animals, including humans. In mice, progesterone stimulates epithelial proliferation and ductal side branching, whereas progesterone has limited effect on the mammary epithelium of larger animals and humans [79]. Table 1.2 below further summarizes the similarities and differences seen in mammary gland development in mice, humans, pigs, and ruminant animals like sheep, goats, and cows. However, the main drawback of using a larger sized animal is the cost of the animal. Large animals are much more expensive than smaller animals and fewer researchers are trained in, and have the facilities for, the proper care of these larger animals [79]. Because of this fact, fewer research grants and funding are available for projects that focus on the use of larger animal models [79, 81].

Table 1.2: *Comparative Aspects of Mammary Gland Development [79]*

Attribute	Mice	Humans	Pigs	Ruminants
Morphology	Sparse ducts; alveolar	TDLU	TDLU	TDLU
Stromal histology	Adipose » connective	Intralobular, interlobular connective » adipose	Intralobular, interlobular connective » adipose	Intralobular, interlobular connective » adipose
No. of ductules/TDLU (Types 1, 2, and 3, respectively)	N/A	11, 47, 81	9, 24, 64	Not defined
No. of galactophores	1	~8–15	2	1
Epithelial proliferation	Concentrated in endbuds and alveoli	Concentrated in endbuds or TDLU	Concentrated in endbuds or TDLU	Peripheral Zones of TDLU
Response to E	Endbud	Epithelial	Endbuds, TDLU	Epithelial
Response to P	Alveoli	Negative, or No Effect	No Effect	No Effect
Mammary tumors	Spontaneous, viral origin	Spontaneous	Rare, few cases	Rare, few cases
Tumor precursor	AH, ADH, DCIS	ADH, DCIS	Unknown	Unknown
Tumor hormone dependence	Rare	50–60%	Unknown	Unknown

Abbreviations: AH: alveolar hyperplasia; ADH: atypical ductal hyperplasia; DCIS: ductal carcinoma *in situ*; E: estrogen; P: progesterone; TDLU: terminal ductal lobular unit.

Tannic Acid Introduction and Structure

Tannic acid is a compound that was previously used medically for the treatment of burns but certain characteristics of it show promising abilities in the field of breast reconstruction and breast cancer research, particularly its ability to cross-link collagen to form a scaffold along with its anti-cancer properties.

Tannic acid is a polyphenolic compound that contains a central pentagalloylglucose (PGG) core surrounded by gallic acid molecules through ester bonds at all hydroxyl functional groups [82, 83]. Figure 1.4, illustrates this structure with the encircled PGG core and the esterified gallic acid molecules found on the outside of the circle. The ester bonds within the tannic acid are hydrolysable, resulting in the release of the gallic acid molecules as metabolites of tannic acid [82, 85].

Tannic acid is commonly found in certain plant products, including food grains (such as sorghum, peas, fava beans, and other legumes) and fruits (such as apples, grapes, bananas, peaches, pears, and cranberries) [82]. Tannins can also be readily found in products made from these plant products, such as wines and tea [82]. Tannic acid molecules are found in two different forms, condensed and hydrolysable, where the chemical structure of the tannic acid molecule is the main difference between the two. Condensed tannins are natural polymers of different flavanol groups, see Figure 1.5 below [85]. Condensed tannic acid is not used readily in biomedicine due to the limited bioactivity and, therefore, any mention of tannic acid from this point on will be in reference to hydrolysable tannic acid.

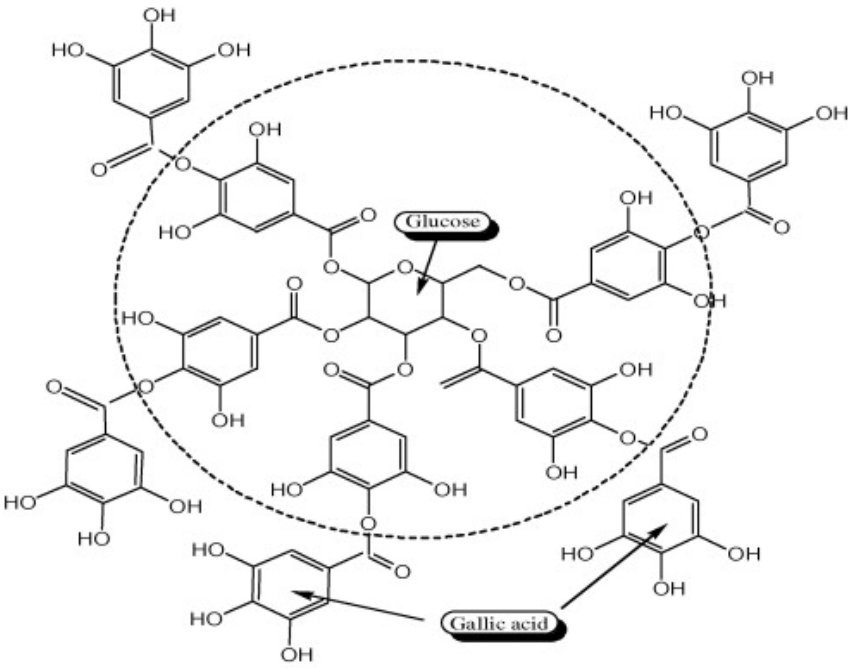

Figure 1.4: *The structure of hydrolysable tannic acid [84]*

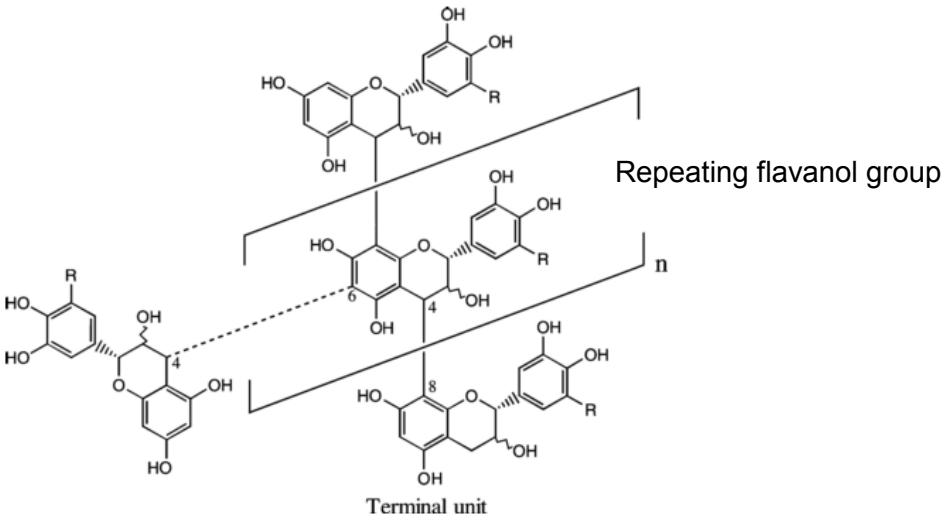

Figure 1.5: *The structure of condensed tannic acid [86]*

Tannic Acid for Burn Treatments

The first documented medical use for tannic acid was in the 1920s as a burn treatment [87]. It was believed that the burned skin released toxins, which then entered the blood stream and caused organ damage and failure [87]. However, by applying tannic acid, the toxins would be fixed to the burn wound and not allowed to enter into the body [87]. In addition to these theorized benefits, patients who underwent tannic acid treatment also reported that they had reduced pain, a lower infection risk, stimulation of epidermal regeneration, faster wound healing, reduction of plasma loss, and a reduced mortality [87]. Clinician Lindsay performed a study on a burn patient who had extensive second degree burns on both thighs. One the right side, the burns were treated with wet saline solution bandages while the left side was treated with wet saline bandages, followed by bandages that had been saturated in a 5% tannic acid solution [88]. It was noted that after 24 hours, the lesions on the left side of the patient looked so markedly improved that the tannic acid treatment was then applied to the right side of the patient [88]. After three days of the tannic acid bandage treatment, a tannic acid ointment was used. The burned tissue was noted as being dry and well-tanned and, after a few days, the necrotic tissue was removed in a continuous bath in which the patient lies supported in a bath of tepid water [88]. Sixty-five days after admission, the patient was discharged as completely healed [88]. Lindsay made a note, stating that the use of the tannic acid treatment resulted in immediate and continued relief from pain, a greatly reduced level of shock, and markedly reduced level of absorbed toxins [88].

However, opposition to tannic acid treatments was introduced in the 1940s when it was proposed that there was a relationship between liver necrosis and the application of tannic acid [87]. Autopsies of 16 patients treated with tannic acid showed that 14 of

them had liver necrosis [87]. Animal studies showed that a 10% tannic solution, introduced intravenously or subcutaneously, caused liver pathology but tannic acid applied to burns did not alter liver function [87]. In 1963, Lucke and colleagues examined five cases of patients who died unexpectedly after receiving barium enemas containing 0.25% tannic acid [89]. After autopsy, all five patients were shown to have fatal liver damage which the authors attributed to the tannic acid within the enemas [89]. However, the authors do state that proof that the patients died from exposure to tannic acid is lacking and that there is a low recorded incidence of liver damage after exposure to the barium enemas containing tannic acid [89]. The authors merely wanted to point out the suspicions that incidences like this raise, and they wanted to investigate a common variable between these five outstanding cases [89]. Because of the concerns raised by this research study and others, it was justified to discontinue the use of tannic acid in the treatment of burns, and new methods were developed [87].

By as early as the 1950's, there was opposition to the notion that tannic acid caused fatal liver damage. It was cited that the mortality of burn victims decreased from 25% to 10% after the introduction of the tannic acid treatment method [87]. Opponents to the use of tannic acid stated that this was due to the advancements of burn and shock treatments. However, proponents for the use of tannic acid stated that if tannic acid was the cause for liver damage, then the mortality rate should have increased, not decreased, after the introduction of tannic acid [87]. The animal studies previously conducted by the opponents of the tannic acid treatment were also scrutinized. In the animal studies, the administration of tannic acid intravenously would have greatly increased the amount of tannic acid in the blood plasma far beyond what would be seen when applied topically [87]. The concentration of tannic acid used in these animal

studies, >10%, was much greater than the concentration actually used in the clinical setting, <5% [87]. A follow up animal study was performed on guinea-pigs with experimental burns and an applied 3% tannic acid solution. The results of this study showed that liver structure changes were less in those that had been treated with the tannic acid compared to those that had not been treated with tannic acid. This outcome lead to the conclusion that the use of tannic acid on a burn wound diminishes liver damage caused by the resorption of toxins [87]. A recent study performed by Halkes and colleagues explains that the tannic acid used in the 20s to 40s was not very purified and actually contained contaminants like gallic acid, flavonoids, and condensed tannins, and only 35% of the solution was actually tannic acid [90]. The negative effects seen from the use of these tannic acid solutions was not caused by the tannic acid but, rather, by the contaminants found in the solution. The authors showed, using a hemoglobin assay, that free gallic acid is unable to cause the precipitation of hemoglobin and may actually completely block the binding of hemoglobin when present in low doses [90]. They hypothesized that the gallic acid contaminants within the tannic acid solution were responsible for preventing the binding of proteins in the burn wound, delaying the healing process, and allowing more tannic acid to be introduced into the blood stream and causing the negative effects that were seen [90]. The authors believe that the use of current, purified tannic acid will remove the opposition to use tannic acid in burn wound treatments [90].

Tannic Acid as a Cross-linking Agent

The use of tannic acid as a burn wound treatment stems from the observation of tannic acid's ability to form cross-links with proteins. This ability has led to the use of

tannic acid as a cross-linking agent for the formation of scaffolds that are used in tissue engineering applications. The most common fixative used for tissue scaffold development is glutaraldehyde because of its low cost, high availability, and solubility in aqueous solutions [91]. Glutaraldehyde is able to crosslink proteins by bonding to the primary amine groups and forming chemical bridges between the protein molecules [91]. The exact mechanism of collagen fixation is not fully understood, but it is hypothesized that it is through covalent bonds [91]. Glutaraldehyde has limitations that can cause medical complications and result in the failure of the implant [91]. For example, bioprosthetic heart valves are most commonly fixed using glutaraldehyde, and the principle cause of failure for these valves is calcification [91]. Residual glutaraldehyde has been implicated in the process of calcification, although a direct link has not been proven [91]. Studies have shown that glutaraldehyde-fixed bioprostheses become more biocompatible and show less calcification when treated with amino acid solutions, further supporting the link between glutaraldehyde and valve calcification [91].

Another complication associated with glutaraldehyde fixation is the limitation of proteins glutaraldehyde can crosslink. Glutaraldehyde is unable to crosslink elastin, a major component of valves and blood vessels [92]. Due to the elastin remaining unprotected, bioprosthetic valves and blood vessels fixed in glutaraldehyde are broken down at an increased rate and can fail early in their lifetime [92]. However, tannic acid has been shown to crosslink elastin and thus provides protection of elastin. A study by Isenburg and colleagues showed that when glutaraldehyde-fixed blood vessels are also exposed to tannic acid during the fixation process, the degradation rate of these implants is reduced by 15-fold, extending the life span of the implant [92]. Another advantage of

these glutaraldehyde/ tannic acid fixed prostheses is a reduction in the calcification by 66% compared to those fixed with glutaraldehyde alone [92].

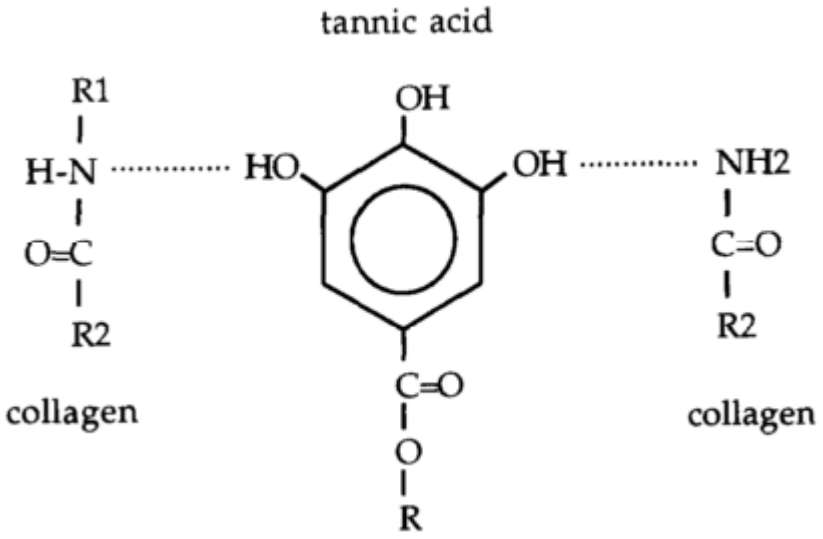

Figure 1.6: *Cross-linking of collagen by tannic acid [93]*

Tannic acid is able to cross-link proteins by forming hydrogen bonds between its many hydroxyl groups and the amine groups of proteins, see Figure 1.6. A study by Heijman and colleagues used dermal sheep collagen as a human skin analog to test the degree of cross-linking as well as the release of tannic acid from the collagen implants [93]. This study showed that the degree of cross-linking of collagen is proportional to the concentration of the tannic acid solution used in the cross-linking process [93]. It also showed that the degradation rate of tannic acid cross-linked collagen was greatly reduced, compared to other scaffolds cross-linked with glutaraldehyde [93]. The authors also explored the thermal denaturation temperature of tannic acid cross-linked collagen scaffolds as a way to measure the degree of cross-linking. Their research results showed that, at a tannic acid cross-linking concentration between 2% to 3%, the thermal

denaturation temperature was at its maximum [93]. At higher concentrations, the thermal denaturation temperature did not increase, but the measured uptake of tannic acid did increase, suggesting that the maximum amount of cross-linking occurs between 2% and 3% and any cross-linking concentration above this results in only an increase of bound tannic acid to the collagen scaffold [93].

Another factor that influences the degree of cross-linking by tannic acid is the pH of the cross-linking solution. A study by Van Buren and coworkers explored the effects pH has on the ability of tannic acid to cross-link with gelatin [94]. Their studies showed that, as the pH decreased and the solution became more acidic, the ability of the tannic acid to form complexes with gelatin decreased as more tannic acid and gelatin were found in solution [94]. It is hypothesized that the decrease in ability of tannic acid to form complexes with the gelatin is due to a deaggregating effect on the gelatin and alteration of its electrostatic charge [94].

Tannic Acid as a Cancer Treatment

In addition to being able to cross-link proteins and form complexes, tannic acid has also been shown to have anti-cancer properties. However, the exact mechanism by which tannic acid affects cancer cells is still not fully understood. A study by Nam and coworkers shows that tannic acid potentially inhibits the activity of specific proteasomes and causes a build-up of proteasome substrates, specifically the cyclin-dependent kinase inhibitor $p27^{kip1}$ and the pro-apoptotic protein Bax [95]. A build-up of these substrates causes the arrest of the cell growth cycle in the G1 phase followed by the induction of apoptosis [95]. This study showed that after the introduction of a tannic acid solution, Jurkat T cells increased both $p27^{kip1}$ expression and G1 population in a time

dependent manner, and increased Bax expression and cell death [95]. They also showed that, as the concentration of tannic acid increased, the percent of cells within a pre-G1 phase also increased after a 24 hour exposure time [95]. These results showed that the initial concentration of tannic can be proportionately related to the level of apoptosis and cell death observed.

Others have proposed that tannic acid affects tumor cells by inhibiting the C-X-C chemokine receptor type 4 (CXCR4) from recognizing the chemokine (C-X-C motif) ligand 12 (CXCL12) chemoattractant [96]. The CXCR4 receptor is commonly expressed by most types of cancer cells and it is noted that CXCL12 is commonly found at sites of cancer metastasis [96]. It is hypothesized that the CXCL12/ CXCR4 complex is a major component in the process of metastasis for cancers [96]. In a study by Chen and coworkers, they observed that certain herbal Chinese medicines inhibited this complex. They further investigated the components of the Chinese medicines and found that extracts from the fruit of the forsythia tree contained tannins that played a role in this inhibition [96]. They showed that after exposure to tannic acid, migration of cancer cells by CXCL12 was greatly inhibited but there was no significant effect on the migration of non-cancerous cells [96]. The results indicate that tannic acid has the ability to selectively inhibit the migration of cells that express the CXCR4 receptor while allowing other cells to grow and proliferate [96].

Tannic acid has also been studied as a chemotherapy drug to be used in conjunction with others, as a way of overcoming the negative side effects of the other drugs as well as enhancing the positive effects. Tikoo and colleagues assessed cancerous cells exposed to both tannic acid and another chemotherapy drug, doxorubicin [97]. Doxorubicin is an anthracycline antibiotic that is used commonly for

the treatment of solid tumors. However, it is limited in terms of use because of its noticed toxicities to different tissues, including cardiac tissue (cardiotoxicity) [97]. The authors completed both *in vitro* testing, with embryonic rat heart myoblasts and human breast cancer cells, and *in vivo* testing, with Sprague Dawley rats induced to have breast cancer tumor growths [97]. Their results showed that, when the embryonic rat heart myoblasts were exposed to tannic acid with the doxorubicin, the levels of Bax were decreased and the amount of Bcl-2 (an anti-apoptotic protein) increased compared to levels resulting from treatment with doxorubicin alone. They also observed a decrease in the amount of cellular death [97]. However, when the human breast cancer cells were exposed to doxorubicin and tannic acid, the measured levels of p53 (a tumor suppressing gene) were shown to have increased beyond that resulting from introduction of doxorubicin alone [97]. The same results were seen for the experimental Sprague Dawley rats with breast cancer tumors [97]. These results suggest that the combination of tannic acid with doxorubicin results in an increase in the overall potency of breast cancer treatment, as well as a reduction of the unwanted side effects.

Researchers have proposed that tannic acid negatively affects cancer cells by inhibiting the enzyme nitric oxide synthase (NOS). Nitric oxide is an important inorganic gas synthesized by NOS and has been found to play crucial roles in many cellular and organ functions [98]. Recently, it has been cited as a signaling molecule that regulates the processes of tumorigenesis; several types of cancer cells overexpress NOS as compared to normal cells [98]. Therefore, Cosan and colleagues performed a study to determine the effect of tannic acid as well as another polyphenolic compound, resveratrol, on the activity of NOS in two types of cancer cells, colon cancer and breast cancer [98]. Tannic acid and resveratrol were selected because of their documented

anti-carcinogenic and anti-inflammatory properties [98]. This study showed that the NOS activity of these cancer cell lines was reduced when exposed to resveratrol and tannic acid, suggesting that these compounds are able to reduce the amount of nitric oxide synthesized by these cancer cell lines and, therefore, reduce the amount of tumor formation [98].

Tannic Acid in Diabetes Research

Another area of tannic acid research is focused around diabetes research. A major complication of diabetes is that the amount of glucose in the blood stream must be regulated but most anti-diabetic drugs that are hypoglycemic also promote adipose tissue formation and weight gain [99, 100]. Ideally, one would want a drug that is able to reduce blood glucose levels but also inhibit adipogenesis, thus combating the symptoms of diabetes without causing the weight gain side effect. It was noticed that extracts from the leaves of the banaba tree, a species of tree found in tropical southern Asia, stimulated these two desired effects on 3T3-L1 preadipocytes [99]. It was also found that the extract from the leaves of the banaba tree contained tannic acid. Liu and coworkers exposed the 3T3-L1 cells to the banaba extract and compared that result with 3T3-L1 cells exposed to banaba extract with tannic acid removed. This study showed that when the tannic acid was removed from the extract, the two desired effects of the extract were lost [99]. This led the researchers to the hypothesis that the tannic acid in the banaba extract was responsible for these desired effects. To test this hypothesis, they exposed 3T3-L1 cells to pure tannic acid to see the effects tannic acid alone would have on the cells. The results of this test showed that tannic acid by itself stimulated the same two activities as the banaba extract [99]. This proved to the authors that the tannic

acid was responsible for the inhibition of the adipogenesis as well as the increase in the uptake of glucose from the blood stream [99].

A similar study was done by Muthusamy and coworkers, except a different source of tannic acid was used. Instead of using a banaba extract, they used extracts from the chicory plant, found in Europe, North America, and Australia. Much like banaba extract, extract from the chicory plant has also been shown to be rich in tannic acid [100]. The authors exposed 3T3-L1 cells to the pure extract from the chicory plant as well as to the extract with tannic acid removed [100]. Their study initially contradicted the results seen by Liu and coworkers. When they exposed the 3T3-L1 cells to both the pure extract and the extract with tannic acid removed, the cells increased their glucose uptake. This result led the authors to hypothesize that the tannic acid may not be the crucial molecule that triggers the desired effects [100]. However, after further investigation, it was determined that the extract that had the tannic acid removed also contained a molecule that caused the activation of a signaling pathway, which also resulted in the uptake of glucose [100]. The results from their adipogenesis inhibition study confirmed what Liu and colleagues had seen in their study and therefore, confirmed the results that showed that tannic acid was an effective inhibitor of adipogenesis as well as a promoter of glucose uptake by preadipocytes [100].

Maximizing the Usefulness of Tannic Acid

With all of these characteristics and abilities of tannic acid in mind, a study was performed by Cass and colleagues that incorporated a majority of the different advantages tannic acid has to offer. The study explored the ability of tannic acid to act as a cross-linking agent for a collagen scaffold used to co-culture MCF-7 cells, human

breast cancer cells, and D1 mesenchymal stem-like stromal cells, [101]. The hypothesis was that tannic acid would cross-link the collagen effectively enough to form a viable scaffold on which cells could grow and that, as the scaffold was remodeled by the cells, tannic acid would be released and cause cancerous MCF-7 cells to undergo apoptosis but also allow non-cancerous D1 cells to proliferate and eventually differentiate into mature adipocytes [101]. The results showed that collagen gels that were exposed to a higher concentration of tannic acid solution had a higher thermal denaturation temperature [101], suggesting a direct correlation with the concentration of tannic acid and the degree of cross-linking within the scaffold. However, it was noted that the interaction between the tannic acid and the collagen is a weak interaction and that, under normal physiological conditions, the scaffolds may not be durable and may prematurely break down [101].

The results of these studies also indicated that MCF-7 cells decreased in metabolic activity after 48 and 72 hour exposure times coupled with a 0.025 and a 0.05 mg/ mL tannic acid concentration [101]. Undifferentiated D1 cells had a significant decrease in metabolic activity at all time-points and all concentrations of tannic acid [101]. Differentiated D1 cells fared better and showed much more stability compared to undifferentiated D1 cells. Differentiated D1 cells showed extremely similar metabolic activity levels at all time-points and at all concentrations compared to cellular behavior on collagen gels without tannic acid cross-linking [101]. The results of this study showed that MCF-7 cell metabolic activity increased when grown on collagen gels cross-linked with 0.1 mg/mL of tannic acid. Metabolic activity of MCF-7 cells did not decrease until they were cultured on gels cross-linked with 1.0 mg/ mL [101]. D1 cells were unaffected by any of the cross-linking concentrations for the first 24 hours of culture. However, after

48 hours, D1 cells on all cross-linked concentrations showed a significant decrease in metabolic activity [101].

Studies further showed that, as the concentration of the tannic acid solution used for cross-linking increased, the level of triglycerides and lipid production decreased, suggesting that the tannic acid prevents the D1 cells from differentiating [101]. However, it was suggested that this differentiation inhibition could be used as a tool to ensure that any stem-like cells implanted using this type of scaffold would be allowed to differentiate only at a specific time, thus ensuring the maximal success of the implant [101].

Synthesis

When considered in sum, the many relevant publications in the literature suggest that the approaches to treatment and reconstruction for breast cancer fall in one or more of three categories: therapeutic, cosmetic, and functional, with the ideal approach combining all three.

Treatments that are considered therapeutic are those that are specifically designed to neutralize the cancerous cells. Often, these therapies result in the destruction of neighboring cells or a radical change in the overall physique of the patient. While these types of therapies have negative side effects, they are more focused on the neutralization of the cancerous cells. Some treatments that fall exclusively in this category include mastectomy as well as radiation and chemo therapies. Mastectomies neutralize the cancerous cells but also result in the removal of the entire breast. Radiation and chemo therapies also have a positive result against cancerous cells but have a negative effect on normal, noncancerous cells.

Cosmetic therapies are those therapies that are designed to minimize or undo the physical changes a patient may undergo after treatment. Typically, these therapies follow a mastectomy procedure and target reconstruction of the breast mound. These therapies include muscle flaps, artificial implants, and tissue expanders, and restore only the physical appearance of breast tissue but none of the functions of the breast.

Functional therapies are a relatively new alternative and thus there are very few currently in use. Therapies that are found in this category are those that are capable of replacing the functionality of the breast tissue lost from breast cancer. Currently, there is only one type of therapy that falls exclusively in this category, tissue engineering. However, tissue engineering approaches have not yet moved out of the laboratory and are currently not being used in human patients.

It is also important to note that these three categories are not exclusive and there is a number of therapies that are found in more than one category. Two examples of these types of therapies include lumpectomies and the use of scaffolds that have incorporated therapeutic agents within them. A lumpectomy is able to fall within both the therapeutic category and the cosmetic category because, like a mastectomy, a lumpectomy effectively removes the cancerous mass from the breast, but leaves the overall shape of the breast relatively unaffected. Scaffolds with incorporated therapeutic agents can fall in both the therapeutic category, because of the additives included within the scaffold itself, and the functional category, because the concept behind the use of a scaffold is to grow functional tissue to replace tissue that was lost due to the cancer.

While some therapies are classified in two categories, none of the therapies are classified in all three. The ideal therapy is one that is effective in neutralizing the cancerous tissue without severely altering the overall appearance of the patient and

providing replacement tissue that could resume the lost functions of the breast tissue. Therefore, the ideal therapy would be classified in all three categories. Very few studies reported in the literature show an equal focus on all three of these classifications, i.e. there is a significant gap in the current research to achieve such an end.

The goal of this work was to develop a scaffold that would fill the void where all three criteria intersect. This scaffold would be cosmetic in that it will fill the void created by the lumpectomy and provide a reconstructive option for lumpectomy patients. The scaffold would also be therapeutic in that it would be made with TA incorporated into it. As the scaffold is remodeled, the TA will be released into the surrounding tissue and negate any of the cancerous cells that may have been missed during the lumpectomy procedure, resulting in a reduced risk of recurrence. And finally, the scaffold would restore functionality in that the void would be filled with living tissue comprised of cells obtained from the patient. These studies will evaluate the functionality of collagen bead scaffolds that have been cross-linked with TA to allow for preadipocyte cells to attach and proliferate on while, at the same time, increase the incidence of apoptosis amongst cancerous cells.

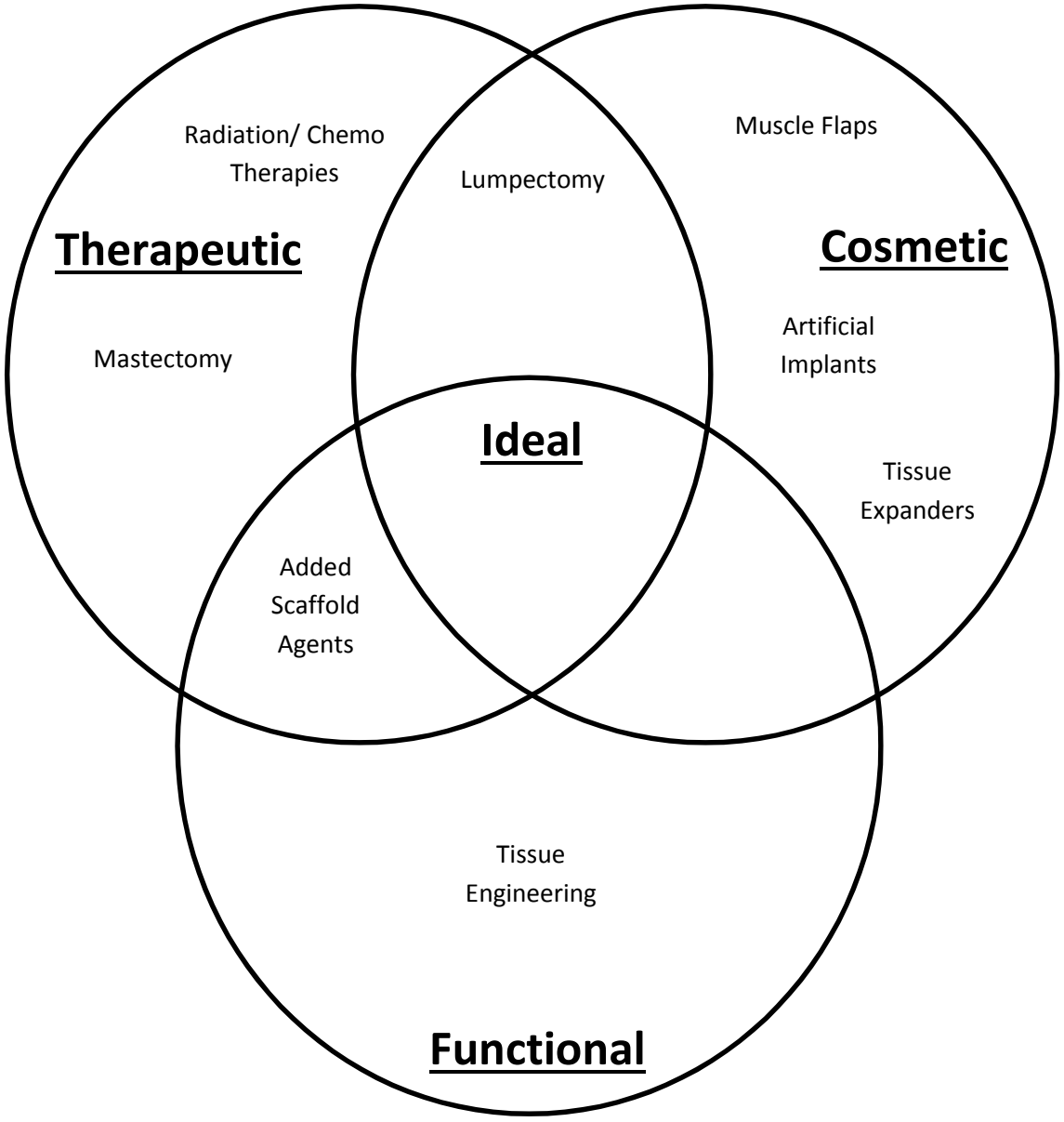

Figure 1.7: *Synthesis Venn Diagram*

CHAPTER 2

BEAD DEVELOPMENT AND CHARACTERIZATION

2.1 Background

One of the overall objectives of this research was to develop a scaffold that was injectable. It order to do this, it was conceived that beads would provide the needed injectable quality desired. A solution containing these beads could be loaded into a syringe and then injected into the lumpectomy void site. Previous studies had developed collagen scaffolds cross-linked with TA but these were in sheet form and would not fulfill the purpose intended for this research. Therefore, a new method for the production of the collagen beads needed to be developed.

2.2 Materials and Methods

Bead Development

Collagen beads were developed using an adapted procedure from Tebb and coworkers [102]. All procedures were conducted in a biologic safety hood using sterile technique. All solutions were either prepared using sterile components or the prepared solution was sterile filtered using a 0.22 μm filter (Corning; Corning, NY) under vacuum.

The procedure started by making a 1.0 mg/ mL type I bovine collagen solution (PureCol; Advanced BioMatrix; San Diego, CA) using the method outlined by Vernon and coworkers [103]. Briefly, the final volume of collagen solution was calculated and divided by the concentration of the stock collagen solution. This amount was the working volume of the stock collagen solution. The working volume of collagen was then multiplied by 0.111 to determine the amount of 10x Dulbecco's Phosphate Buffered

Saline Solution (10x DPBS) (Sigma Aldrich; St. Louis, MO) needed. The final volume of collagen solution was divided by ten to determine the amount of fetal bovine serum (FBS) (Corning; Manassas, VA) needed. The volumes of the working stock collagen solution, the 10x DPBS, and the FBS were added together and then subtracted from the final volume of the collagen solution to determine the needed amount of serum-free Dulbecco's Modified Eagle's Medium (DMEM). Once all these volumes were combined, 1 N sodium hydroxide (NaOH) (Sigma Aldrich; St. Louis, MO) was added until the solution reached a neutral pH. A neutral pH was determined by a distinct color change in the overall collagen solution caused by the presence of phenol red in the serum-free DMEM. Table 2.1 shows an example calculation of this procedure, using a 3.0 mg/mL stock collagen solution to make 6.0 mL of a 1.0 mg/mL collagen solution. This volume was consistently used to make a single batch of beads.

Table 2.1: *Collagen Solution Procedure*

Solution	Amount
Working Collagen Solution (3.0 mg/mL)	6.0 / 3.0 = **2.0 mL**
10x DPBS	0.111 x 2.0 mL = **0.222 mL**
FBS	6.0 mL / 10 = **0.6 mL**
Serum free DMEM	6.0 – (2.0 + 0.222 + 0.6) = **3.178 mL**
1N NaOH	Enough to Neutralize pH (**~20 µL/ batch**)

The next solution made was a sterile 1.4% m/v alginate solution (Sigma Aldrich; St. Louis, MO) using deionized water filtered through a MilliQ system (Millipore Direct 8; Darmstadt, Germany). A ratio of 60:40 collagen to alginate was used to produce the beads. Using the previous example of 6 mL of collagen solution, the procedure would require 4 mL of 1.4% alginate. However, the process of sterile filtering alginate caused some loss of the initial volume, so it was necessary to prepare 2 – 3 mL more than that required. The alginate powder was dissolved in the MilliQ water using a stir bar (VWR;

Radnor, PA) and stir plate (Corning; Manassas, VA) set to 6 on a scale to 10 with low heat and covered with parafilm. Once the alginate was fully dissolved, the solution was sterile filtered overnight in a biologic safety hood (SterilGARD III Advance; The Baker Company; Sanford, ME).

Before use, the components of a bead generator (Var V1; Nisco; Zurich Switzerland) were autoclaved. This included the probe, the glassware dish and petri dish, stir bar, silicone tubing (3/32" inner diameter, 5/32" outer diameter), and a 27G blunt tip needle, see figure 2.1. In addition to these, a steel spatula and a stainless steel wire mesh strainer were also autoclaved in autoclave pouches at 121°C for 45 minutes. The electrostatic box, syringe pump (KDS100; KD Scientific; Holliston, MA), and both power cords were sprayed with ethanol, wiped with gauze, and placed inside the biological safety hood. After being sterile filtered, the prepared 1.0 mg/mL collagen solution was combined with the 1.4% alginate solution at a ratio of 60:40 collagen to alginate and loaded into a 20 cc syringe (BD; Franklin Lakes, NJ). The autoclaved components were then arranged as pictured below with the taller glassware dish inside the shorter glassware dish. The stir bar was placed within the taller glassware dish and all three components were placed underneath the holder arm, adjusting the position to ensure that the stir bar was freely able to rotate at 25% rotational speed. The 27 G needle was attached to the tubing and also placed in the holder arm, with the tubing placed within the notch at the top of the electrostatic box. The probe was then placed inside the plastic connector on the holder arm and locked in place with the locking screw with about a quarter of an inch of the probe locked above the plastic connector. A sterile 1.5% calcium chloride ($CaCl_2$) (Fisher Scientific; Fair Lawn, NJ) solution was then loaded into the tall glassware dish until it started overflowing into the short glassware dish. The

holder arm was then lowered by loosening the holder screw until the probe was slightly immersed in the $CaCl_2$ solution. The doors to the electrostatic box were then closed, the 20 cc syringe containing the collagen/ alginate solution was connected to the tubing and loaded into the syringe pump. The syringe pump was set to flow at a speed of 10.0 mL/hr and the beads were allowed to drop into the 1.5% $CaCl_2$ solution with the electrostatic box set to 6.0 kV.

After the initial formation of the beads, they were removed from the 1.5% $CaCl_2$ solution using the mesh strainer and then transferred to a cross-linking solution made of 100 mL of MilliQ water, tannic acid (Sigma Aldrich; St. Louis, MO), and enough 10 N NaOH to produce a neutral pH. Table 2.2 below summarizes the cross-linking solutions used for this procedure. The beads were kept in the cross-linking solution overnight while on a shaker plate set to 130 RPM (VWR Microplate Shaker; VWR; Radnor, PA). The mesh strainer and metal spatula were autoclaved after the beads were transferred. After remaining overnight in the cross-linking solution, the beads were removed and placed in a 50 mM sodium citrate solution for 3 hours on a shaker plate in order to remove the alginate. After 3 hours, the beads were removed, rinsed well with phosphate buffered saline (PBS) (Sigma Aldrich; St. Louis, MO), and stored at 20 °C in a 50 mL centrifuge tube with enough PBS to cover them. This method produced beads with an average diameter of 1.2 mm.

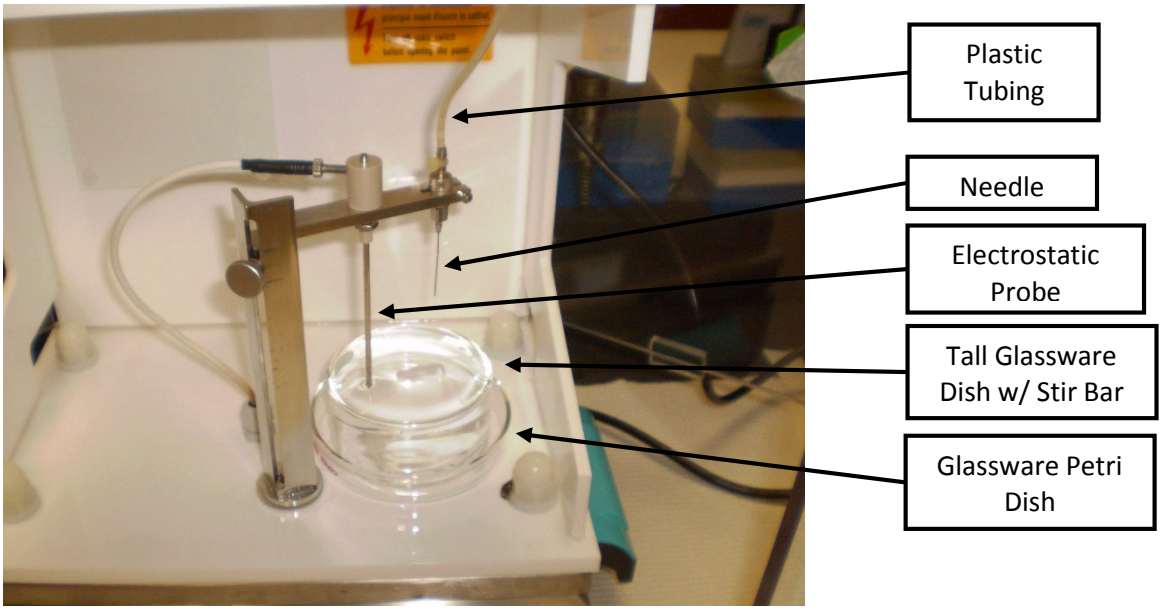

Figure 2.1: *Electrostatic Bead Generator Setup*

Table 2.2: *Cross-linking Solutions*

Cross-linking Solution	Tannic Acid (g)	10 N NaOH (mL)
0.1% Tannic Acid	0.1	0.018
1.0 % Tannic Acid	1.0	0.180
10.0% Tannic Acid	10.0	1.800

Thermal Denaturation

To determine the degree of cross-linking, the developed beads underwent a thermal denaturation study. Thermal denaturation was studied because of the direct correlation between denaturation temperature and the degree of collagen cross-linking: i.e., the higher the denaturation temperature, the greater the degree of collagen cross-linking. For this procedure, a sample of beads from each of the three different cross-linking solutions was dyed overnight using green food coloring, to allow better visualization, and was then washed to remove any excess dye. Next, a 100 mL beaker was placed on a hot plate (Corning PC-200; Corning; Manassas, VA) and filled with 25 mL of deionized (DI) water. A thermometer was placed in the DI water to monitor the

temperature. For the procedure, a single bead was placed in the DI water and the hot plate was turned on. The bead was monitored until shrinkage took place, at which point the temperature of the DI water was recorded.

Histological Evaluation

Once the beads were developed, it was important to determine the internal structure as well as ensure that the alginate was completely removed, leaving only collagen present. To perform this evaluation, finished beads were put into Z-Fix (Anatech LTD; Battle Creek, MI), a fixative solution, overnight to completely fix the beads. The fixed beads were then put into a tissue processor (Sakura Tissue-Tek VIP E150/300; Southeast Pathology; Charleston, SC) for 3 hrs to remove any remaining water within the beads using a series of washes with ethanol, formalin, and xylenes and infuse the entire bead structure with paraffin wax. After processing, the beads were embedded in paraffin and allowed to harden overnight on an embedding center (Sakura Tissue-Tek 4710; Southeast Pathology; Charleston, SC). The next day, the paraffin block was sectioned into 5 μm sections using a manual microtome (Microm H320; Southeast Pathology; Charleston, SC) until bead sections could be seen. These bead sections were then collected on a glass slide (Platinum Line; Mercedes Medical; Sarasota, FL) and then placed in a drying rack which was then placed into a drying oven (Stabil-Therm Gravity Oven; Blue M.; Blue Island, IL) overnight. The drying oven removed the majority of the paraffin from the collected samples. Once drying was completed, the collected slides were ready for staining.

The first stain that was performed was the hematoxylin and eosin (H&E) stain (Poly Scientific; Bay Shore, NY). This stain was performed using a series of washes

involving ethanol, DI water, xylenes, clarifying agents, blueing agent, and the two dyes to show the internal structure of the beads and determine if the beads were porous.

The second stain performed was a Masson's Trichrome stain (Poly Scientific; Bay Shore, NY). This stain was done to verify that the beads are comprise only collagen. Masson's Trichrome is commonly used to distinguish between different connective tissue types, staining muscle fibers red, collagen and bone a blue or green, cytoplasm pink, and cell nuclei a black color.

Storage Standard Operating Procedure (SOP)

It was important to determine if there was a significant amount of TA eluting from the beads during the period of storage in PBS, in order to ensure that the beads would have the same concentration of TA contained within if they were used 1 day or 5 days after being made.

For this study collagen beads cross-linked with 0.1%, 1.0%, and 10.0% TA were developed and then placed in PBS and stored in the refrigerator. A 0.5 mL sample of the storage PBS was collected every 24 hrs over a 2-week period. The 1.0% TA beads were made 24 hrs before the 0.1% and the 10.0% TA beads and, therefore, have 14 data points, whereas the 0.1% and the 10.0% TA beads have 13 data points.

At the end of the 2-week time period, the collected samples underwent the modified Folin-Ciocalteu (F-C) assay, described in further detail in the next chapter. For this assay, standards of 0%, 0.001%, and 0.002% TA were prepared using PBS. Due to the lack of phenol red within the collected samples, further dilution of the samples was not needed. Solutions of 10% F-C reagent (Sigma Aldrich; St. Louis, MO) and 700 mM sodium carbonate (Fisher Scientific; Fair Lawn, NJ) were prepared. A 100 µL of sample/

standard was added into 1.5 mL microtubes (VWR; Radnor, PA) with 200 µL of 10% F-C reagent solution and 800 µL of 700 mM sodium carbonate. However, after the addition of the sodium carbonate to the samples collected from the 10.0% TA beads, it became apparent that the color was saturated. Therefore, the original samples were further diluted by 1/10th their original concentration and these new samples were then treated with the F-C assay and analysis, using new 10% F-C reagent and sodium carbonate solutions. The standards were re-run with the new solutions to ensure continuity between the 10.0% samples being measured and the standards being used.

After briefly vortexing the microtubes using an analog vortex mixer (VWR, Radnor, PA) to ensure adequate mixing had occurred, the tubes were incubated for 2 hrs at room temperature. After the incubation period, 200 µL of the resulting mixture was loaded in triplicate into black-side, clear-bottom, 96-well plates (Greiner Bio One; Monroe, NC) and the absorbance was read at 765 nm using a multi-mode microplate reader (Synergy™ Mx; Biotek; Winooski, VT). Using Microsoft Excel, the absorbance values for the standards were plotted against their known concentrations and a linear trend line was fit to the data. The trend line equation was then used to calculate the %TA concentrations of the unknown samples. The ANOVA test was performed for statistical analysis on the obtained concentration values to determine if there was statistical significance between the readings ($p<0.05$).

Quantification of TA Incorporated into the Beads

This study was done to evaluate the amount of TA that was being incorporated into the beads during the cross-linking process. For this study, 0.1%, 1.0%, and 10.0% TA cross-linking solutions were prepared and three 1.0 mL samples were taken of each

solution before the introduction of the collagen/ alginate beads and were labeled as the "before" samples. Once these samples were collected, collagen/ alginate beads were introduced to the cross-linking solutions and then placed on the shaker plate at 130 rpm overnight. After reacting overnight, three samples of each cross-linking solution were collected and were labeled as the "after" samples.

After the collection of the samples, a blank, 1.0%, 2.0%, and 3.0% TA standards were created along with a 700 mM sodium carbonate solution and a 10% F-C reagent solution. All the collected samples and standard solutions were then diluted with DI water till the expected concentration was within the 0.01 magnitude, for example the 10.0% before and after samples were diluted by $1/10^{th}$ three times. These diluted samples and standards then underwent the F-C assay using the prepared F-C reagent and sodium carbonate solutions. Into 1.5 mL microtubes was added 100 µL of the collected samples or the standards, 200 µL of the 10% F-C reagent, and 800 µL of the sodium carbonate solution. These were then vortexed for a few seconds and allowed to incubate at room temperature for 2 hrs. After the incubation period, 200 µL of the resulting mixture was loaded in triplicate into black-side, clear-bottom, 96-well plates and the absorbance was read at 765 nm using a multi-mode microplate reader. Using Microsoft Excel, the absorbance values for the standards were plotted against their known concentrations and a linear trend line was fit to the data. The trend line equation was then used to calculate the %TA concentrations of the average "before" and "after" absorbance values. The concentration of TA contained within the beads was calculated by subtracting the average concentration of the "after" samples from the average concentration of the "before" samples. To account for the dilutions that were performed,

the resulting value for the 10.0% TA solution was multiplied by 10 and the value for the 0.1% TA solution was divided by 10.

2.3 Results

Thermal Denaturation

For this study, five beads from each TA concentration were tested and their denaturation temperatures are shown below in Table 2.3.

Table 2.3: *Thermal Denaturation Temperatures*

Sample	0.1% TA Beads	1.0% TA Beads	10.0% TA Beads
1	59 °C	61 °C	63 °C
2	60 °C	62°C	65 °C
3	58 °C	63 °C	65 °C
4	59 °C	60 °C	61 °C
5	56 °C	60 °C	65 °C
Average	58.4 ± 1.52°C	61.2 ± 1.30°C	63.8 ± 1.79°C

Histology

Figure 2.2 reveals that there are several pores throughout the entire structure of the bead. Figure 2.3 shows that the entirety of the bead stains a blue color which corresponds to the bead being composed of collagen.

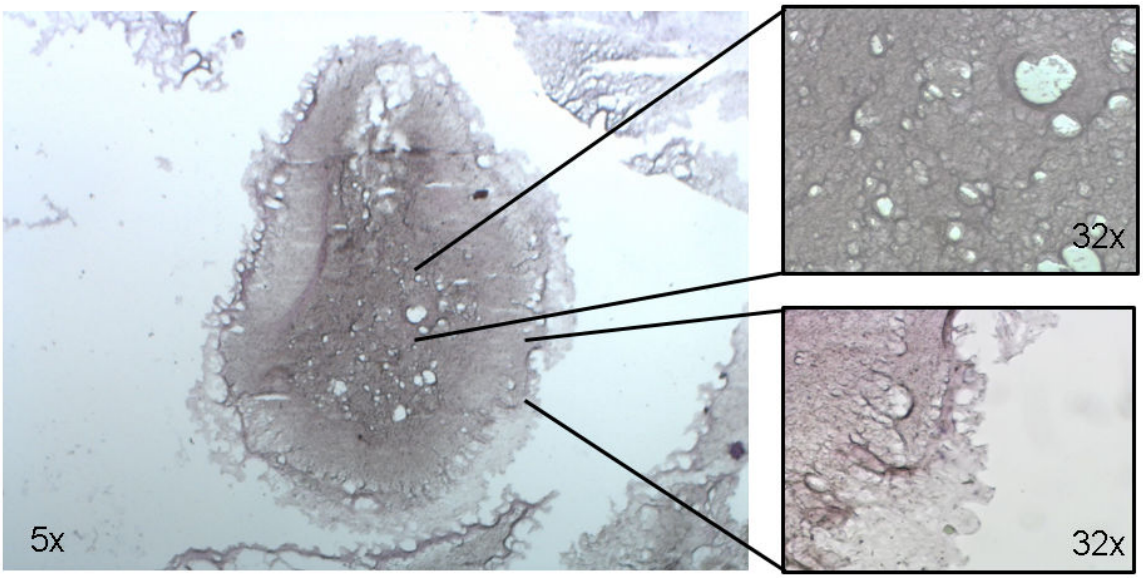

Figure 2.2: *H&E Stain*

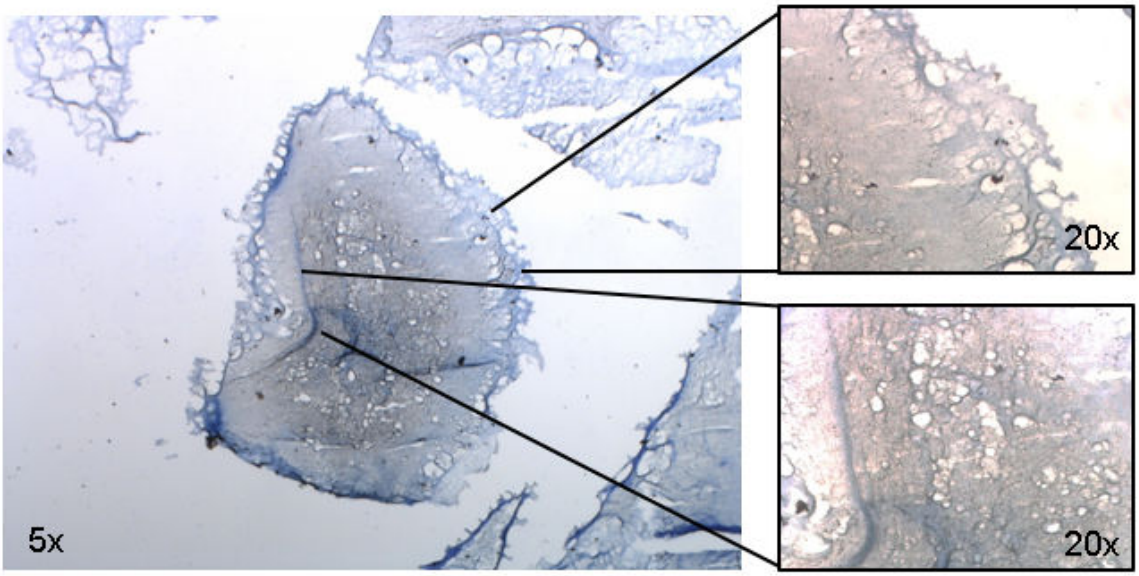

Figure 2.3: *Masson's Trichrome Stain*

Storage Standard Operating Procedure (SOP)

Below are the TA concentrations of the storage PBS samples which are graphed in figure 2.4. These values were obtained by using the standard equations developed from the graphs of the standards seen in figure 2.5.

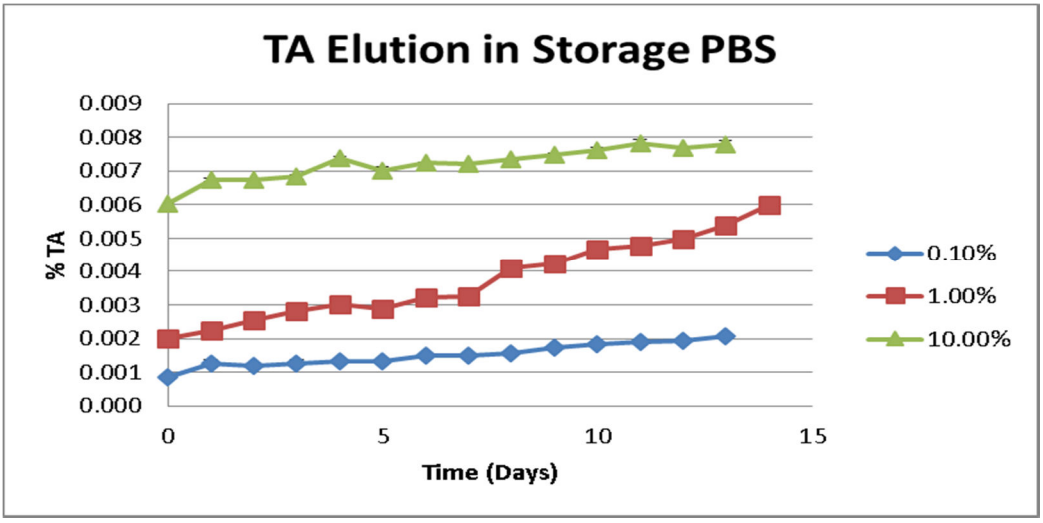

Figure 2.4: *TA Elution Measurements for Storage PBS*

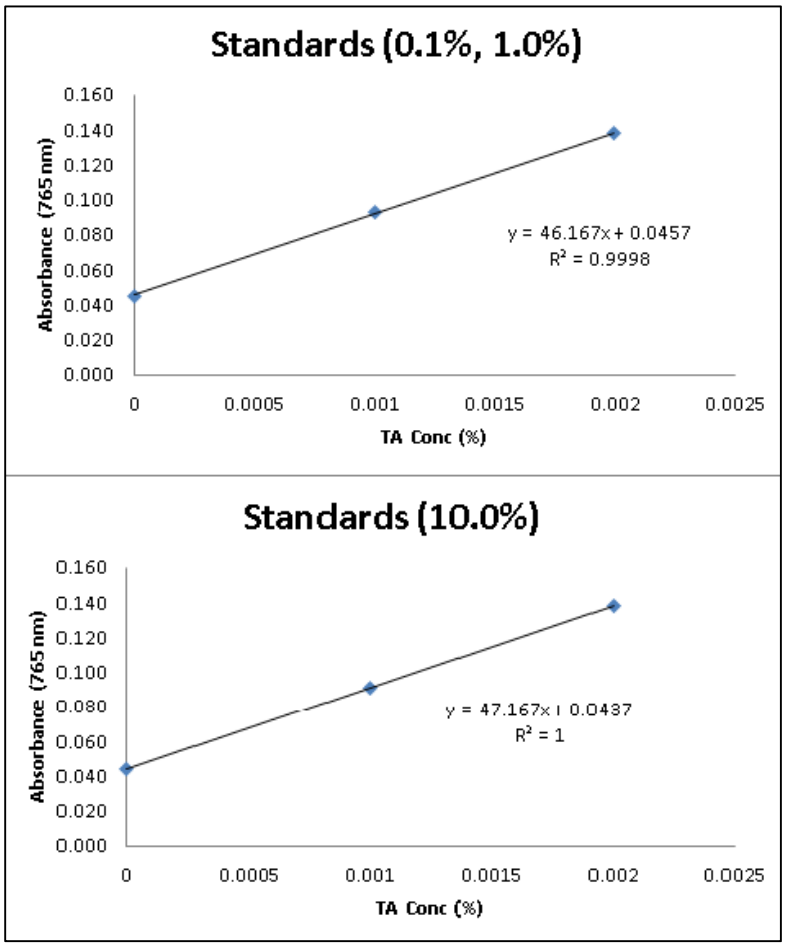

Figure 2.5: *Standard Measurements for Storage SOP*

Quantification of TA Incorporated into the Beads

Below are the TA concentrations of the "before" and "after" samples, their differences, and their corrected values which are shown in table 2.4. These values were obtained by using the standard equations developed from the graphs of the standards seen in figure 2.6.

Table 2.4: TA Concentrations of "Before" and "After" Samples

	0.1% Before	0.1% After	1.0% Before	1.0% After	10.0% Before	10.0% After
Sample Absorbance Values	0.420	0.349	0.483	0.475	0.436	0.441
	0.416	0.350	0.472	0.466	0.442	0.435
	0.418	0.348	0.483	0.469	0.438	0.443
Average Absorbance	0.418	0.349	0.479	0.470	0.439	0.440
Calculated Concentration (%)	1.010	0.760	1.220	1.190	1.080	1.090
Corrected Concentration (%)	0.101	0.076	1.220	1.190	10.800	10.900
Difference (%)	0.025		0.030		-0.100	

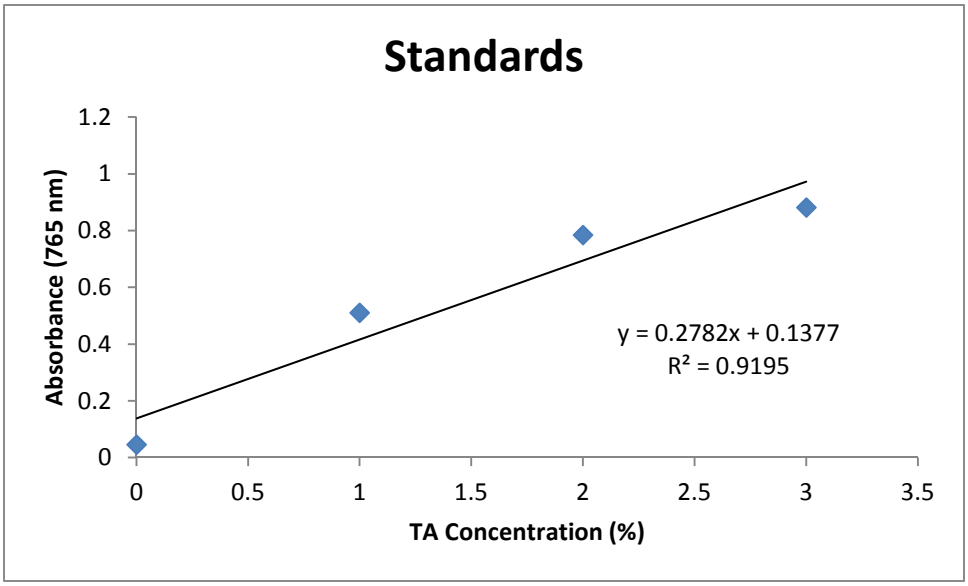

Figure 2.6: *Standard Measurements for Bead TA Quantification*

2.4 Discussion and Conclusions

Thermal Denaturation

Based on statistical analysis using ANOVA with $p<0.05$, the denaturation temperature for the beads cross-linked with 0.1% TA was found to be statistically significantly different from that of the 1.0% TA beads and the 10.0% TA beads. However, the denaturation temperatures of the 1.0% TA beads and the 10.0% TA beads were not statistically different from each other.

Histology

The pink coloration of the H&E stained cross-section is what was expected from the staining procedure. Alginate, if it had been present, would have been stained by a dark blue color; the absence of this color suggests the absence of alginate within the bead structure.

Based on the blue/ green coloration seen in the Masson's Trichrome stain throughout the bead, it can be concluded that the bead is composed of collagen, with no visual evidence of any other material type.

Storage Standard Operating Procedure (SOP)

The results of this study showed that the starting TA concentrations in the PBS storage solutions and the final concentrations after 2 weeks of storage were statistically different. However, the measured difference was so small between the start and end points that the scientific significance of the difference was negligible. Therefore, it was determined that the beads should be used within 2 weeks of manufacture to ensure consistency of the TA bead concentration. This conclusion enabled the comparison of

results between studies when examining the overall effects of the beads on the different cell types.

Quantification of TA Incorporated into the Beads

The results of this study show that there is not a huge difference in bead TA concentration as higher concentrations of TA were used for cross-linking. However, this experimentation may need to be revised due to the different dilutions used for the different concentrations. When these dilutions were corrected for in the calculations, the error associated with the calculated value could have been magnified which could account for the negative value obtained with the 10% TA cross-linked beads.

CHAPTER 3

FOLIN-CIOCALTEU (F-C) ASSAY MODIFICATION

3.1 Background

A reliable method for the quantification of tannic acid (TA) has been elusive, particularly when the TA is found within a sample of cell culture medium. A way of overcoming this shortfall is through modification of the Folin-Ciocalteu (F-C) assay. The F-C assay works by electron transfer from phenolic compounds to phosphomolybdic/ phosphotungstic acid complexes in an alkaline medium. The complexes that form are blue and are therefore measureable with a spectroscope [104].

3.2 Methods and Results

Modified Methodology Development

It was hypothesized that an additional dilution with deionized water (diH_2O) was needed to overcome the reactivity of the medium to the reagents of the F-C assay. To test this hypothesis, a modified method of the F-C assay was implemented. Standards of 1% and 2% m/v TA solutions (Sigma Aldrich; St. Louis, MO) were prepared with Dulbecco's Modified Eagle's Medium (DMEM) (Atlanta Biologicals; Flowery Branch, GA). A blank of DMEM alone was used as the 0% TA standard. A test solution was also prepared at a concentration of 1.682% m/v TA in DMEM. The standard solutions as well as the variable solution were diluted with 1:10 serial dilutions in DMEM till their final concentrations were $1/1000^{th}$ of their original.

The diluted standards and test solution then underwent four different dilutions with diH_2O; 90:10, 75:25, 50:50, and 0:100 diH_2O: TA solution. Folin-Ciocalteu's (F-C)

phenol reagent was purchased from Sigma-Aldrich (St. Louis, MO) and sodium carbonate was purchased from Fisher Scientific (Pittsburgh, PA). A multi-mode Synergy™ Mx microplate reader was used for this assay (BioTek; Winooski, VT). A volume of 100 µL of the final dilutions was transferred into micro centrifuge tubes (VWR; Radnor, PA). A 10% v/v F-C reagent solution was prepared using diH_2O. A volume of 200 µL of the prepared F-C reagent was added to each micro centrifuge tube and each tube was briefly vortexed (VWR Analog Vortex Mixer; Radnor, PA); 800 µL of a prepared 700 mM sodium carbonate solution was then added to each tube. The micro centrifuge tubes were allowed to incubate at room temperature for 2 hours, after which they were vortexed and 200 µL transferred from each tube to a clear bottom, black-side 96-well plate, in triplicate. The absorbance of the solutions was measured at 765 nm with the multi-mode microplate reader.

Modified Methodology Results

The absorbance values for the standard solutions were used to develop an equation to calculate the TA concentration of the test solution. Both the R^2 of the standard equation and the closeness of the calculated test concentration to its actual concentration were used to determine the best dilution method, see Table 3.1. The results indicate the 75:25 dilution had the closest linear relationship between standards, with R^2=0.9914, but the calculated TA concentration of the test solution was the farthest from the actual concentration. To further test these results, a second trial was performed using only the 75:25 dilution. The second test solution had a concentration of 1.59% TA and the same procedure was followed as before. The results of the second trial resulted in an R^2 of 0.9835 and a calculated concentration of 1.63%. These results

suggest that the 75:25 dilution method is best suited to prevent the color saturation caused by culture medium, while preserving enough sensitivity to TA concentrations to give accurate measurements.

Table 3.1: *R^2 and calculated TA concentrations of the different dilution methods. Actual TA concentration is 1.682% TA.*

Dilution (diH_2O:TA Sample)	R^2	Calculated %TA
90:10	0.9357	1.31 %
75:25	0.9914	2.09 %
50:50	0.9574	1.02 %
0:100	0.9122	1.89 %

Example Experiment Implementation Methods

An experiment was designed to measure the amount of TA that elutes from tannic acid cross-linked beads into surrounding Dulbecco's Modified Eagle Medium: F12 (DMEM: F12) (ATCC; Manassas, VA). A volume of 20 mL of porous collagen beads was developed; the beads were approximately 1-mm in diameter and cross-linked with TA purchased from Sigma-Aldrich (St. Louis, MO). The TA concentrations of the cross-linking solutions were 0.1%, 1.0%, and 10% TA m/v. Approximately 0.2 mL of beads were placed into nine transwell inserts, three inserts per bead type, of a 12-well plate with DMEM: F12. The remaining three wells did not contain any beads and served as a negative control group. Samples of the DMEM: F12 were collected once every 24 hours for a 72-hour period.

Standard solutions of 1%, 5%, and 10% m/v of TA were prepared with DMEM: F12. Serial 1:10 dilutions of these standard solutions were performed with DMEM: F12 until the final concentrations were 1/1000th the original concentration. These dilutions

were necessary to obtain standards with concentrations in the same order of magnitude as the concentrations of the unknown samples. The order of magnitude of the sample solutions was determined through trial and error. A "blank" of DMEM: F12 was designated the 0% TA solution standard. These diluted 1%, 5%, and 10% TA solutions as well as the blank 0% TA solution are termed the standard solutions.

Example Experiment Results

The same 75:25 dilution methodology as described previously was used. A standard curve was developed using the averages of the readings from the diluted standard solutions. Using Microsoft Excel, a linear trend line was fit to these data points to generate an equation that could be used to calculate the TA concentrations, see Figure 3.1. The linear equation was used to calculate the concentration of TA within each unknown sample.

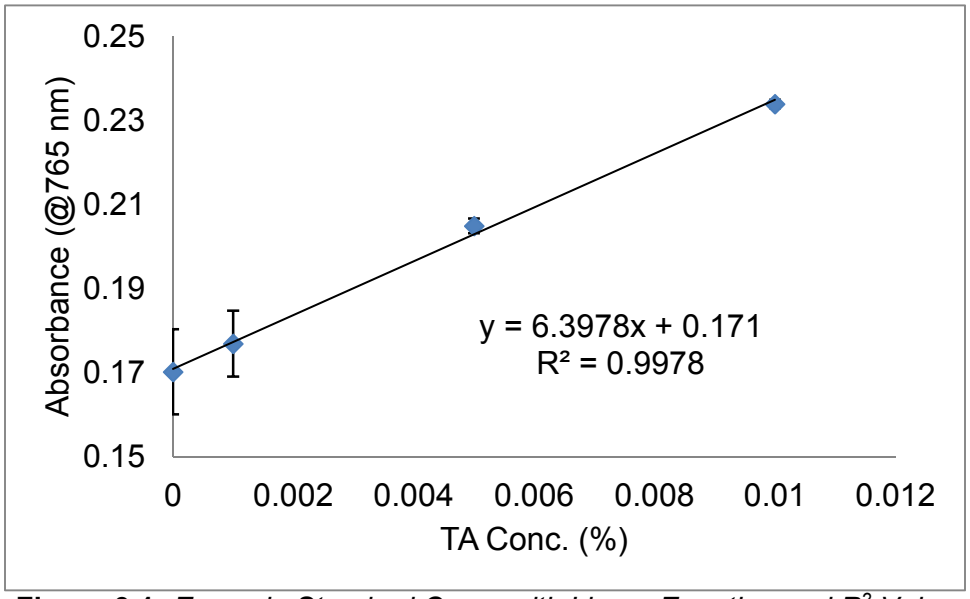

Figure 3.1: *Example Standard Curve with Linear Equation and R^2 Value*

3.3 Discussion

Standard preparation should be determined using a trial-and-error type experimental set up. It is important that the standard solutions are on the same order of magnitude in TA concentration as the unknown samples, to provide the most accurate results. If the unknown sample is a concentration two orders of magnitude below the diluted 1% TA standard, or the measured TA concentration is close to the 0% standard measurement, it is recommended that all standards be diluted another order of magnitude and the assay conducted again to ensure that the results are accurate.

It is important to understand the reasons behind the dilution methodology as well as the assay methodology. The DI water dilution is performed because the DMEM: F12 reacts with the chemicals in the assay and can cause a color change. If the dilution is not performed, the samples will be oversaturated, resulting in identical absorbance readings for all samples. By performing the dilution with DI water, oversaturation is avoided and accurate readings can be obtained. The color change caused by DMEM: F12 alone is accounted for in the 0% standard solution. It is also important that the sodium carbonate is added after the F-C reagent solution in order to prevent the phenols from undergoing air-oxidation and reducing the accuracy of the assay results [104].

3.4 Conclusions

This method works well in measuring the concentration of TA within samples of DMEM: F12. The assay is sensitive enough to measure very small concentrations of TA within a given sample and reliably provide quantifiable results. The method also takes into account the color change that occurs due to the presence of medium, making the results more accurately reflect the actual TA concentration within the sample. While this

modified assay has only been performed using DMEM and DMEM: F12, the methods should be readily translated to systems with other media types.

CHAPTER 4

EVALUATION OF THE EFFECTS OF TANNIC ACID CROSS-LINKED COLLAGEN BEADS ON CANCEROUS CELLS IN TWO-DIMENSIONAL (2-D) CULTURE USING TRANSWELL INSERTS

4.1 Background

Once the process for the development of the collagen beads was fully established and the collagen beads characterized, the next step was to determine the efficacy of the bead system as an anti-cancer treatment and as a scaffold. This was a two-step process, with the first step being the examination of the effect the beads alone have on cancerous and noncancerous cells growing distal from the beads. The second step assessed the addition of cells growing on the beads and explored the effectiveness of the beads to function as a scaffold as well as how the addition of cells affected the release kinetics of the tannic acid from the collagen beads.

Transwell inserts were used because of their ability to suspend tannic acid (TA)-cross-linked beads within the medium and allow the diffusion of the TA throughout the medium while preventing the beads from being in direct contact with the cancerous cells. This setup better mimics a 2D model of a lumpectomy site, where the cancerous cells would not be found proximal to the implanted TA cross-linked collagen beads.

The first goal of this study was to simulate how the beads would affect the surrounding tissue within a breast that had cancer cells still present within. MCF-7 cells, immortalized human breast cancer cells, were used in this model as the cancerous cells being targeted for neutralization. As a control for comparison, SW872 cells, human preadipocyte cells that originate from a liposarcoma, were used as the model for normal

preadipocyte cells that are found within normal breast tissue. These cells were used for comparison to ensure that the TA targets, most effectively, the cancerous MCF-7 cells, with minimal negative effects on the SW872 cells. In addition to the variable cell types, collagen beads that have been cross-linked in different concentrations of TA will be compared in order to determine which TA cross-linking concentration is most effective at negating the cancerous cells while minimizing the negative effects on the preadipocyte cells. The concentrations of TA cross-linking solutions selected are based on previous work performed by another lab member [101]. The second goal of this study is to determine the added effect of preadipocytes growing directly on TA beads within the previously mentioned transwell lumpectomy model. The added effect of cells growing directly on the TA beads will alter the elution rate of the TA from the beads, which may alter the apoptotic activity of the cells.

To ensure that the results of this study are reliable, the study was repeated with a second batch of 1.0% TA beads because of the hypothesized duality of the concentration in which it will allow the preadipocytes to survive but also cause apoptosis of the cancerous cells. All materials and methods used were the same for the repeat studies.

4.2 Materials & Methods

Cell Culture

SW872 and MCF-7 cells were obtained from American Type Culture Collection (ATCC; Manassas, VA) and cultured with Dulbecco's Modified Eagle's Medium (DMEM: F12), also purchased from ATCC. The use of DMEM: F12 medium was recommended for use with the SW872 cells and, in order to keep variables consistent, the MCF-7 cells

were also cultured in this medium. The medium was also supplemented with 10% fetal bovine serum (FBS) (Corning, Manassas, VA) as well as 1% antibiotic- antimycotic (AA) (Gibco; Great Island, NY) and 0.2% fungizone (Gibco; Great Island, NY) to help prevent contamination. Both cell types were grown in T-75 cell culture flasks (Corning; Corning, NY) incubated at 37 °C with 5.0% CO_2 (Panasonic MCO-18ACL; Chicago, IL).

Bead Preparation and Cell Seeding

Beads were prepared as previously described and cross-linked by either 0.1%, 1.0%, or 10.0% TA. Two batches of each bead type were made to examine the effect of beads alone on cells and two batches per bead type were made to evaluate how the beads function as a scaffold. Two double batches were made of the 1.0% TA beads for the repeat study, one double batch per study objective.

For the evaluation of the beads to function as a scaffold, 1000 mL roller bottles (Corning; Corning, NY) were treated with Sigmacote (Sigma Aldrich; St. Louis, MO) to prevent cellular attachment to the bottles. The storage phosphate buffered saline (PBS; Sigma Aldrich; St. Louis, MO) was aspirated from the centrifuge tubes in which the beads were stored and replaced with DMEM: F12. The beads were then placed in the roller bottles, one double batch of one bead type per bottle, and the bottles were held on the bottom edge of the roller bottle to allow the beads to collect in one location. Enough medium was then added to just cover the beads within the roller bottles. To the roller bottles was then added 1 mL of an SW872 cell suspension with a concentration of 4.0 x 10^6 cells per mL. The roller bottles were then put in the incubator at 37°C and 5.0% CO_2, still balanced on the bottom edge of the roller bottle, for 1 hr. During that hour, the bottles were removed from the incubator every 20 minutes and shaken slightly to re-

suspend any cells that may have settled on the bottom of the roller bottle and then placed back in the incubator on edge. These steps were executed to allow the cells another opportunity to attach to the beads. At the end of the hour, an additional 40 mL of DMEM: F12 was added to each of the roller bottles and then the bottles were placed in a roller bottle apparatus within an incubator set to 37 °C with 5.0% CO_2. The roller bottles were kept in the roller bottle apparatus (WSR Bot Drive 7"R 5 x 03 Deck; Wheaton; Millville, NJ) for 72 hrs, allowing additional SW872 cell attachment and proliferation on the beads.

Transwell Model Setup

For this experiment, samples were collected every 24 hrs over a 3-day period. With three data collection time points, two different cell types, and two different conditions for the beads, a total of twelve 12-well transwell plates (Costar; Corning, NY) were used for the main study. Additionally, there were four 12-well transwell plates used for the repeat study: two cell types and two different conditions for the beads. A single transwell plate allowed enough room for all three data collection time points. Therefore, a total of sixteen 12-well transwell plates were used for the entire study.

SW872 cells were seeded at 3.0 x 10^5 cells into each of the wells of eight 12-well transwell plates, and the same amount of MCF-7 cells were seeded into each of the wells of the eight remaining 12-well transwell plates. A volume of 1 mL of fresh DMEM: F12 was also added to each well and the transwell plates were placed in the incubator for 72 hrs to allow cell attachment and growth. After 72 hrs, the medium was aspirated from all wells. For all transwell plates, the transwell inserts for the first column were removed and 2.0 mL of fresh DMEM: F12 was added. Transwell inserts were retained in

the other three well columns and 1.5 mL of fresh DMEM: F12 was added. The main study used all three bead types, one per column, with the first column serving as the control group and each transwell plate comprising an individual time point. The repeat study only used 1.0% TA beads so each column was used for an individual time point, with one of the wells in the first column serving as a control for that time point. Diagrammed below is the transwell plate setup for each of the studies. Once the beads were placed in the transwell inserts, 0.5 mL of DMEM: F12 was added to each of the inserts and all transwell plates were placed in the incubator at 37 °C with 5.0% CO_2. Figure 4.2 below shows the final schematic for a transwell setup.

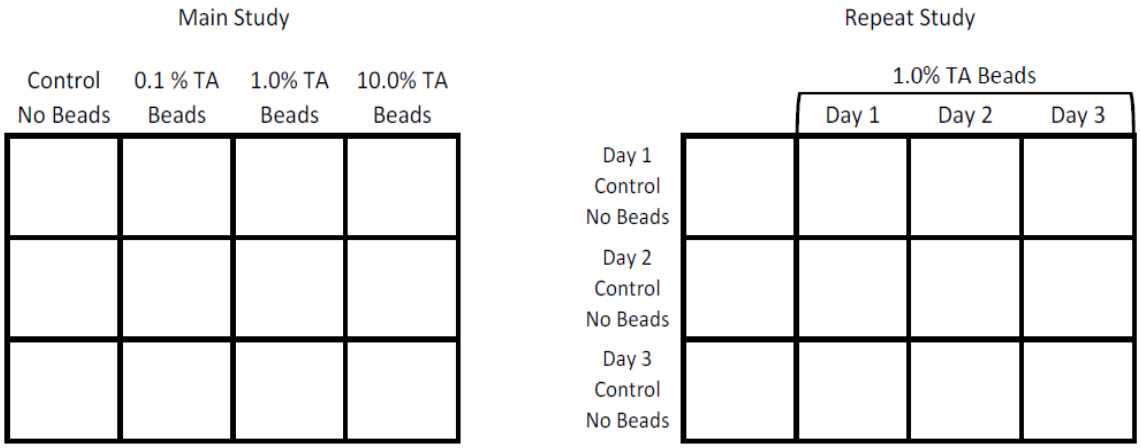

Figure 4.1: *Transwell Plate Setup for the Main Study and Repeat Study*

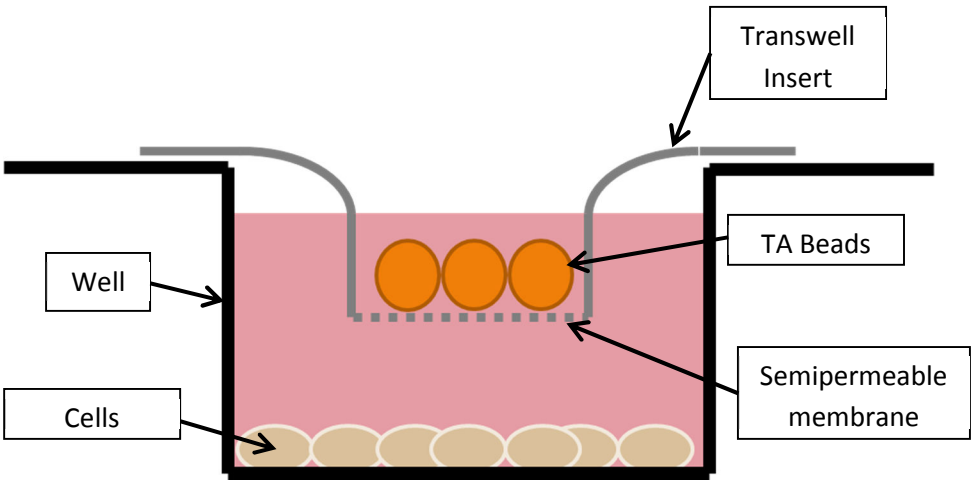

Figure 4.2: *Transwell Schematic*

Sample Collection

Every 24 hrs, for the main study 3-day time period, two SW872 transwell plates and two MCF-7 transwell plates, one plate with seeded beads and one plate with non-seeded beads per cell type, were removed from the incubator. For the transwell plates with seeded beads, the beads were removed from the transwell inserts and collected in a 6-well plate (Costar; Corning, NY). The transwell insert was then discarded. For the transwell plates with non-seeded beads, the transwell insert and the beads were discarded. From each well, 1 mL of medium was collected and stored in the refrigerator. The remaining medium was aspirated and then each well was washed with 1 mL of PBS which was then also aspirated. Subsequently, 1 mL of Z-fix (Anatech LTD; Battle Creek, MI) solution was added to each well to fix the cells that were growing on the bottom of the wells. The well plates were then stacked, wrapped in paraffin, and stored in the refrigerator.

For the repeat study, every 24 hrs, a control well and a single column of wells on each well plate underwent the same procedure as described above. However, after the addition of Z-fix to the wells at the 24 hr and 48 hr time points, the transwell plates were placed back in the incubator instead of in the refrigerator.

The collected beads were analyzed using a Live/ Dead assay (Invitrogen; Eugene, OR) to qualify the cells that were growing on the beads. The collected medium samples were used for the F-C assay to measure the amount of TA that eluted from the beads. The medium samples from the transwell plates with non-seeded beads were also used for biochemical analysis (YSI 2900; YSI Life Sciences; Yellow Springs, OH) to measure glucose and lactate levels and gain an approximation of the metabolic activity of the cells growing on the bottom of the wells. The fixed cells were analyzed using the

TUNEL assay (Abcam; Cambridge, MA) to quantify the amount of apoptotic activity that was occurring.

F-C Assay

To perform this assay, standards of 0.01%, 0.005%, 0.001%, and 0% TA (Sigma Aldrich; St. Louis, MO) were prepared using DMEM: F12. These standards and the collected medium samples were then diluted with MilliQ water (Direct 8; Millipore; Darmstadt, Germany), to prevent color saturation from occurring due to the presence of the DMEM: F12 medium. For each standard and collected medium sample, 25 µL of the medium sample was combined with 75 µL of MilliQ water in a 1.5 mL micro centrifuge tube (VWR; Radnor, PA). After performing the dilution, 200 µL of a 10% Folin-Ciocalteu (F-C) reagent solution (Sigma Aldrich; St. Louis, MO) was added to each micro centrifuge tube followed by 800 µL of a 700 mM sodium carbonate solution (Fisher Scientific; Fair Lawn, NJ). All micro centrifuge tubes were then vortexed for a few seconds (VWR Analog Vortex Mixer; Radnor, PA) and allowed to incubate for 2 hrs at room temperature. At the end of the 2 hrs, the solutions were loaded in triplicate into clear bottom, black side 96-well plates (Greiner Bio One; Monroe, NC) and the absorbance of the solutions was read at 765 nm with a multi-mode micro plate reader (Synergy™ Mx; BioTek; Winooski, VT).

The absorbance readings were loaded into a Microsoft Excel 2013 (Microsoft; Redmond, WA) worksheet, and the absorbance readings of the standards were averaged and graphed against their known concentrations. A linear trend line was fitted to the standard data points, providing an equation to model the relationship between absorbance readings and TA concentration values. This equation was then used to

calculate the TA concentration of the experimental medium samples collected. The calculated TA concentrations were then averaged and graphed.

Minitab 16 (Minitab; State College, PA), a statistics program, was then used to perform the analysis of variance (ANOVA) statistical analysis on the calculated TA concentrations. For statistical analysis, all absorbance readings were first used to calculate all TA concentration values and then these calculated values were averaged to obtain the overall average concentration for each condition.

Biochemical Analysis

Samples of the collected medium from the transwell plates that did not have SW872 cells seeded on the TA cross-linked beads were loaded into a 96-well plate (Costar; Corning, NY) with a sample of fresh DMEM: F12 loaded in between each time point group. The fresh DMEM: F12 provided the baseline for the biochemical analyzer (YSI 2900; YSI Life Sciences, Yellow Springs, OH) as the instrument measure the levels of glucose and lactate in the samples. Once loaded, the 96-well plate was placed in the biochemical analyzer to perform the analysis. The obtained values for each group were averaged.

Live/ Dead Assay

Per individual transwell plate, all beads that were seeded with SW872 cells and cross-linked by the same TA concentration were collected into a single well of a 6-well plate. A Live/ Dead solution (Invitrogen; Eugene, OR) was prepared using calcein-AM, ethidium homodimer-1, and PBS according to the protocol supplied with the assay kit.

The medium was aspirated from the collected beads and enough Live/ Dead solution was added to the wells to cover the beads. The well plates were then placed in a drawer to protect them from light and allowed to incubate at room temperature for 10 minutes. The beads were then examined under fluorescence and pictures were taken using the microscope (Axiovert 40 CFL; Zeiss; Peabody, MA) and attached camera (AxioCam MRc5; Zeiss; Peabody, MA).

TUNEL Assay

After the completion of the 3-day collection time points, the well plates were removed from the refrigerator, the Z-Fix solution was aspirated, and the TUNEL assay was conducted according to the protocol provided in the kit. After the completion of the assay, the plates were imaged under red fluorescence at 488 nm using the microscope. Images were taken at three independent locations per well. At one location, a picture of all the cells was taken as well as a picture of all cells that stained positive for apoptotic activity. The total number of cells and the number of apoptotic cells were counted in each picture set and these two numbers were then used to find the percent apoptosis that was occurring in each location.

Due to a weak green fluorescence captured in the analysis of the wells exposed to beads that had not been seeded with SW872 cells, a different TUNEL assay was used to analyze the plates that had contained seeded beads. The company that supplied the kits verified that the results of both assays would be comparable.

4.3 Results

F-C Assay

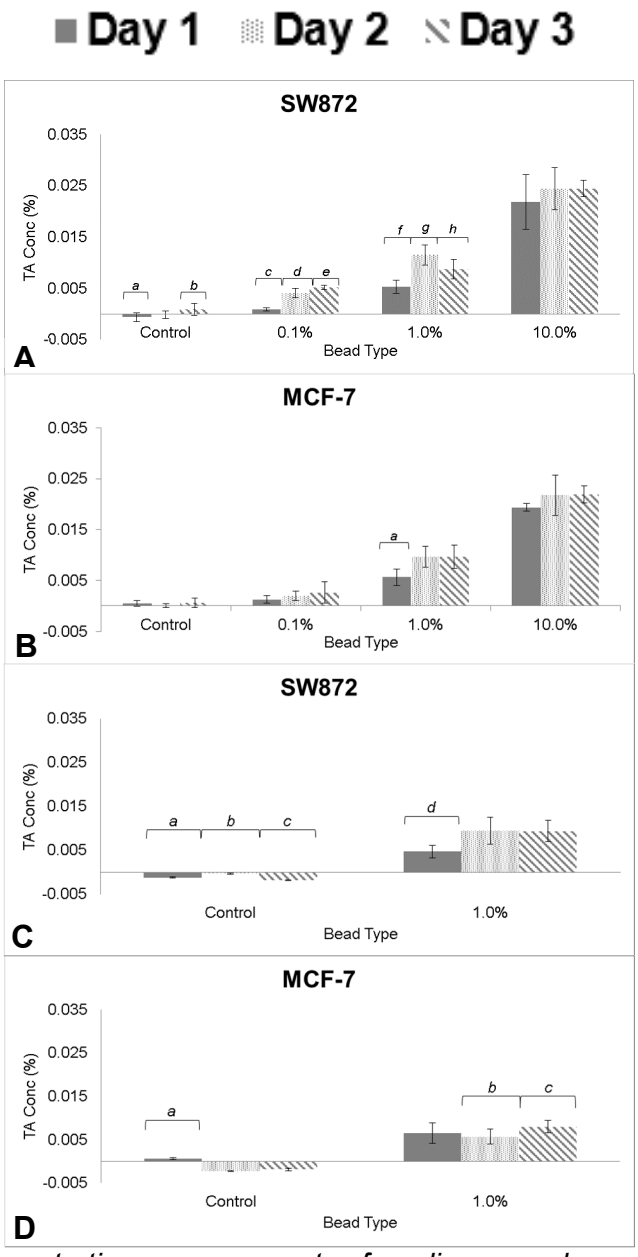

Figure 4.3: *TA concentration measurements of medium samples collected from transwell plates with no cells seeded on the TA cross-linked collagen beads. (A) SW872 transwell plates in the main study. (B) MCF-7 transwell plates in the main study. (C) SW872 transwell plates in the repeat study. (D) MCF-7 transwell plates in the repeat study. Letters signify statistical significant difference (p>0.05) between time points within groups. The controls for the repeat study had n=3, all other time points had n=9.*

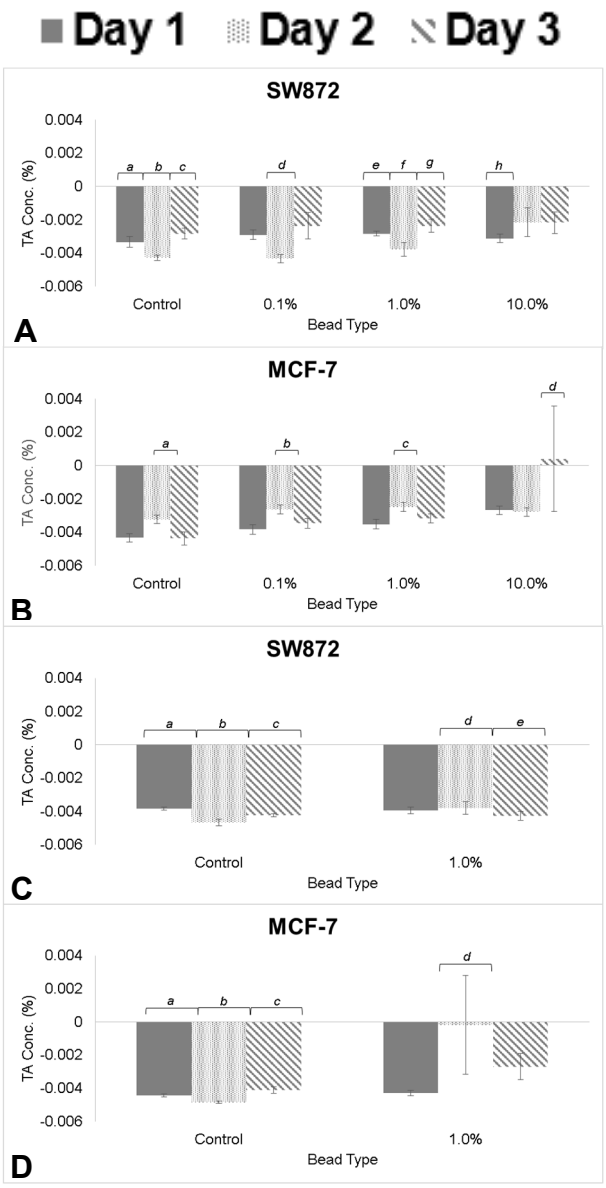

Figure 4.4: *TA concentration measurements of medium samples collected from transwell plates with SW872 cells seeded on the TA cross-linked collagen beads. (A) SW872 transwell plates in the main study. (B) MCF-7 transwell plates in the main study. (C) SW872 transwell plates in the repeat study. (D) MCF-7 transwell plates in the repeat study. Letters signify statistical significant difference (p>0.05) between time points within groups. The controls for the repeat study had n=3, all other time points had n=9.*

Biochemical Analysis – Glucose and Lactate

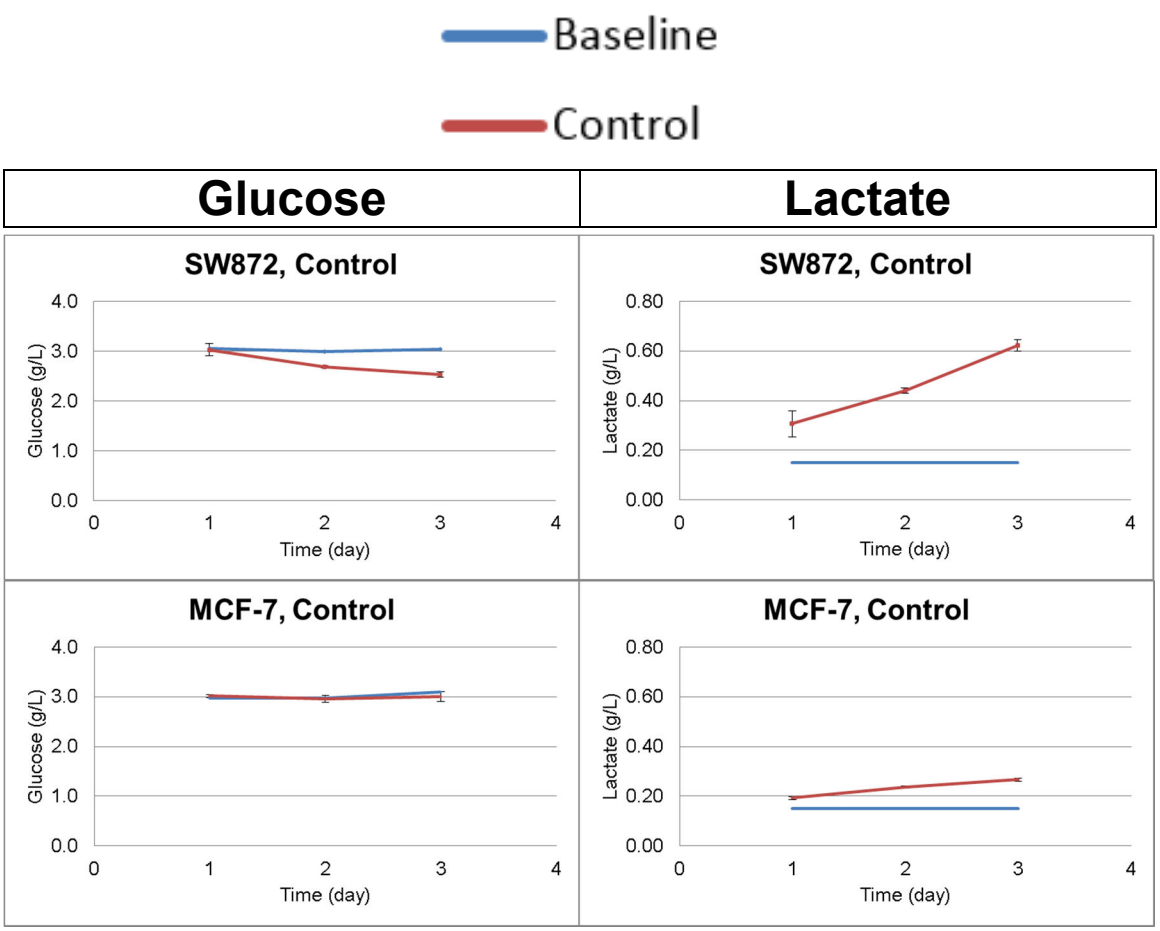

Figure 4.5: *Biochemical analysis of glucose and lactate levels for transwell plates with SW872 cells and MCF-7 cells that were not exposed to beads. Error bars represent the standard error for all data points. Each data point represents a mean average of n=3 per condition and time point.*

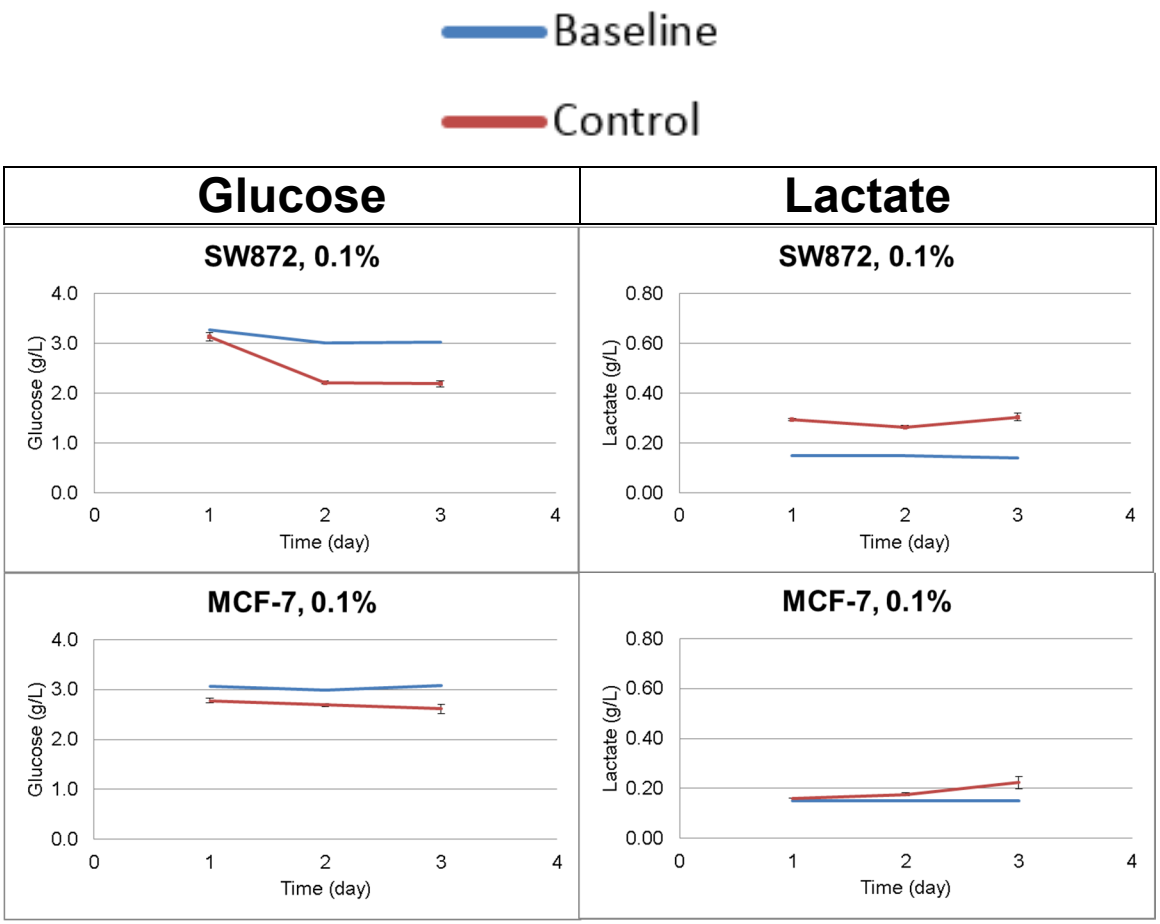

Figure 4.6: *Biochemical analysis of glucose and lactate levels for transwell plates with SW872 cells and MCF-7 cells that were exposed to 0.1% TA beads. Error bars represent the standard error for all data points. Each data point represents a mean average of n=3 per condition and time point.*

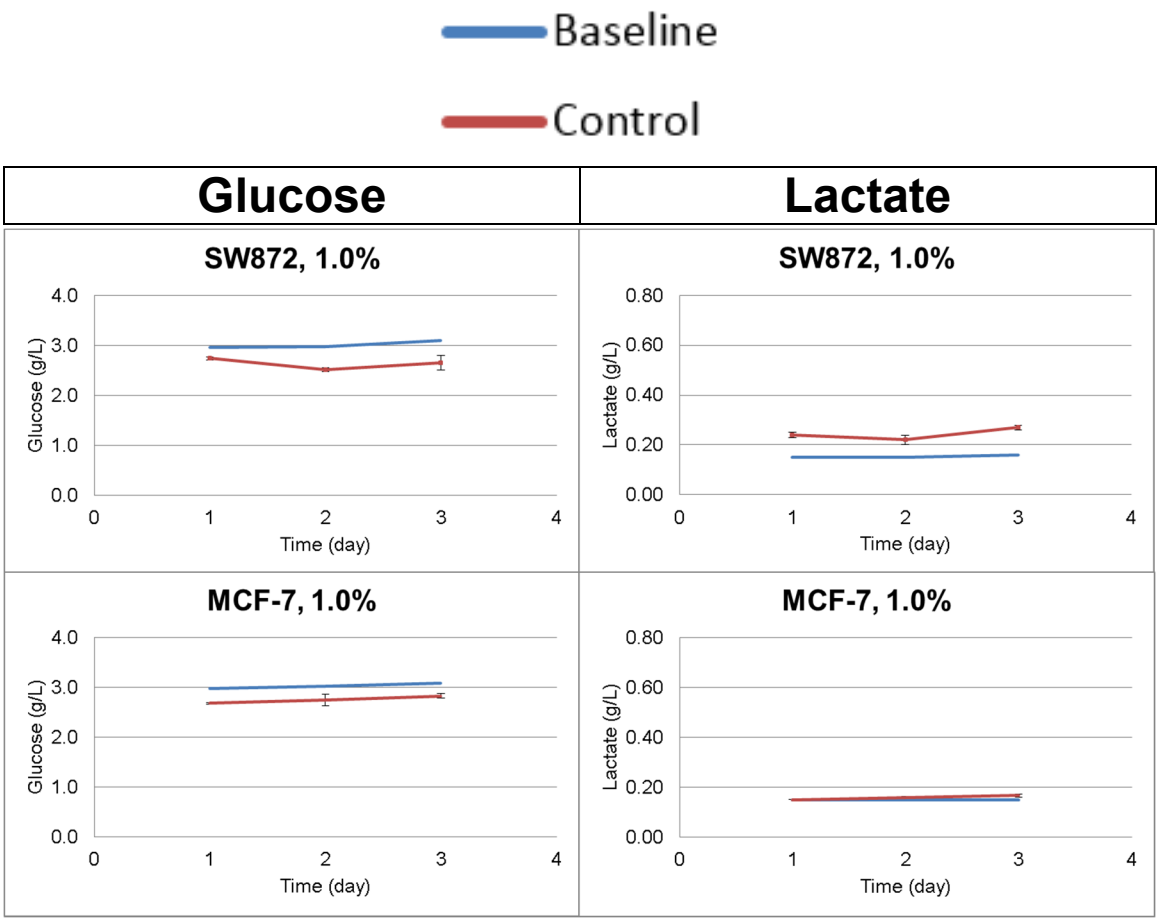

Figure 4.7: *Biochemical analysis of glucose and lactate levels for transwell plates with SW872 cells and MCF-7 cells that were exposed to 1.0% TA beads. Error bars represent the standard error for all data points. Each data point represents a mean average of n=3 per condition and time point.*

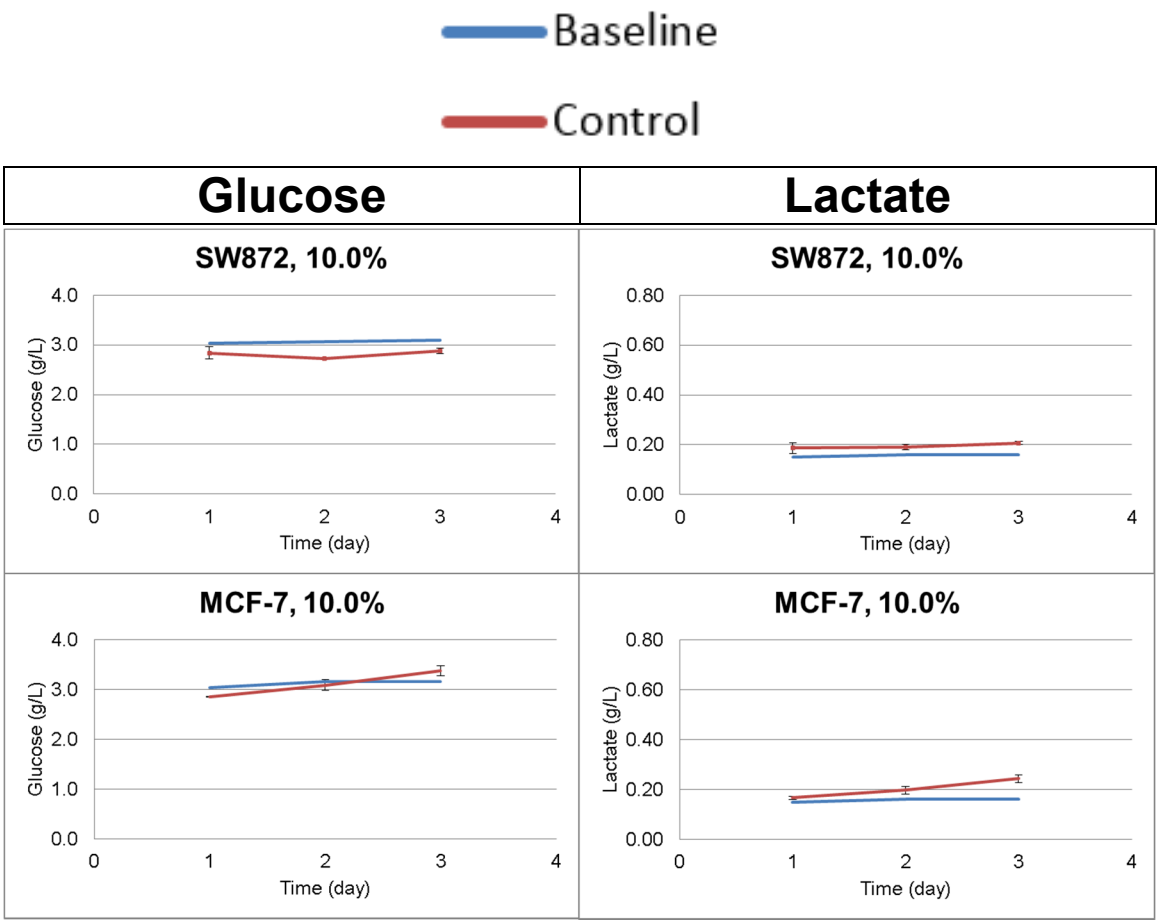

Figure 4.8: *Biochemical analysis of glucose and lactate levels for transwell plates with SW872 cells and MCF-7 cells that were exposed to 10.0% TA beads. Error bars represent the standard error for all data points. Each data point represents a mean average of n=3 per condition and time point.*

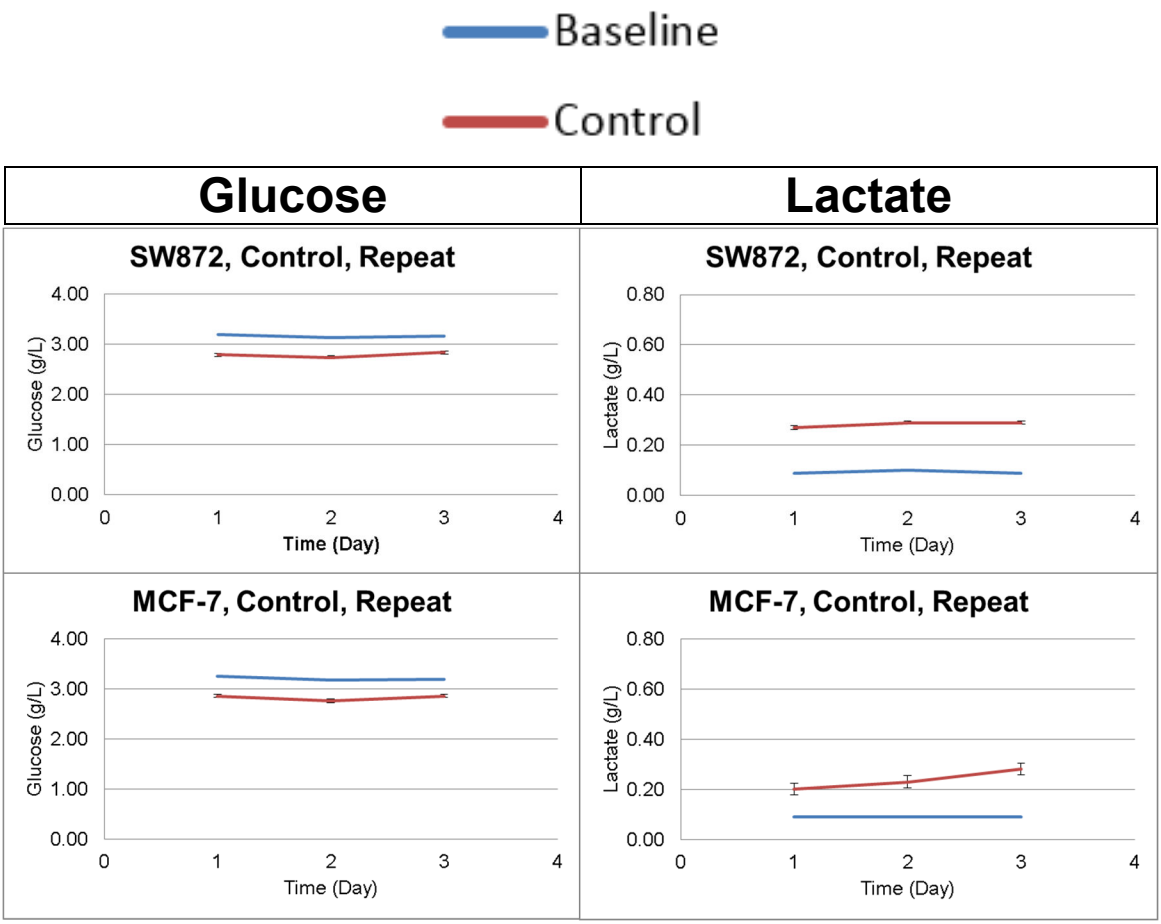

Figure 4.9: *Biochemical analysis of glucose and lactate levels for transwell plates in the repeat study with SW872 cells and MCF-7 cells that were not exposed to beads. Error bars represent the standard error for all data points. Each data point represents a mean average of n=3 per condition and time point.*

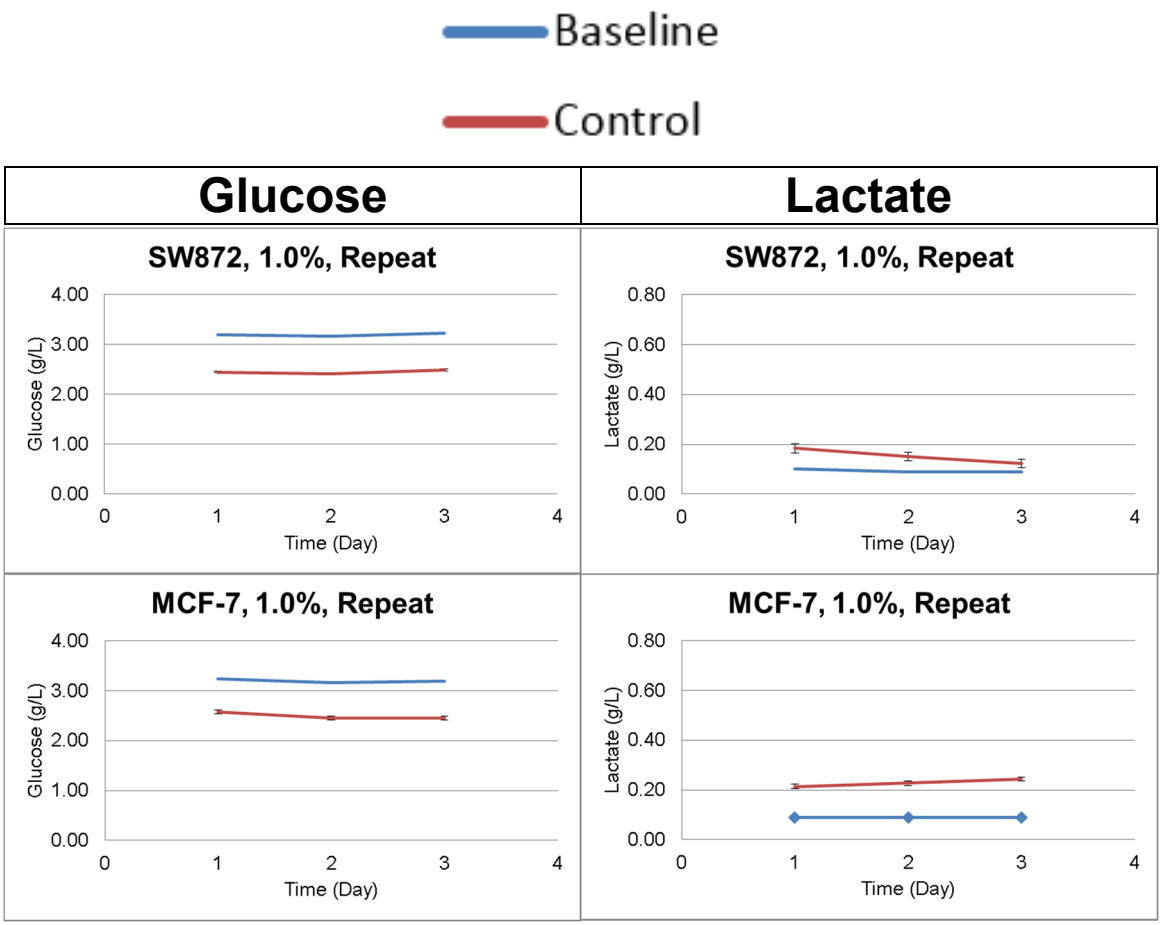

Figure 4.10: *Biochemical analysis of glucose and lactate levels for transwell plates in the repeat study with SW872 cells and MCF-7 cells that were exposed to 1.0% TA beads. Error bars represent the standard error for all data points. Each data point represents a mean average of n=3 per condition and time point.*

Live/ Dead Assay

The primary function of the beads, beyond being the source for TA in the model, is to also provide a viable scaffold on which the SW872 preadipocyte cells can grow and proliferate. Live/ Dead images of the beads over the 3-day period show if cells are able to survive when in direct contact with the beads.

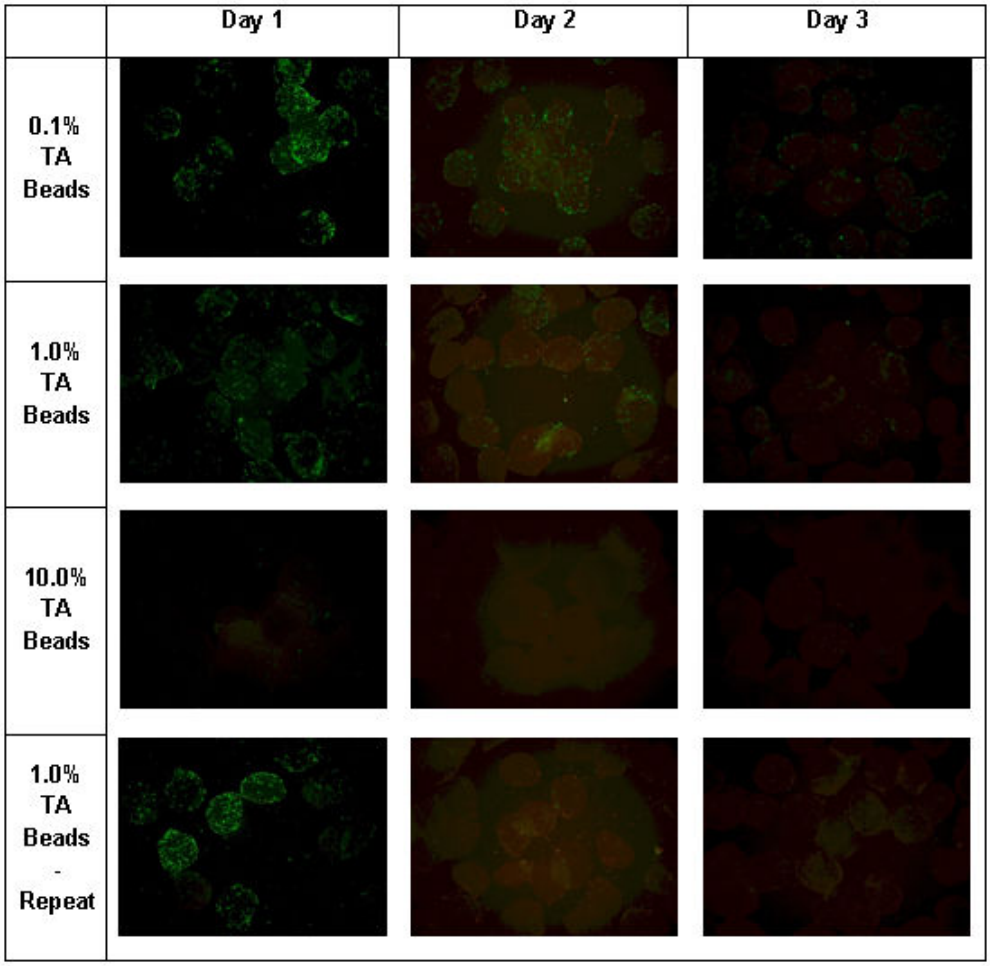

Figure 4.11: *Live/ Dead analysis on the SW872 cells growing on the TA cross-linked beads. Bright green dots signify a live cell. There were no noticeable differences between beads that had SW872 or MCF-7 cells growing in the bottom of the wells. All pictures were taken at a total magnification of 250x.*

TUNEL Assay

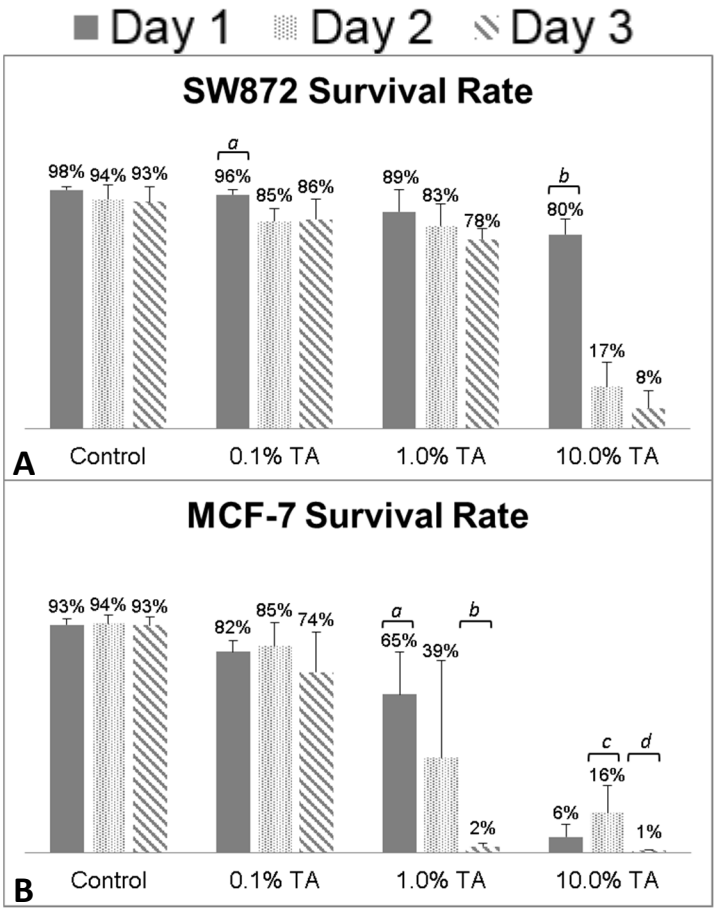

Figure 4.12: *TUNEL assay results showing the survival rates of SW872 cells (A) and MCF-7 cells (B), exposed to non-seeded beads, growing in the bottom of the wells for the main study. Letters designate statistical significant difference (p>0.05). All groups comprised n=9 samples.*

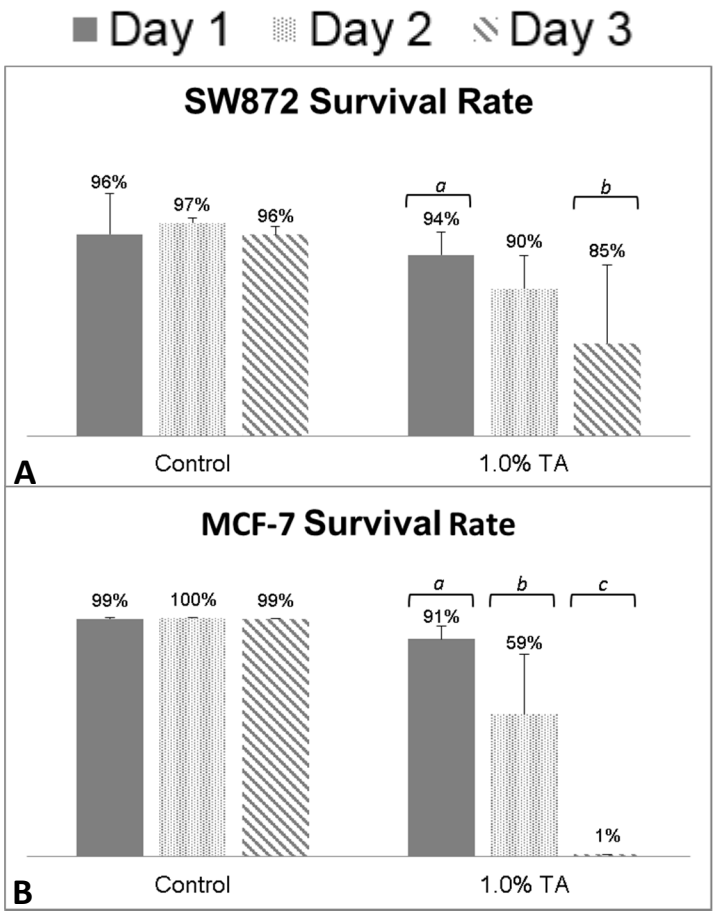

Figure 4.13: *TUNEL assay results showing the survival rates of SW872 cells (A) and MCF-7 cells (B), exposed to non-seeded beads, growing in the bottom of the wells for the repeat study. Letters designate statistical significant difference (p>0.05). Control groups comprised of n=3 samples. All other groups were comprised of n=9 samples.*

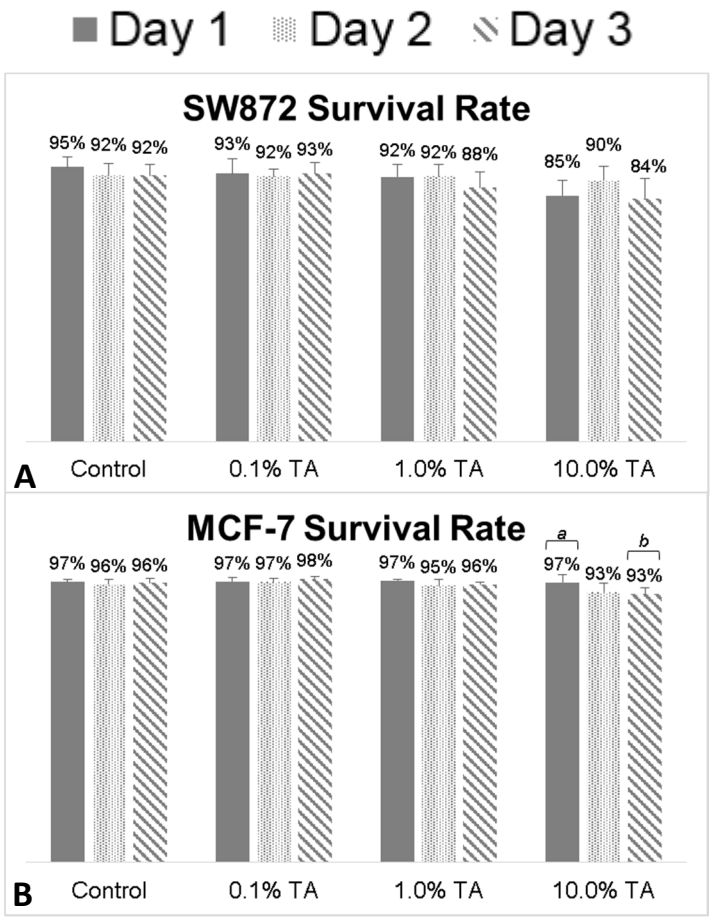

Figure 4.14: *TUNEL assay results showing the survival rates of SW872 cells (A) and MCF-7 cells (B), exposed to seeded beads, growing in the bottom of the wells for the main study. Letters designate statistical significant difference (p>0.05). All groups were comprised of n=9 samples.*

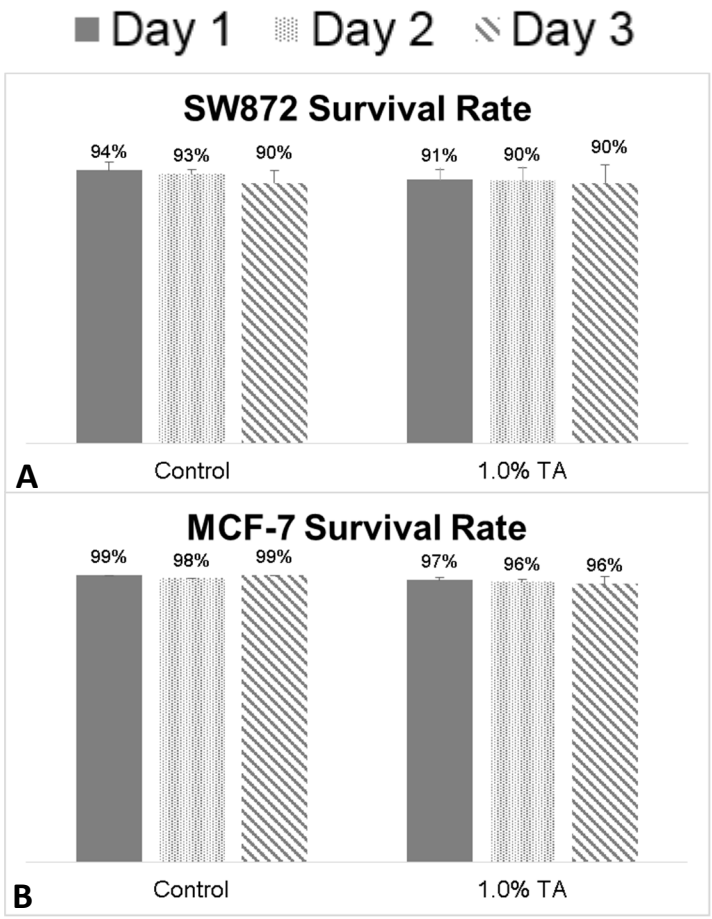

Figure 4.15: *TUNEL assay results showing the survival rates of SW872 cells (A) and MCF-7 cells (B), exposed to seeded beads, growing in the bottom of the wells for the repeat study. Letters designate statistical significant difference (p>0.05). Control groups comprised of n=3 samples. All other groups were comprised of n=9 samples.*

4.4 Discussion

The results, derived from the F-C assay for the beads that did not have SW872 cells seeded on them, showed that the majority of the TA eluted from the beads during the first 48 hrs of incubation. Since there were not any cells present to facilitate the remodeling of the collagen beads, the release that was seen could be attributed to TA that was contained within the porous structure of the beads but not bound to the collagen in the form of crosslinks. Another factor that may have added to the release of the TA could be the conditions for incubation; i.e., the morphology of the beads alters when exposed to the temperature and CO_2 of the incubator. The FC results also show that the amount of TA released by the beads increases as the cross-linking concentration of the beads increases. This observation follows the logic that the increased amount of TA present during the production of the beads would lead to an increased level of TA captured within the beads. With the increasing TA present within the beads, the amount eluted by the beads should increase as well. It was also observed that the cell type that was growing in the bottom of the wells had no effect on the elution rates of the beads. This is what was expected since there was no direct interaction between the beads and the cells in the bottom of the wells.

It then follows that the same wells with the non-seeded beads would show an increased amount of apoptotic activity as the TA cross-linking solution for the beads increases. Previous studies have shown that TA causes apoptosis of MCF-7 cells [101]. With the increased prevalence of TA within the medium, it would be expected that wells with MCF-7 cells would show an increased level of apoptotic activity. The results also show that cells in these wells have a higher level of apoptosis as exposure time to the TA increases. This is also what was expected because a longer exposure time allows a

greater chance for TA to act on the cancerous cells and induce apoptosis. The wells with SW872 cells also showed the same effect, with more apoptotic activity being seen in wells with beads cross-linked by a higher concentration of TA. However, for the SW872 cells, the levels of apoptosis are much less pronounced than those seen by the MCF-7 cells, demonstrating the ability of TA to selectively target the cancerous cells to a greater extent. However, once the bead TA concentration reaches 10.0%, the concentration of TA within the medium is too high for the SW872 cells to survive.

The biochemical analysis of glucose and lactate levels describes, in part, the metabolic activity of the cells growing in the bottom of the wells with non-seeded beads. Under normal conditions, it would be expected that glucose levels will decrease as cells metabolize it and produce lactate as a byproduct, causing lactate levels to increase over time. Measuring the levels of both glucose and lactate levels over time should provide insight into the metabolic activity of the cells being examined. What these results show is that the MCF-7 cells are less metabolically active when exposed to TA. There also appears to be an inverse correlation between the cross-linking concentration of TA for the beads and the effect the beads have on metabolic activity. As the bead TA cross-linking concentration increases, the metabolic activity of the MCF-7 cells becomes more inhibited, the cells producing less lactate and a constant level of glucose. This is most likely due to the increased level of apoptosis occurring as the levels of TA increase. The same correlations between metabolic activity and TA levels can be seen for the SW872 cells. However, the results of the TUNEL assay suggest that the metabolic activity of the SW872 cells was inhibited by the TA, but the cells were still able to survive.

When the results for the wells containing beads that were seeded with SW872 cells are examined, there are some striking differences. The F-C assay shows that very

little TA has eluted from the beads over the 3-day time period. The order of magnitude of the readings, along with the standard deviation of each group, suggests that the values obtained are simply noise readings that occur in a colorimetric assay when levels are very close to zero. It is hypothesized that the little amount of TA elution that occurred was due to the cell seeding process used. The previously discussed results showed that the non-seeded beads eluted the majority of TA during the first 48 hrs. However, for the beads that were seeded with SW872 cells, the first 48 hrs of incubation occurred while the beads were in the roller bottles for cell seeding rather than during the actual experiment. Therefore, the majority of the TA eluted from the beads before the beads were placed in the transwell inserts, resulting in the decreased levels of TA present.

The TUNEL assay for the seeded bead well plates also revealed the low levels of TA present within the medium. With little TA present, there was little induction of apoptosis which resulted in a much higher rate of survival for the MCF-7 and SW872 cells, especially at the 1.0% and 10.0% TA levels. The Live/ Dead assay results show that SW872 cells were able to adequately attach and grow on the collagen beads cross-linked with 0.1% and 1.0% TA after the initial cell seeding process. The 10.0% TA beads did not show any significant cellular attachment after the initial cell seeding process and, therefore, did not demonstrate any significant cellular activity over the three day time period of the study. As the study continued, the 0.1% TA cross-linked beads continued to show a high level of viable cells attached to the beads over the 3-day period, suggesting that these beads are capable of providing a scaffold for the preadipocytes. The number of viable cells on the 1.0% TA cross-linked beads significantly decreased as the study progressed over the 3 days. By day three, the 1.0%

TA beads had very low numbers of viable cells when compared to numbers after day one.

4.5 Conclusions

The results collected from the well plates with the non-seeded beads showed that the 1.0% and 10.0% TA beads are able to induce apoptosis of cancerous cells. However, the 10.0% TA beads also caused the apoptosis of the preadipocytes. Only the 1.0% TA beads were able to cause apoptosis of cancerous cells while allowing the preadipocytes to proliferate, suggesting that the concentration of TA within these beads may be ideal for the overall intended goal of this project. These results were verified by the repeat study.

However, results gleaned from the well plates with the seeded beads show that the 1.0% TA beads are not able to provide a viable scaffold upon which preadipocytes can grow and proliferate. The preadipocytes are able to survive when they are found distal to the TA source but direct contact with the 1.0% TA beads exposes the preadipocytes to too great of a TA concentration and they are not able to survive. The preadipocytes growing on the 0.1% TA beads were able to attach at a high number after the initial seeding and remain viable over the 3 days. This result suggests that the ideal TA cross-linking solution concentration is between 0.1% and 1.0% TA.

CHAPTER 5

EVALUATION OF THE EFFECTIVNESS OF TA CROSS-LINKED BEADS IN A THREE-DIMENSIONAL (3-D) ENVIRONMENT

5.1 Background

Once the effects of the beads had been evaluated in a 2-D model, it was important to determine if the beads showed the same effects in a 3-D environment. A 3-D environment better simulates how cells will behave in an *in vivo* environment and ensures that the previous work and results seen can be translated to a more physiologically relevant model.

The purpose of this study is to determine the effectiveness of the TA, released from the beads, on cancer cells that are in a 3-D construct. Accordingly, cancerous cells were embedded in a collagen/ agarose gel. This gel had a pit molded into the middle of it, in which TA beads that had been seeded with SW872 cells were placed. The assumption was that the preadipocyte cells would attach and proliferate on the TA beads, releasing the TA into the surrounding medium and gel and causing the death of the cancerous cells contained within. This 3-D setup had the advantage of being a 3-D scaffold system that would better mimic aspects what could be expected in a physiological environment.

Collagen/ agarose gels were selected for this study for two primary reasons. For a lumpectomy to be performed on a patient, the cancerous cells cannot be very metastatic and cannot be expanding beyond the original cancerous tumor in the breast. A collagen/ agarose gel does not provide much motility to any cells encapsulated within, thus better mimicking the condition where the cancerous cells are not metastatic and

attempting to spread out beyond their original location. The second reason behind the selection of collagen/ agarose gels is for their physical properties. Other gels types that were tested did not provide the mechanical strength necessary for sectioning. The collagen/ agarose gels were able to be sectioned in the way intended without falling apart.

5.2 Materials and Methods

Cell Culture

SW872 and MCF-7 cells were obtained from ATCC (Manassas, VA) and cultured with Dulbecco's Modified Eagle's Medium (DMEM): F12 medium, also purchased from ATCC (Manassas, VA). The use of DMEM: F12 medium was recommended for use with the SW872 cells and, in order to keep variables consistent, the MCF-7 cells were also cultured in this medium. The MCF-7 cells had also been tagged with red fluorescent protein using lentiviral transfection in order to distinguish the two cell types during analysis. The medium was also supplemented with 10% fetal bovine serum (FBS) (Corning; Manassas, NY) as well as 1% antibiotic- antimycotic (AA) (Gibco; Great Island, NY) and 0.2% fungizone (Gibco; Great Island, NY) to help prevent contamination. Both cell types were grown in T-75 cell culture flasks (Corning; Corning, NY) incubated at 37 °C with 5.0% CO_2 (Panasonic MCO-18ACL; Chicago, IL).

To perform the lentiviral transfection of the MCF-7 cells, MCF-7 cells were seeded in a 96 well plate in normal growth medium and proliferated in an incubator at 37ºC. The media was removed and Cignal Lentiviral particle-RFP (Qiagen; Venlo, Netherlands) with SureENTRY transduction reagent (Qiagen; Venlo, Netherlands) in

growth media without antibiotics was added. The plate was incubated for 18-20 hrs, after which the media containing the lentiviral particles was removed and normal growth media containing antibiotics was added and the MCF-7 cells were allowed to grow to confluency. Once confluent growth media containing the selective agent, 2 ug/ml puromycin (Fisher; Fair Lawn, NJ) was added. The selection media was replaced every 3-4 days until puromycin resistant positive colonies appeared. The RFP-positive cells were expanded in selection media to obtain RFP positive cultures.

Modified Well Plate Lid and Teflon Plugs

In order to mold a pit within the collage/ agarose gels, a modified well plate lid was fabricated. Measurements of a 12-well plate were taken and loaded into Solid Edge V20 (Siemens; Plano, TX), a computer aided design (CAD) program. The measurements were used to create the top of the modified well plate lid and side fins were added to help secure the lid on top of the well plate base. Measurements of the location of the wells of the well plate were also taken. At the center location of the 12 wells was placed a 10-mm diameter hole where polytetrafluoroethylene (PTFE) plugs could be inserted. The entire modified well plate lid was made out of aluminum to allow easy sterilization using an autoclave.

In addition to the modified well plate lid, PTFE plugs also needed to be manufactured to serve as the actual molds around which the gels would set, thus creating the desired pit in the gels. PTFE was selected because of its ability to prevent gels and other substances from sticking to it, allowing the easy removal of the plugs from the gels once they had been set. PTFE was also selected because of its ability to be easily sterilized in an autoclave. Each peg was designed to have a handle that was 15-

mm diameter and a central peg with a diameter of 10 mm. The central peg was inserted into the hole of the modified well plate lid and suspended within the gel as the gel set, causing the formation of a pit within the gel once the plugs were removed. Below is a schematic to show how the modified well plate lid and the PTFE plugs were used to create the mold for the gels.

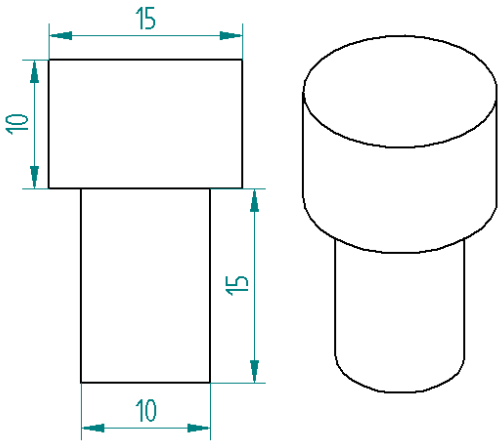

Figure 5.1: *Design of the PTFE plugs. All measurements are in mm.*

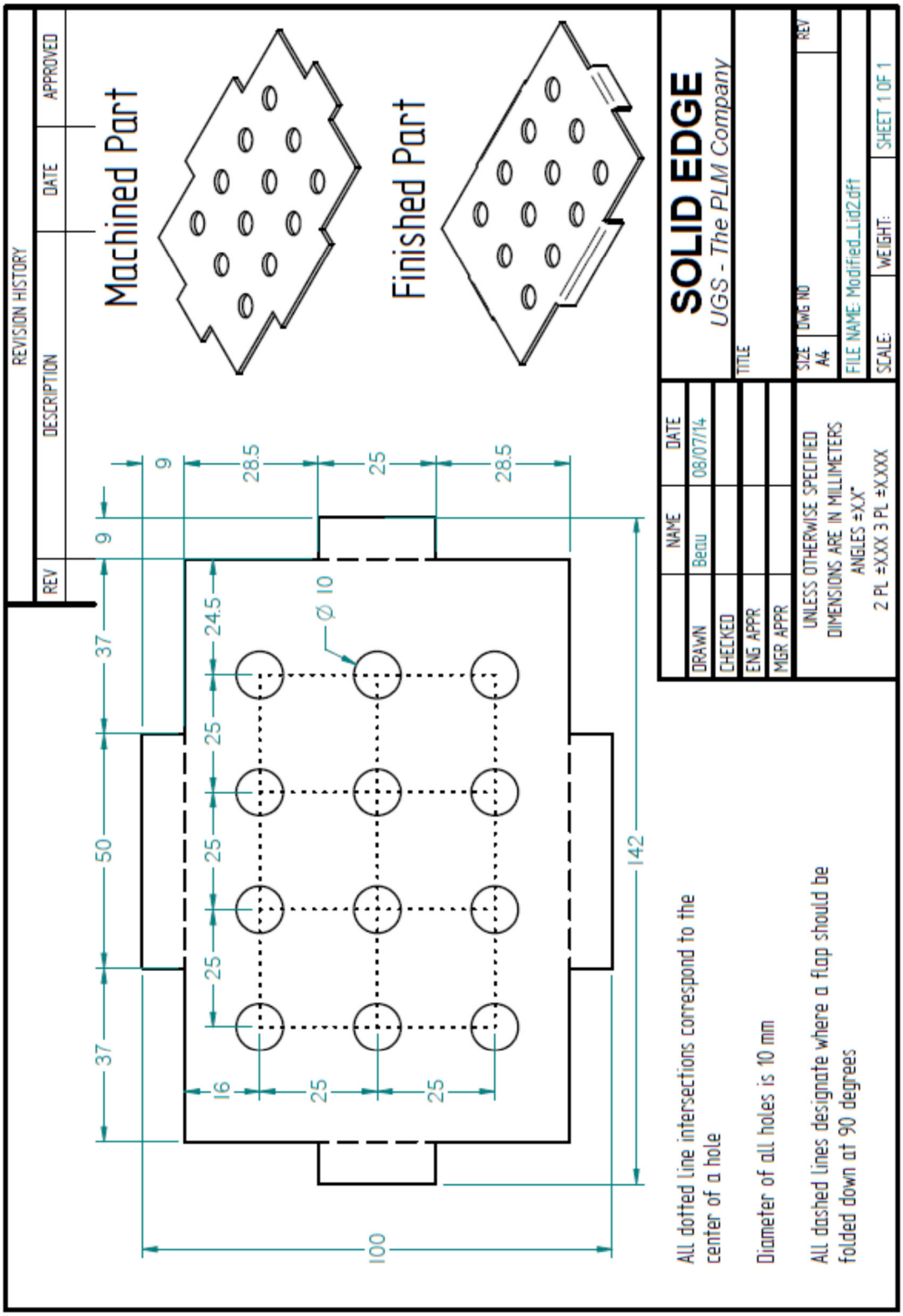

Figure 5.2: *Solid Edge drawing of the modified well plate lid*

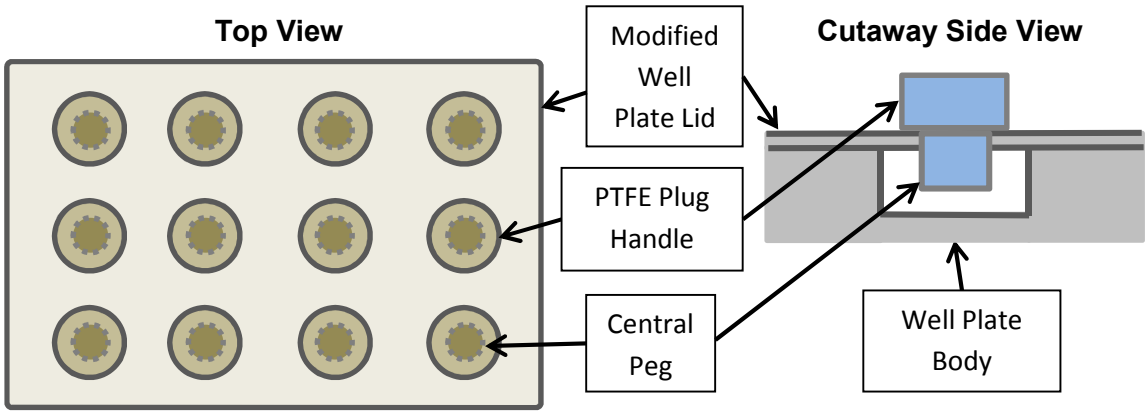

Figure 5.3: *Schematic showing how the PTFE plugs and the modified well plate lid are put together to form the mold for the gels. In the image on the right, the Teflon plug handle and central peg are one continuous piece that passes through a hole in the modified well plate lid.*

Collagen/ Agarose Gel Setup

There were three data collection time points for this experiment; day 1, day 4, and day 7. The main experiment incorporated 0.1%, 1.0%, and 10.0% TA beads, some of which were seeded with SW872 cells, some of which were control wells that were not exposed to TA beads. In addition to the main experiment, there was a repeat experiment using the same methods as the main experiment but using only 1.0% TA beads to verify the results of the main experiment. The 1.0% beads were chosen because the previous results showed survival of preadipocytes and apoptosis of cancerous cells.

One 12-well plate (Costar; Corning, NY) was used for each time point for the main experiment. A 12-well plate served as the control group, in which only three columns were used, one per time point. In addition to these plates, a 12-well plate was

used for all three time points of the repeat study and one 12-well plate was used for the control group, just as in the main experiment. In total, six 12-well plates were used for the entire experiment. However, since only three columns of the control plates were used, only 66 wells were used in total.

Based on previous studies, it was determined that the best ratio for of collagen to agarose to use was 1:2. At this ratio, the gel was firm enough to allow acquisition of complete histological sections, and the collagen concentration was not high enough to vigorously react with the TA eluting from the beads and cause the gel to become flakey. A 1% agarose solution (Low Gelling Temperature; Fisher Scientific; Fair Lawn, NJ) was prepared by first calculating the volume of agarose needed for the experiment. Into each well was dispensed 3 mL of the 1:2 collagen/ agarose gel mixture, 1 mL of collagen and 2 mL of agarose per well. There were 66 wells used in total, with 2 mL of agarose per well, resulting in 132 mL of 1% agarose solution. For backup purposes, 150 mL of 1% agarose solution was prepared. Accordingly, 1.50 g of high gelling temperature agarose was weighed and the powder was placed in a glass bottle. The glass bottle with the agarose was then autoclaved to sterilize both the agarose and the glass bottle. After being autoclaved, 78 mL of DMEM: F12 medium was added to the bottle and the bottle was then placed in a 65 °C water bath (Grant SUB 28; Keison Products; Grants Pass, OR) till the agarose was dissolved. A volume of 78 mL of DMEM: F12 was used to suspend the agarose powder and account for the addition of the cell suspension that was added in the final steps of the initial setup. The addition of the cell suspension brought the concentration of the agarose solution to the desired 1.0%.

As the agarose dissolved in the DMEM: F12, a 1.0 mg/mL collagen solution was prepared. A total of 66 wells was used, each well needing 1 mL of collagen solution;

hence, a total of 66 mL of 1.0 mg/mL collagen solution was needed. To serve as a backup supply, 80 mL of collagen solution was prepared. The procedure used to prepare the bead collagen solution was used to prepare this collagen solution. Briefly, the stock solution of collagen (PureCol; Advanced Biomatrix; San Diego, CA) had a concentration of 3.0 mg/ mL. In order to obtain 80 mL of a 1 mg/mL collagen solution, 26.67 mL of the stock collagen solution was needed. This volume was then multiplied by 0.111 to calculate the amount of 10x PBS (Sigma Aldrich; St. Louis, MO) required, 2.96 mL. One tenth of the total volume of the final solution comprised FBS (Corning; Manassas, NY), 8.0 mL. Finally, the rest of the desired volume comprised serum-free DMEM: F12 (ATCC; Manassas, VA), 42.37 mL. Once these volumes were combined, enough 1.0 N NaOH (Sigma Aldrich; St. Louis, MO) was added to yield a neutral pH, as indicated by a color change from yellow to pink. This color change was caused by the presence of phenol red in the DMEM: F12.

The last component of the gel model is the embedded cancerous MCF-7 cells. Confluent T-150 cell culture flasks (Corning; Corning, NY) of MCF-7 cells were removed from the incubator (Panasonic MCO-18ACL; Chicago, IL) and the total number of MCF-7 cells was counted. A total of 5.0×10^4 cells was desired per well. This number was chosen to simulate the situation of a lumpectomy, where the majority of the cancerous cells are removed by removing the cancerous mass, leaving only a few cancerous cells on the periphery of the cancerous mass' original location. For this experiment, the total number of MCF-7 cells was approximately 7.4×10^6, resulting in a cell suspension of 2.0×10^5 cells/ mL. Therefore, 0.25 mL of the MCF-7 cell suspension and 0.75 mL of DMEM: F12 was placed in each well.

Once all components were prepared, 1 mL of 1% agarose solution, 1 mL of 1.0 mg/mL collagen solution, 0.25 mL of MCF-7 cells suspension, and 0.75 mL of DMEM: F12 were added to each well and mixed. The modified well plate lid was placed on top of the well plate and the PTFE plugs were inserted into the holes of the lid. The gels were allowed to set for 15 minutes in the incubator. While the gels were solidifying, the 1% agarose solution was placed back in the hot water bath to prevent it from solidifying. After 15 minutes, the well plate was removed from the incubator, the PTFE plugs were removed from the holes, and the modified well plate lid was removed and replaced with the original well plate lid. This procedure was repeated for all well plates with the two control well plates only receiving gel mixture in the first three columns.

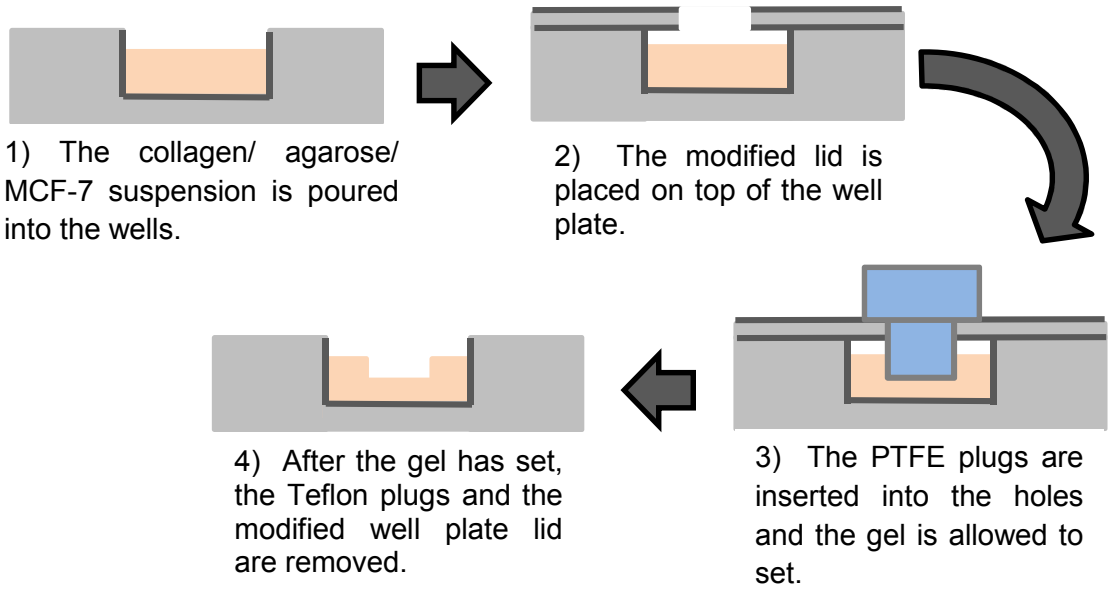

Figure 5.4: *Outlined process of how the gels were molded with the PTFE plugs and the modified well plate lid.*

TA Bead Setup

Four double batches of TA (Sigma Aldrich; St. Louis, MO) cross-linked beads were prepared, one batch cross-linked with 0.1% TA, two batches cross-linked with 1.0% TA, and one batch cross-linked with 10.0% TA. One batch from each cross-linking solution type was used in the main study, and the remaining 1.0% TA batch was used in the repeat study. Each batch was stored in phosphate buffered saline (PBS; Sigma Aldrich; St. Louis, MO) in the refrigerator.

Sigmacote (Sigma Aldrich; St. Louis, MO) was applied to four 50 mL centrifuge tubes (Corning; Corning, NY) and allowed to dry overnight, prior to setting up the gels. This was done to prevent cells from attaching to the centrifuge tubes during the cell seeding process. The four batches of beads were removed from the refrigerator and the PBS was removed and replaced with DMEM: F12. Approximately two thirds of the beads from each batch were placed into the individual Sigmacote-treated centrifuge tubes. SW872 cells were removed from the incubator and counted from confluent T-75 cell culture flasks (Corning; Corning, NY). The total SW872 cell count was 5.25×10^6 cells; the cells were suspended in 4 mL of DMEM: F12. To each of the Sigmacoted centrifuge tubes, 1 mL of the SW872 cell suspension was added, approximately 1.30×10^6 cells per centrifuge tube. The centrifuge tubes with the beads and the SW872 cells was gently shaken and then placed in the incubator, set to 37 °C at 5.0% CO_2 for one hour. During that hour, every 20 minutes, the centrifuge tubes were gently shaken and then placed back in the incubator.

At the end of the hour, the beads were removed from the incubator. The beads were then placed into the molded wells of the collagen/ agarose gels, each well receiving approximately 0.2 mL of the bead suspension. For the original experiment, the

first column of the well plate received the beads that had not been seeded with SW872 cells. These samples served as bead control groups that allowed differentiation between the effects the beads alone had on the MCF-7 cells and any added effects the SW872 cells caused by growing on the beads. Each well of the first column received a different bead type. The other three columns of the well plate received a different bead type. This setup was repeated for all three experimental well plates of the main study. The control well plate did not receive any beads. For each data collection time point, one well plate was used, as well as one column of the control well plate.

The well plates in the repeat study had the same experimental setup as the original, except all bead control wells received 1.0% TA beads that had not been seeded with SW872 cells, while the other three columns of the experimental plate received 1.0% TA beads that had been seeded. For each data collection time point, one bead control well was used, along with one column from the experimental well plate and one column from the control well plate. A volume of 1 mL of DMEM: F12 was then added to each well and the well plates were placed in the incubator at 37°C with 5.0% CO_2. Every 24 hrs, the DMEM: F12 would be replaced with 1 mL of fresh medium.

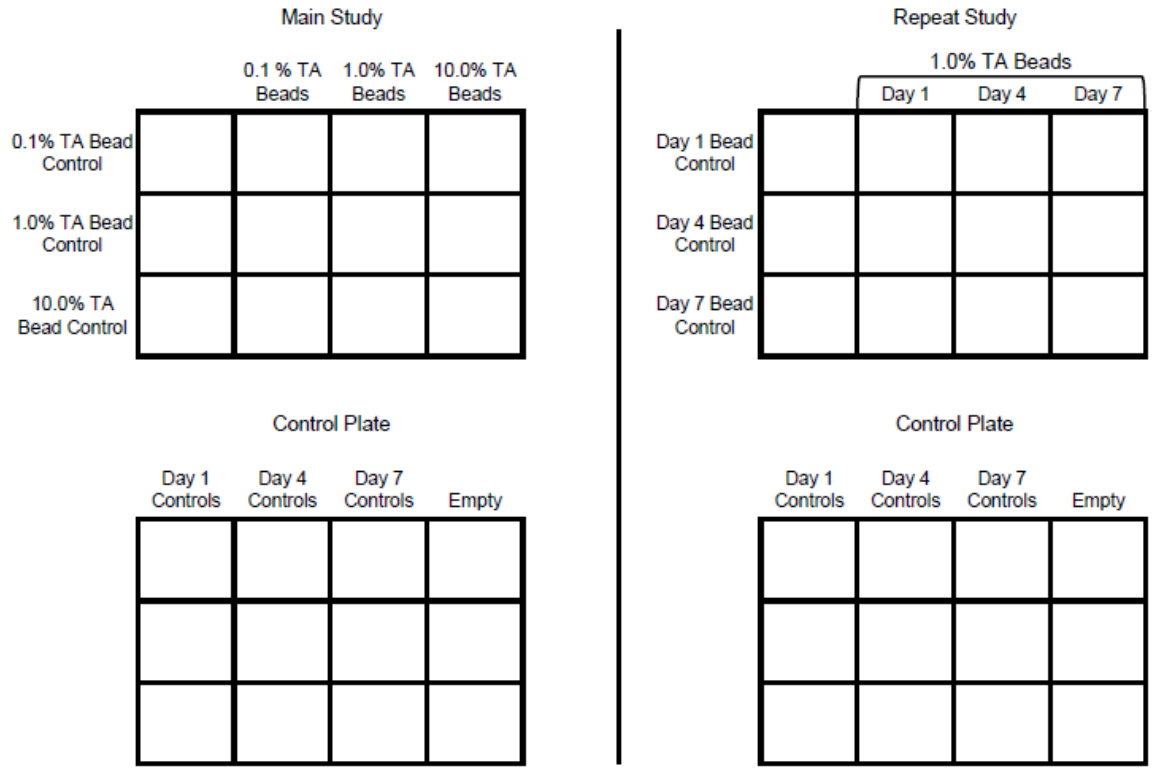

Figure 5.5: *Diagram showing the lay out for the well plates in the main study and the repeat study*

Sample Collection

Every 24 hrs, samples of the medium from the wells of the day 7 data collection time point well plate were collected along with samples from the day 7 control column of the control well plate. These samples were later used for F-C analysis to measure the rate of elution of the TA from the beads.

Two metal surgical spatulas were autoclaved before gel samples were collected. At the designated data collection time points, the well plates were removed from the incubator, along with the control well plate. The beads were removed from the wells of the experimental groups, collected in a 6-well plate (Costar; Corning, NY) and set aside.

The remaining medium was removed from the wells. Using the straight edge of the metal spatula, the gel was loosened from the walls of the well. Using the scooping end of the spatula, the gel was then removed from the well and placed in a well of a 6-well plate. After all the gels had been removed, the straight edge of the metal spatula was used to slice the gel down the middle. Subsequently, the two scooping ends of the two spatulas were used to reposition the two gel halves so the cut surfaces were face down in the well (Figure 5.6). This was done for all gels.

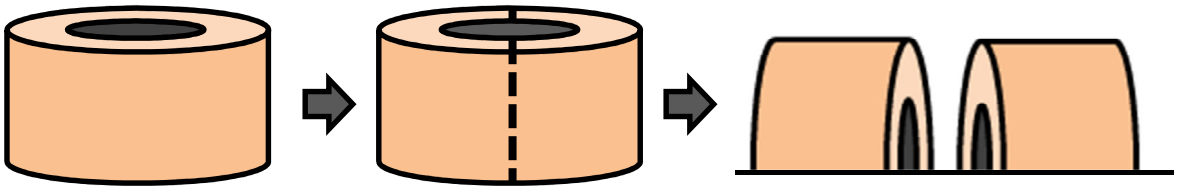

Figure 5.6: *Sectioning process of the collagen/ agarose gels.*

Live/ Dead Assay – TA Beads

After the beads had been placed in the 6-well plate, any remaining medium was aspirated from the wells. A partial Live/ Dead solution was prepared with calcein-AM (Invitrogen; Eugene, OR) and PBS alone. This solution only tags live cells with a green fluorescence and does not tag dead cells. A volume of 2.0 mL of the partial Live/ Dead solution was then added to each well containing the beads. The 6-well plate was then placed in a dark drawer until imaged under fluorescent light with the microscope (Axiovert 135 Inverted Microscope; Zeiss; Thornwood, NY) and attached camera (ProgRes™ C10 Plus; Jenoptic Optical Systems; Jupiter, FL) and the ProgRes™ Capture Pro 2.6 software (Jenoptic Optical Systems; Jupiter, FL).

Live/ Dead Assay – Collagen/ Agarose Gels

After the gels had been sectioned and repositioned, they were washed with PBS. The same partial Live/ Dead solution was made for the imaging of the collagen/ agarose gels as was used for the TA beads. Normally, this Live/ Dead solution would also tag dead cells with a red fluorescence, but the MCF-7 cells were already tagged with a red fluorescent protein, which would make them indistinguishable from dead cells if exposed to a complete Live/ Dead solution. To each well containing a sectioned gel, 2.0 mL of the partial Live/ Dead solution was added. These well plates were then placed in a dark drawer till they were ready to be imaged using fluorescent light and a microscope.

Images were then taken of the gels under both red and green fluorescent light. The red light revealed the tagged MCF-7 cells and the green light revealed live cells. Using Adobe Photoshop, these two pictures were overlaid. Yellow MCF-7 cells were fluorescing in both pictures; red fluorescence overlaid with green fluorescence produces a yellow fluorescence. Dead MCF-7 cells only appeared red in the overlaid picture because they did not fluoresce green; any live SW872 cells appeared green in the overlaid picture because they did not fluoresce red.

F-C Assay

Standards of 0.01%, 0.005%, 0.001%, and 0% TA were prepared using DMEM: F12. These standards and the collected medium samples were then diluted with MilliQ water (Direct 8; Millipore; Darmstadt, Germany). This was done to prevent color saturation from occurring due to the presence of the components of the DMEM: F12 medium. For each standard and collected medium sample, 25 µL of the medium sample was combined with 75 µL of MilliQ water in a 1.5 mL micro centrifuge tube (VWR;

Radnor, PA). After performing the dilution, 200 µL of a 10% Folin-Ciocalteu (F-C) reagent solution (Sigma Aldrich; St. Louis, MO) was added to each micro centrifuge tube, followed by 800 µL of a 700 mM sodium carbonate solution (Fisher Scientific; Fair Lawn, NJ). All micro centrifuge tubes were then vortexed and allowed to incubate for 2 hrs at room temperature. At the end of the 2 hrs, the solutions were loaded in triplicate into clear bottom, black side 96-well plates (Greiner Bio One; Monroe, NC) and the absorbance of the solutions was read at 765 nm with a multi-mode micro plate reader (Synergy™ Mx; BioTek; Winooski, VT).

The absorbance readings were loaded into a Microsoft Excel worksheet, and the absorbance readings of the standards were averaged and graphed against their known concentrations. A linear trend line was fitted to the standard data points, providing an equation to model the relationship between absorbance readings and TA concentration values. This equation was then used to calculate the TA concentration of the experimental medium samples collected. The calculated TA concentrations were then averaged and graphed. Minitab 16 (Minitab; State College, PA), a statistics program, was then used to perform the analysis of variance (ANOVA) statistical analysis on the calculated TA concentrations.

5.3 Results

Live/ Dead Assay – TA Beads

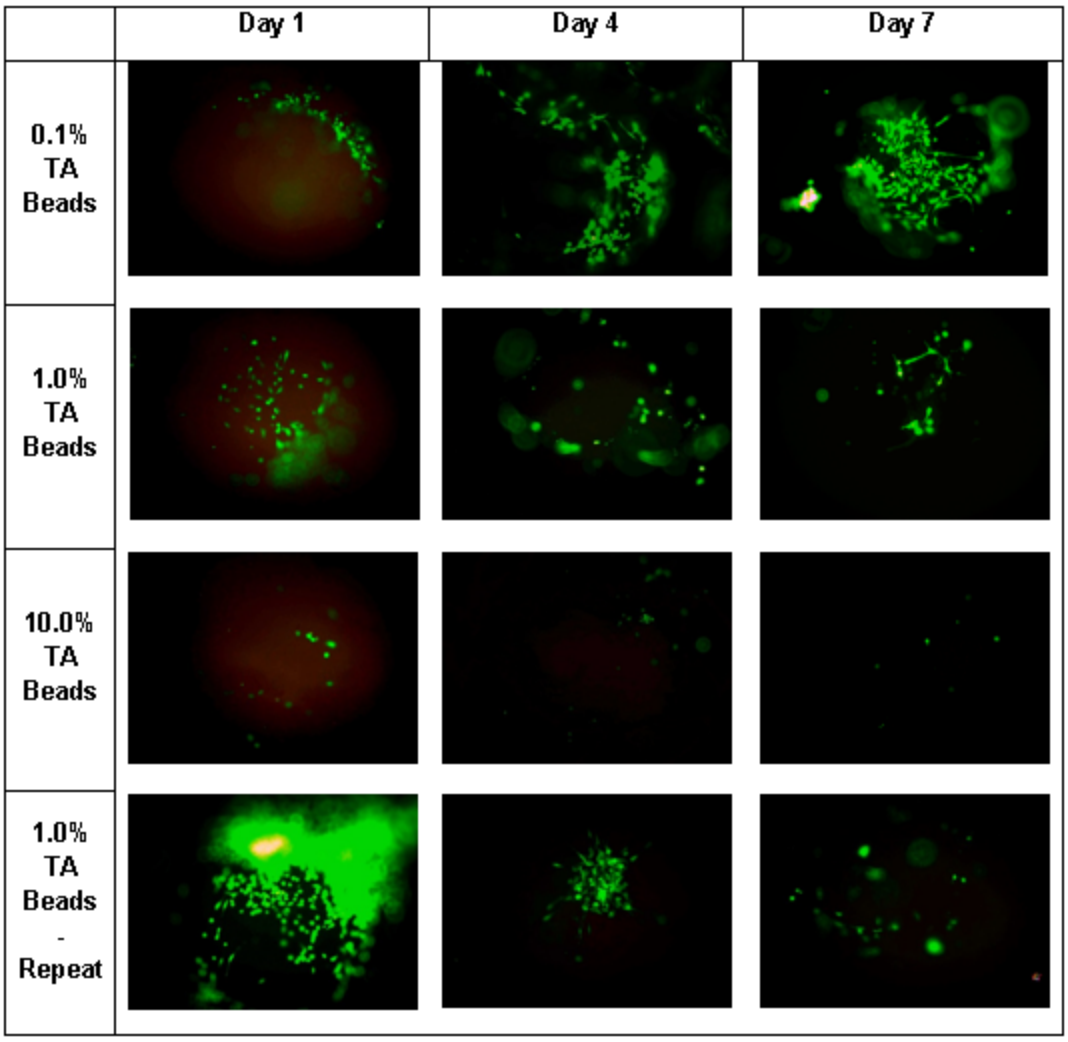

Figure 5.7: *Live/ Dead analysis on the SW872 cells growing on the TA cross-linked beads. Three pictures were taken of each bead type at each data collection time point. These pictures best represent the average appearance of the three pictures in each group. Bright green dots signify a live cell. All pictures were taken at a total magnification of 1000x.*

Live/ Dead Assay – Collagen/ Agarose Gels

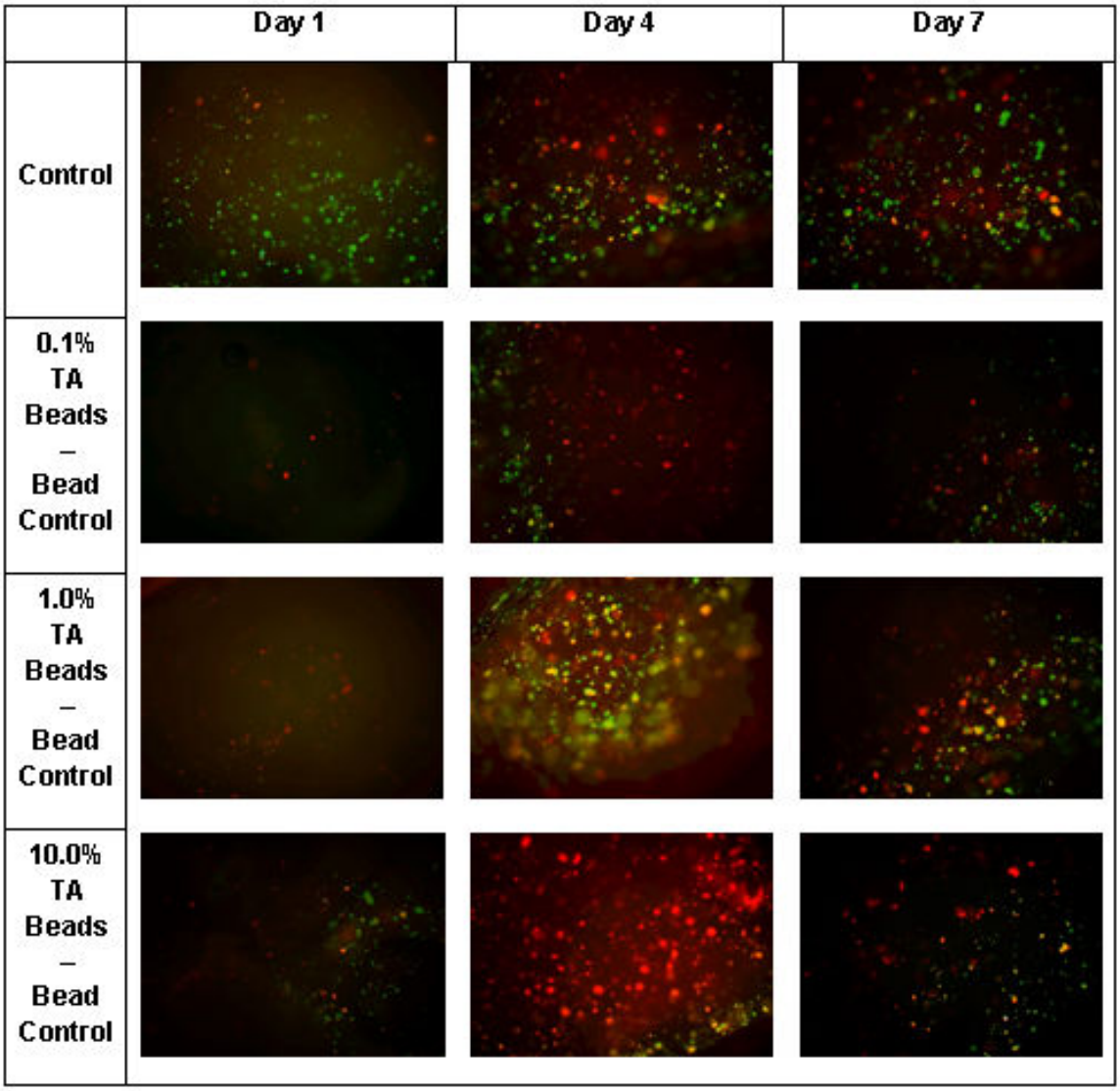

Figure 5.8: *Live/ Dead analysis on the collagen/ agarose gels in the main study that were exposed to beads that were not seeded with SW872 cells. Red dots signify dead MCF-7 cells, green dots signify live SW872 cells, and yellow dots signify live MCF-7 cells. All pictures were taken at a total magnification of 250x.*

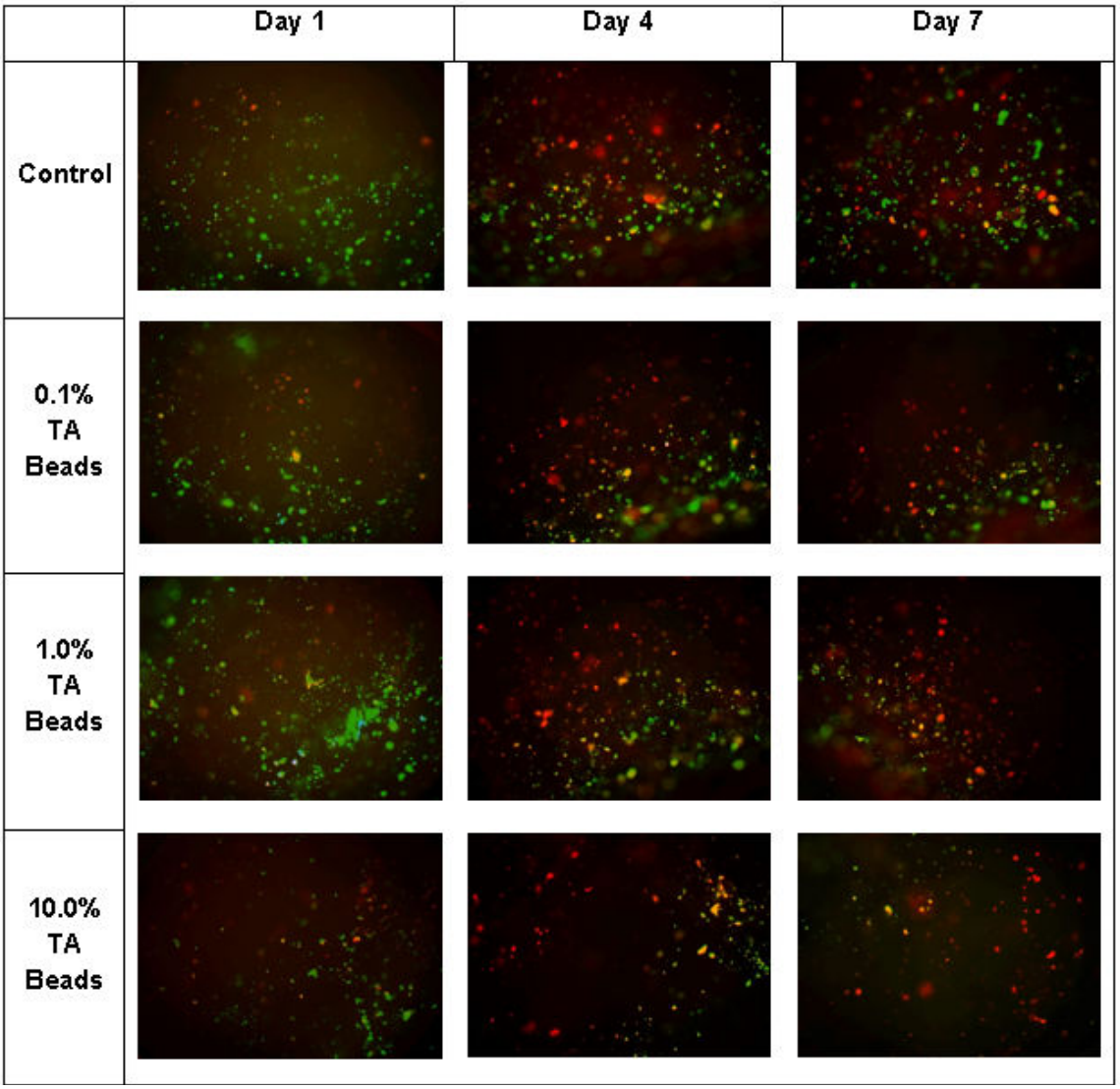

Figure 5.9: *Live/ Dead analysis on the collagen/ agarose gels in the main study that were exposed to beads that were seeded with SW872 cells. Red dots signify dead MCF-7 cells, green dots signify live SW872 cells, and yellow dots signify live MCF-7 cells. All pictures were taken at a total magnification of 250x.*

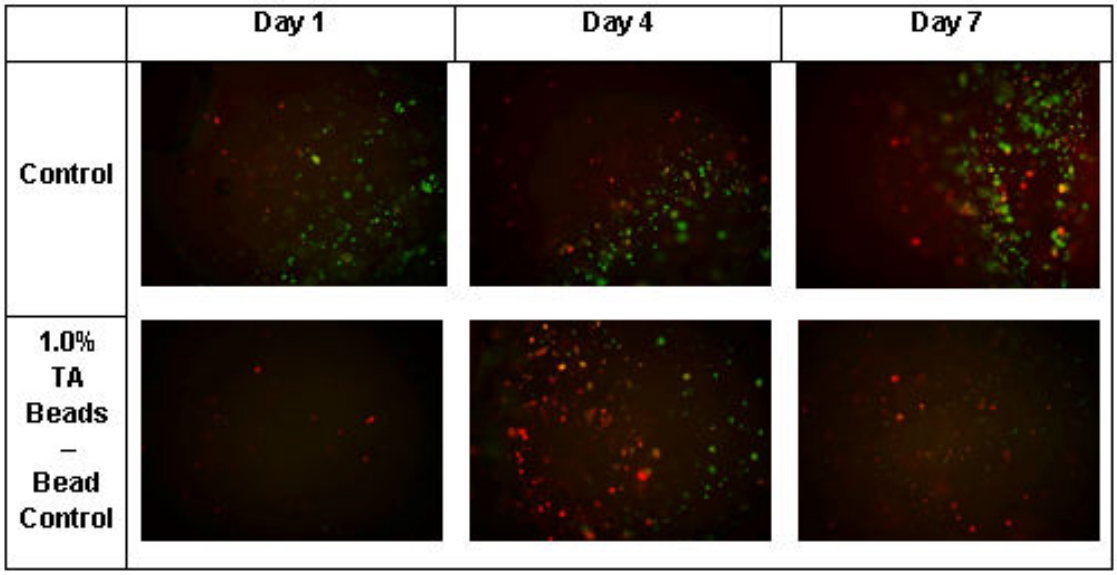

Figure 5.10: *Live/ Dead analysis on the collagen/ agarose gels in the repeat study that were exposed to beads that were not seeded with SW872 cells. Red dots signify dead MCF-7 cells, green dots signify live SW872 cells, and yellow dots signify live MCF-7 cells. All pictures were taken at a total magnification of 250x.*

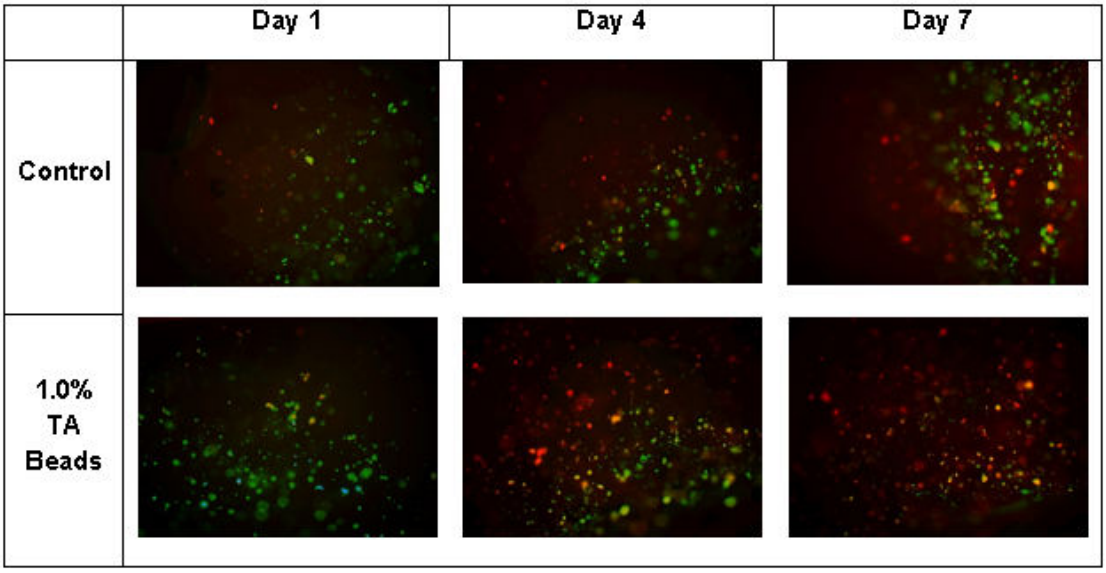

Figure 5.11: *Live/ Dead analysis on the collagen/ agarose gels in the repeat study that were exposed to beads that were seeded with SW872 cells. Red dots signify dead MCF-7 cells, green dots signify live SW872 cells, and yellow dots signify live MCF-7 cells. All pictures were taken at a total magnification of 250x.*

F-C Assay

For statistical analysis, all absorbance readings were first used to calculate all TA concentration values and then these calculated values were averaged to obtain the overall average concentration for each condition.

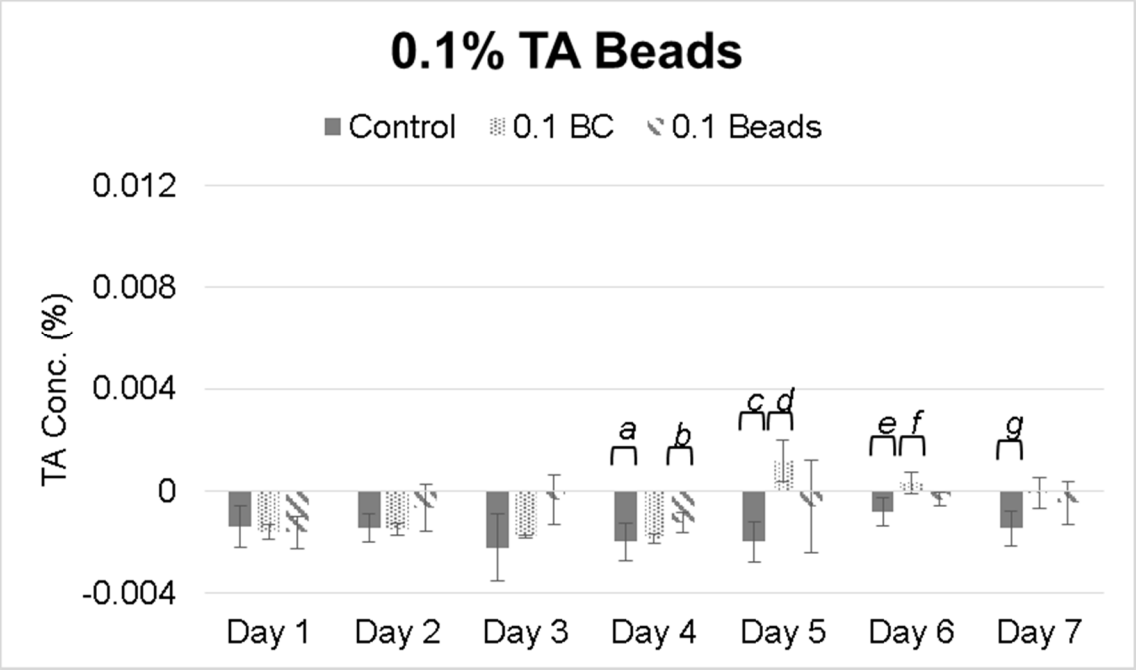

Figure 5.12: *TA concentration measurements of medium samples collected from the wells of the day 7 well plate that were exposed to 0.1% TA cross-linked beads as well as the day 7 control wells in the main study. The control group was not exposed to any TA-cross-linked beads. Those marked as 0.1 BC are 0.1% TA bead control beads that were not seeded with SW872 cells. Those marked as 0.1 beads are 0.1% TA beads that were seeded with SW872 cells. Letters signify statistical significant difference (p>0.05) between the three groups within each time point. The bead control group had n=3 for each average TA concentration, all other groups had n=9.*

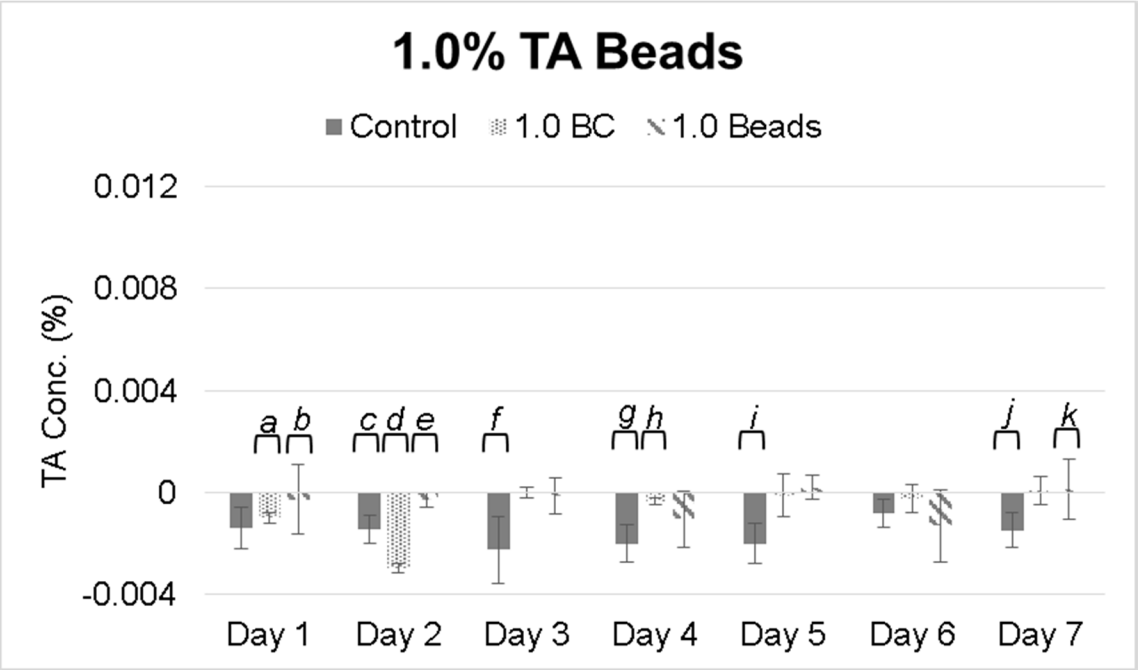

Figure 5.13: *TA concentration measurements of medium samples collected from the wells of the day 7 well plate that were exposed to 1.0% TA cross-linked beads as well as the day 7 control wells in the main study. The control group was not exposed to any TA cross-linked beads. Those marked as 1.0 BC are 1.0% TA bead control beads that were not seeded with SW872 cells. Those marked as 1.0 beads are 1.0% TA beads that were seeded with SW872 cells. Letters signify statistical significant difference (p>0.05) between the three groups within each time point. The bead control group had n=3 for each average TA concentration, all other groups had n=9.*

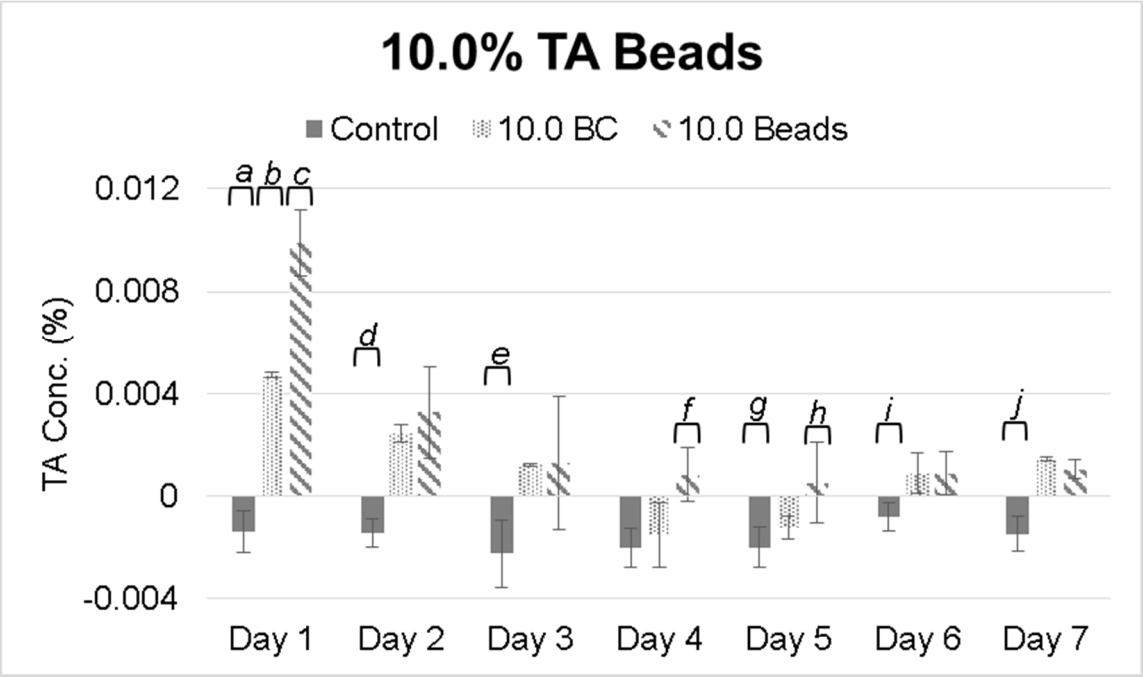

Figure 5.14: *TA concentration measurements of medium samples collected from the wells of the day 7 well plate that were exposed to 10.0% TA cross-linked beads as well as the day 7 control wells in the main study. The control group was not exposed to any TA-cross-linked beads. Those marked as 10.0 BC are 10.0% TA bead control beads that were not seeded with SW872 cells. Those marked as 10.0 beads are 10.0% TA beads that were seeded with SW872 cells. Letters signify statistical significant difference (p>0.05) between the three groups within each time point. The bead control group had n=3 for each average TA concentration, all other groups had n=9.*

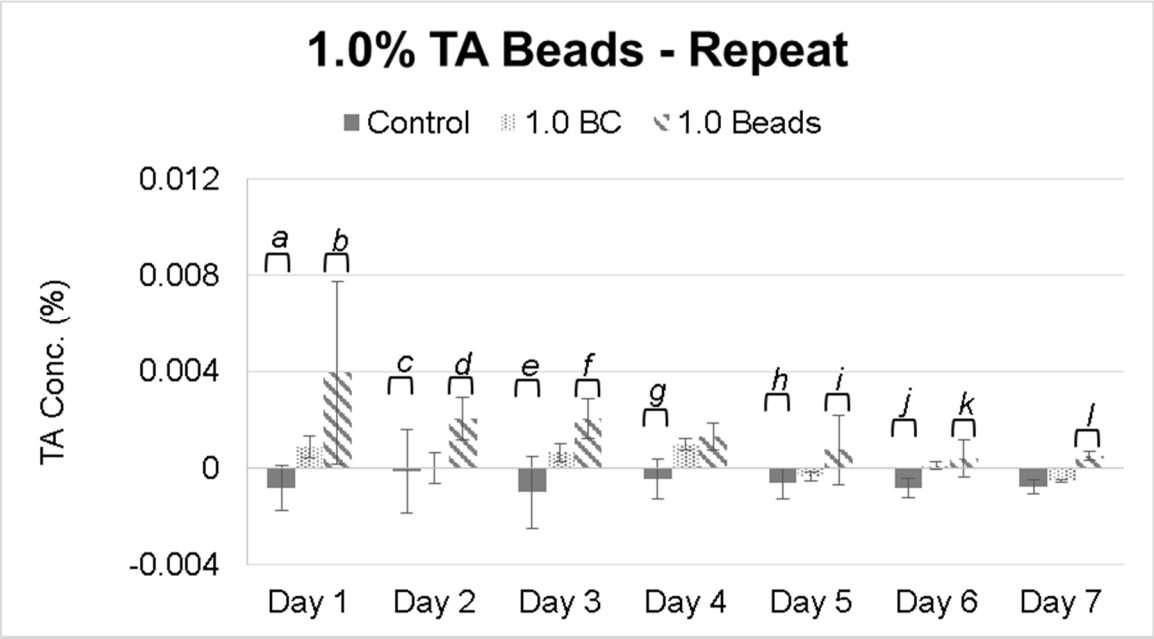

Figure 5.15: *TA concentration measurements of medium samples collected from the wells of the day 7 wells that were exposed to 1.0% TA cross-linked beads in the repeat study. The control group was not exposed to any TA cross-linked beads. Those marked as 1.0 BC are 1.0% TA bead control beads that were not seeded with SW872 cells. Those marked as 1.0 beads are 1.0% TA beads that were seeded with SW872 cells. Letters signify statistical significant difference (p>0.05) between the three groups within each time point. The bead control group had n=3 for each average TA concentration, all other groups had n=9.*

5.4 Discussion

The Live/ Dead assay performed on the different bead types show similar results to those that were seen in previous studies. The images captured by this assay allowed a qualitative assessment of the ability of the TA beads to function as scaffolds for the SW872 cells. Previous studies only explored the functionality of the beads as a scaffold

over a 3-day time period. The results of this assay gave a better overall idea of how the beads might function as scaffolds for a longer duration. For this experiment, the assay shows that both the 0.1% and 1.0% TA cross-linked collagen beads are able to initially provide a viable scaffold on which preadipocyte cells attach and grow. This can be seen in the day 1 results for this assay, where a large number of viable cells can be seen attached to the beads. The 0.1% TA beads continued to show this characteristic through the rest of the 7-day duration for this experiment. However, by day 4, the 1.0% TA cross-linked beads had fewer viable cells attached to the beads and by day 7, the number of viable cells had severely decreased when compared to the initial cell count on day 1. This characteristic was seen in both the main study as well as the repeat study. The 10.0% TA cross-linked collagen beads did not appear to be viable scaffolds for the preadipocytes. Very few viable preadipocyte cells were attached to the 10.0% TA beads on day 1 and this was seen throughout the duration of the experiment.

The live/ dead assay performed on the gels showed the effects the TA eluted from the different bead types had on the embedded MCF-7 cells. The purpose of this assay was to show the effect the TA eluting from the beads had on the cancerous cells embedded within the collagen/ agarose gels. It is important to note that the magnitude of fluorescence for the different fluorescent images is not equal. The green fluorescence was much brighter and easier to detect during image capture compared to that of the red fluorescence. Therefore, some of the images may have overrepresented live SW872 cells, which only fluoresced green. The primary focus while doing this analysis was the prevalence of the dead MCF-7 cells, which only fluoresced red. The red fluorescent protein tagging of these cells enabled the differentiation between the MCF-7 cells and the SW872 cells during this assay. The number of red cells appearing after overlaying

the two fluorescent pictures provided insight on how well the MCF-7 cells were able to survive in the gels. Both beads that had been seeded with SW872 cells and beads that had not been seeded, i.e. the bead controls, were exposed to the gels to also explore the effect cells growing on the beads had on the elution rate of TA from the beads and to explore whether the altered elution rate had an effect on the embedded MCF-7 cells.

The gels that were exposed to the bead controls showed a slight increase in the amount of dead MCF-7 cells as the study progressed from day 1 to day 7. There was also a more pronounced effect seen as the concentration of TA used to crosslink the beads was increased. By day 4, compared to the overall control group, there was a larger number of dead MCF-7 cells, suggesting that the exposure of the gels to the bead controls escalated the death rate of the embedded MCF-7 cells. However, by day 7, the bead control groups had very similar levels of dead MCF-7 cells when compared to the overall control group. This suggests that by day 7, the death rate of the MCF-7 cells had returned to a normal level. This effect was also seen in the repeat study.

A similar effect was seen in the gels that were exposed to beads that had SW872 cells seeded on them. By day 4, there was a clear increase in the number of dead MCF-7 cells for all bead types when compared to the overall control group. However, by day 7, the 0.1% and 10.0% TA bead groups had similar levels of dead MCF-7 cells when compared to the overall control group. Contrary to results seen in the bead control group, the 1.0% TA beads still had a higher level of dead MCF-7 cells by day 7. This was seen in both the main study as well as the repeat study. This suggests that the level of TA within the medium was able to persist longer than that in the bead control group, and continued to cause apoptosis of the cancerous cells at an escalated level.

The F-C assay analysis of the 0.1% TA cross-linked beads showed that the level of TA within the medium did not have a significant difference when compared to either the overall control group or the bead control group for the majority of the study. Past day 3, there were statistically significantly different values obtained, but these values were so very close to each other that there was no scientific significance of these values. The amount of TA that eluted from the beads in either group did not cause a significant change in TA levels over the 7-day time period of the study.

The F-C assay of the 1.0% TA cross-linked beads had similar levels to those seen in the 0.1% TA cross-linked beads. The levels were slightly higher for the 1.0% TA beads when compared to the 0.1% TA beads and the 1.0% TA beads that were seeded with SW872 cells consistently had a statistically different value when compared to the overall control and bead control groups. This pattern was seen in both the main study and the repeat study.

Results of the F-C assay of the 10.0% TA cross-linked beads showed an elevated level of TA concentration for the first 3 days when compared to the other types of beads. It also consistently showed higher levels of TA elution for those beads that had been seeded with SW872 cells for the first 3 days of the experiment and consistently showed higher levels when compared to the overall control group for the 7 days.

5.5 Conclusions

Based on these results, there are some key conclusions that can be made about the effect of the different TA cross-linked collagen beads on a 3D cell culture of cancerous MCF-7 cells. As previous studies have shown, this study also confirms that

the beads are able to provide a viable scaffold for the preadipocyte SW872 cells when the concentration of TA used to crosslink the beads is between 0.1% and 1.0% TA. At 1.0% TA, the cells were able to attach and remain viable for the first 24 hrs but, by day 4, the viable cell number decreased.

The 0.1% TA cross-linked collagen beads, while able to provide a viable scaffold, were not able to elicit a significant negative effect on the embedded MCF-7 cells. This is most likely due to the low concentration of TA contained within the beads themselves. Results from the F-C assay showed very little TA release from either of the bead groups into the surrounding medium compared to the control group. While some effect could be seen in the Live/ Dead assay of these gels, it was not to a significant degree.

The 10.0% TA cross-linked collagen beads showed the reverse characteristics of those seen in the 0.1% TA beads. The preadipocyte SW872 cells were unable to attach and remain viable on these beads due to the high concentration of TA contained within them. However, the high level of TA contained within the beads was able to cause a significant effect on the embedded MCF-7 cells by greatly increasing the level of cell death as seen by the Live/ Dead assay of the gels.

Initially, the 1.0% TA cross-linked collagen beads appeared to hold both the characteristics of providing a viable scaffold for the preadipocytes to grow on as well as cause an increase in the level of cell death for the cancerous MCF-7 cells. However, by day 4, it can be seen that the number of viable cells attached to the 1.0% TA beads had decreased and by day 7, the number of viable cells was drastically reduced when compared to day 1. However, the persistence of the cells to remain viable on the 1.0% TA beads beyond day 1 and up to day 4 suggests a possible explanation as to why the level of cell death of the MCF-7 cells was higher on day 7 as compared to the other

groups. With cells still growing on the 1.0% TA beads, they were able to increase the release rate of the TA from the beads due to their remodeling activities on the beads. Therefore, the release rate of the TA from the 1.0% TA beads stayed at a more consistent rate over a longer period of time.

As stated before, cells were continually growing on the 0.1% TA beads but the level of TA contained within the beads was too low to cause a significant level of cell death to the MCF-7 cells, causing the day 7 results to appear similar to that of the control group. Also, the 10.0% TA beads did not show a significant number of viable cells attached to the beads so most of the TA that it eluted from the beads was free TA that was captured within the porous structure of the bead. With medium changes every 24 hrs, the eluted TA was removed with the old medium and without cellular activity on the beads to cause any further release of TA, by day 4, these beads were not eluting any more TA into the surrounding medium, reducing the effect the beads have on the MCF-7 cells within the gels. However, the 1.0% TA beads were able to allow SW872 cells to remain viable on them for up to 4 days, as can be seen in the Live/ Dead results. Therefore, despite the regular changing of old medium for new, the cellular activity on the beads caused a prolonged release of TA from these beads into the surrounding gel, thus causing a greater impact on the embedded MCF-7 cells by day 7.

CHAPTER 6

EVALUATION OF THE EFFECTIVNESS OF TA BEADS IN A THREE-DIMENSIONAL (3-D) ENVIRONMENT WHEN SEEDED WITH PRIMARY HUMAN PREADIPOCYTES

6.1 Background

The purpose of this experiment was to provide a model that better mimics the *in vivo* environment of the breast. To do this, the preadipocyte cells that were used in this study were primary human preadipocytes harvested from donated breast fat tissue samples. By replacing the preadipocyte cell line developed in a lab with primary human preadipocytes, it provided a better overall image of how the developed TA cross-linked collagen beads interact within an environment similar to the human body. This was done to ensure that the results seen in a laboratory setting are comparable to what a researcher would expect within the human body in terms of cellular reactions.

In order to give an accurate comparison, the methodology of this experiment was performed exactly the same as what was done in the previous 3D environment study except for the substitution of the SW872 cells with the harvested primary human preadipocytes.

6.2 Materials and Methods

Primary Human Preadipocyte Isolation and Cell Culture

After receiving IRB approval to use human tissue samples, the Cooperative Human Tissue Network, CHTN, was contacted to provide donated samples of human fat tissue harvested from the breast. It was designated that the samples be normal

biospecimen with no significant medical conditions and no presence or history of cancer. The donors were required to be females of any race between the ages of 25 and 65 who have not received chemotherapy or radiation therapy, and the samples could be from a surgery, an autopsy, or a transplant procedure. All samples were required to be delivered within the first 48 hrs of retrieval from the patient and be prepared with either RPMI, DMEM, or PBS with antibiotics and antimycotic fungizone. Using these requirements, CHTN supplied two tissue samples.

Prior to the tissue samples arriving, scissors, forceps, and metal strainers were autoclaved to be sterile for use during the preadipocyte isolation procedure. When the tissue sample arrived, it was placed on a sterile disposable petri dish and rinsed 3 times with PBS (Sigma Aldrich; St. Louis, MO) that had been warmed in a 37°C water bath. The rinse was done to remove any access blood or debris from the tissue sample. Then, any excess connective tissue and blood vessels were removed using the autoclaved scissors and forceps. The tissue was then minced with the scissors and placed into a sterile 50 mL centrifuge tube (Corning; Corning, NY). To the centrifuge tube was added 20 mL of a prepared collagenase solution. The collagenase solution was prepared the day before from 500 mL of DMEM medium (Atlanta Biologicals; Flowery Branch, GA) supplemented with 5 mL of AA (Gibco; Great Island, NY) and 1 mL of fungizone (Gibco; Great Island, NY). A volume of 100 mL of the prepared DMEM solution was then mixed with 200 mg of Type I collagenase and 200 mg of Type II collagenase as well as 2% BSA. The prepared collagenase solution was then sterile filtered. After the addition of the collagenase solution to the centrifuge tube containing the minced tissue, any remaining collagenase solution was placed in the freezer to be used again.

The centrifuge tube containing the minced tissue and the collagenase solution was then placed in the incubator at 37°C for 45 minutes. At the end of the 45 minutes, the centrifuge tube was shaken by hand vigorously to aid in the breakup of any remaining large pieces of fat tissue. The digested material was then filtered through the sterilized metal strainer into another sterile 50 mL centrifuge tube to remove any remaining tissue fragments. This solution was then diluted with DMEM: F12 (ATCC; Manassas, VA) to minimize the collagenase activity. The tube was then spun for 10 minutes at 1000 rpm. After the 10 minutes, the fluid within the tube had separated into three layers, a top layer of fat and oil, a middle aqueous layer, and the sediment of preadipocytes and endothelial cells. The top two layers were aspirated off and the cell pellet was resuspended in 20 mL of red blood cell lysis buffer for 10 minutes. The lysis buffer was composed of 77 mL of 1 M NH_4Cl, 50 mL of 100 mM $KHCO_3$, 5 mL of 10 mM EDTA and 368 mL of ddH_2O. The resulting suspension was then spun for 5 minutes at 1000 rpm. Again, the top two layers were aspirated and the final pellet was resuspended in 5 mL of DMEM: F12 supplemented with 5 mL AA, 1 mL of fungizone, and 10% FBS, and then seeded in a T-25 cell culture flask. The flask was the placed in the incubator at 37°C with 5.0% CO_2.

Cell Culture

MCF-7 cells were obtained from ATCC (Manassas, VA). The isolated primary human preadipocytes and the MCF-7 cells were cultured with DMEM: F12 medium, also purchased from ATCC. The use of DMEM: F12 medium was recommended for use with the primary human preadipocyte cells and in order to keep variables consistent, the MCF-7 cells were also cultured in this medium. The MCF-7 cells had also been tagged

with red fluorescent protein in order to distinguish between the two cell types during analysis. The medium was also supplemented with 10% fetal bovine serum (FBS) as well as 1% antibiotic- antimycotic (AA) and 0.2% fungizone to help prevent contamination. Both cell types were grown in cell culture flasks incubated at 37 °C with 5.0% CO_2.

Collagen/ Agarose Gel Setup

This experiment used the same modified well plate lid and Teflon plugs described in the previous experiment. For this experiment, there were three data collection time points; day 1, day 4, and day 7. The main experiment used 0.1%, 1.0%, and 10.0% TA beads, some of which were seeded with primary human preadipocyte cells, as well as have control wells that will not be exposed to TA beads. In addition to this main experiment, there will also be a repeat experiment using the same methods as the main experiment but using only 1.0% TA beads to verify the results of the main experiment. The 1.0% beads were chosen because of the results of previous studies that showed a duality in their effect on the different cell types by allowing preadipocytes to survive but causing apoptosis of cancerous cells.

There was one 12-well plate (Costar; Corning, NY) for each time point for the main experiment. There also was a 12-well plate to serve as the control group, of which only three columns were used, one per time point. In addition to these, there was a 12-well plate for all three time points of the repeat study and one 12-well plate for the control group, same as the main experiment. In total, there were six 12-well plates used for the entire experiment. However, since only 3 columns of the control plates were used, only 66 wells were used in total.

Based on previous studies, it was determined that the best ratio for of collagen to agarose to use is 1:2. At this ratio, the gel is firm enough to allow for proper sectioning without falling apart and the collagen concentration is not high enough to vigorously react with the TA eluting from the beads, causing the gel to become flakey. A 1% agarose solution (Low Gelling Temperature; Fisher Scientific; Fair Lawn, NJ) was prepared by first calculating the volume of agarose needed for the experiment. Each well received 3 mL of the 1:2 collagen/ agarose gel mixture, 1 mL of collagen and 2 mL of agarose per well. There were 66 wells used in total with 2 mL of agarose per well, resulting in 132 mL of 1% agarose solution needed. For backup purposes, 150 mL of 1% agarose solution were prepared. For this, 1.50 g of high gelling temperature agarose was weighed out and the powder was placed in a glass bottle. The glass bottle with the agarose was then autoclaved to sterilize both the agarose and the glass bottle. After being autoclaved, 78 mL of DMEM: F12 medium was added to the bottle and the bottle was then placed in a 65 °C water bath till the agarose was dissolved. 78 mL of DMEM: F12 was used for suspension of the agarose powder to account for the addition of a cell suspension that would then be added in the final steps of the initial setup. The addition of the cell suspension brought the concentration of the agarose solution to the desired 1.0%.

As the agarose was dissolving in the DMEM: F12, a 1.0 mg/mL collagen solution was prepared. With a total of 66 wells being used and each well needing 1 mL of collagen solution, a total of 66 mL of 1.0 mg/mL collagen solution was needed. To serve as a backup supply, 80 mL of collagen solution was prepared. The same procedure was used for preparing the collagen solution as what was used in preparing the collagen solution for the production of the beads. Briefly, the stock solution of collagen (PureCol;

Advanced Biomatrix; San Diego, CA) had a concentration of 3.0 mg/ mL. In order to get 80 mL of a 1 mg/mL collagen solution, 26.67 mL of the stock collagen solution was needed. This volume was then multiplied by 0.111 to calculate the amount of 10x PBS (Sigma Aldrich; St. Louis, MO) required, 2.96 mL. One tenth of the total volume of the final solution needed to be made of FBS (Corning; Manassas, NY), 8.0 mL. Finally, the rest of the desired volume is made up of serum free DMEM: F12 (ATCC; Manassas, VA), 42.37 mL. Once these volumes were combined, enough 1.0 N NaOH (Sigma Aldrich; St. Louis, MO) was added to provide a neutral pH as indicated by a color change from yellow to pink. This color change was caused by the presence of phenol red in the DMEM: F12.

The last component of the gel model is the embedded cancerous MCF-7 cells. Confluent T-150 cell culture flasks of MCF-7 cells were removed from the incubator and the total number of MCF-7 cells was counted. A total of $5.0x10^4$ cells was desired per well. This number was chosen to simulate the situation of a lumpectomy where the majority of the cancerous cells were removed by removing the cancerous mass, leaving only a few cancerous cells behind on the periphery of where the cancerous mass was located. For this experiment, the total number of MCF-7 cells was approximately $7.4x10^6$ cells, resulting in a cell suspension of $2.0x10^5$ cells/ mL. Therefore, each well was going to receive 0.25 mL of the MCF-7 cell suspension and 0.75 mL of DMEM: F12.

Once all components were prepared, 1 mL of 1% agarose solution, 1 mL of 1.0 mg/mL collagen solution, 0.25 mL of MCF-7 cells suspension, and 0.75 mL of DMEM: F12 were added to each well and mixed. The modified well plate lid was placed on top of the well plate and the PTFE plugs were inserted into the holes of the lid. The gels were allowed to set for 15 minutes in the incubator. While the gels were solidifying, the

1% agarose solution was placed back in the hot water bath to prevent it from solidifying. After the 15 minutes, the well plate was removed from the incubator, the PTFE plugs were removed from the holes, and the modified well plate lid was removed and replaced with the original well plate lid. This procedure was repeated for all well plates with the two control well plates only receiving gel mixture in the first three columns.

TA Bead Setup

Four double batches of TA (Sigma Aldrich; St. Louis, MO) cross-linked beads were prepared; one batch cross-linked with 0.1% TA, two batches cross-linked with 1.0% TA, and one batch cross-linked with 10.0% TA. One batch from each cross-linking solution type was used in the main study and the remaining 1.0% TA batch was used in the repeat study. After each batch had been made, they were stored in PBS in the refrigerator.

Sigmacote (Sigma Aldrich; St. Louis, MO) was applied to four 50 mL centrifuge tubes and allowed to dry overnight, prior to setting up the gels. This was done to prevent cells from attaching to the centrifuge tubes during the cell seeding process. The four batches of beads were removed from the refrigerator and the PBS was removed and replaced with DMEM: F12. Approximately two thirds of the beads from each batch were placed into the individual centrifuge tubes that had been treated with Sigmacote. Primary human preadipocyte cells were removed from the incubator and counted from confluent T-75 cell culture flasks. The total primary human preadipocyte cell count was 4.56×10^6 cells which was suspended in 4 mL of DMEM: F12. To each of the Sigmacote centrifuge tubes, 1 mL of the primary human preadipocyte cell suspension was added, approximately 1.14×10^6 cells per centrifuge tube. The centrifuge tubes with the beads

and the cell suspension was gently shaken and then placed in the incubator set to 37 °C at 5.0% CO_2 for one hour. During that hour, every 20 minutes, the centrifuge tubes were gently shaken and then placed back in the incubator.

At the end of the hour, the beads were removed from the incubator. The beads were then placed into the molded wells of the collagen/ agarose gels, each well receiving approximately 0.2 mL of the bead suspension. For the original experiment, the first column of the well plate received the beads that had not been seeded with the primary cells. This was to serve as a bead control group that would allow for the differentiation between the effects the beads alone have on the MCF-7 cells and any added effects the primary cells cause by growing on the beads. Each well of the first column received a different bead type. The other three columns of the well plate received a different bead type. This setup was repeated for all three experimental well plates of the main study. The control well plate did not receive any beads. For each data collection time point, one well plate was used as well as one column of the control well plate.

The well plates in the repeat study had the same experimental setup as the original except all bead control wells received 1.0% TA beads that had not been seeded with primary cells and the other three columns of the experimental plate received 1.0% TA beads that had been seeded. For each data collection time point, one bead control well was used along with one column from the experimental well plate and one column from the control well plate. 1 mL of DMEM: F12 was then added to each well and the well plates were placed in the incubator at 37°C with 5.0% CO_2. Every 24 hrs, the DMEM: F12 would be replaced with 1 mL of fresh medium.

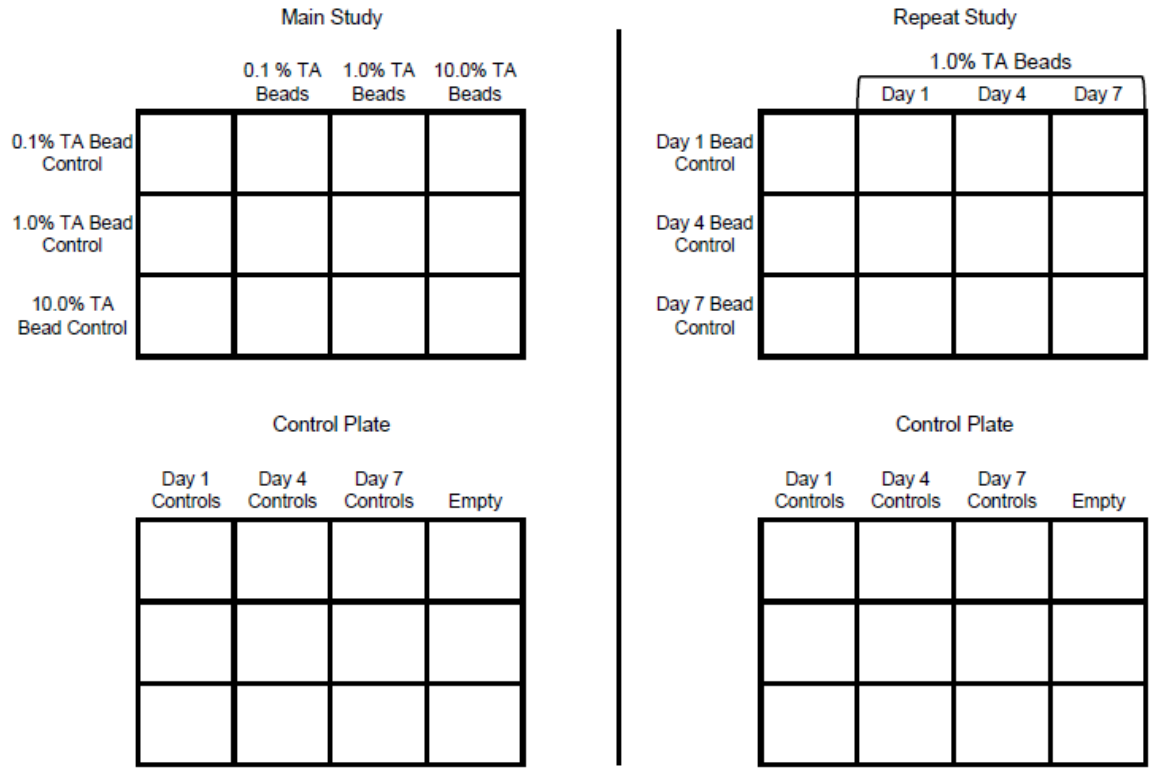

Figure 6.1: *Diagram showing the lay out for the well plates in the main study and the repeat study*

Sample Collection

Every 24 hrs, samples of the medium from the wells of the day 7 data collection time point well plate were collected along with samples from the day 7 control column of the control well plate. These samples were later used for F-C analysis to measure the rate of elution of the TA from the beads.

Two metal surgical spatulas were autoclaved before gel samples were collected. At their designated data collection time points, the well plate would be removed from the incubator along with the control well plate. The beads were removed from the wells of the experimental groups and collected in a 6-well plate (Costar; Corning, NY) and set

aside. The remaining medium was removed from the wells. Using the straight edge of the metal spatula, the gel would be loosened from the walls of the well. Using the scooping end of the spatula, the gel was then removed from the well and placed in a well of a 6-well plate. After all the gels had been removed, the straight edge of the metal spatula was used to slice the gel down the middle. Then, the two scooping ends of the two spatulas were used to reposition the two gel halves so the cut surface was face down in the well. This was done for all gels.

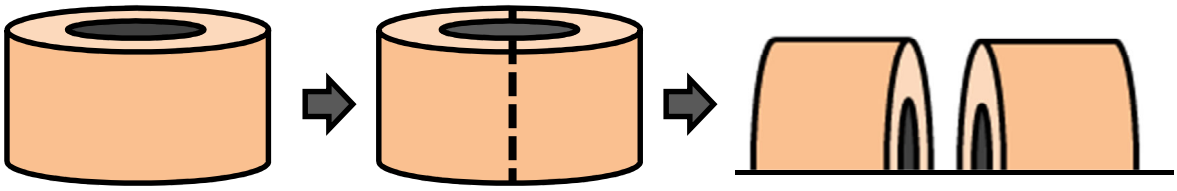

Figure 6.2: *Sectioning process of the collagen/ agarose gels.*

Live/ Dead Assay – TA Beads

After the beads had been placed in the 6-well plate, any remaining medium was aspirated out of the wells. A partial Live/ Dead solution was prepared with calcein-AM (Invitrogen; Eugene, OR) and PBS alone. This solution only tags live cells with a green fluorescence and does no tagging of dead cells. 2.0 mL of the partial Live/ Dead solution was then added to each well containing the beads. The 6-well plate was then placed in a dark drawer until imaged under fluorescent light with the microscope.

Live/ Dead Assay – Collagen/ Agarose Gels

After the gels had been sectioned and repositioned, they were washed with PBS. The same partial Live/ Dead solution was made for the imaging of the collagen/ agarose gels as was used for the TA beads. Normally, this Live/ Dead solution would also tag dead cells with a red fluorescence but the MCF-7 cells were already tagged with a red fluorescent protein, making them indistinguishable from dead cells if they had been exposed to a complete Live/ Dead solution. To each well containing a sectioned gel, 2.0 mL of the partial Live/ Dead solution was added. These well plates were then placed in a dark drawer till they were ready to be imaged using fluorescent light and a microscope.

Images were then taken of the gels under both red and green fluorescent light. The red light would show the presence of the tagged MCF-7 cells and the green light would show the presence of any live cells. Using Adobe Photoshop, these two pictures were then overlaid. Any live MCF-7 cell would appear yellow because it would be fluorescing in both pictures and red fluorescence overlaid with green fluorescence produces a yellow fluorescence. Similarly, dead MCF-7 cells would only appear red in the overlaid picture because they would not also fluoresce green and any live primary cells would appear green in the overlaid picture because they would not also fluoresce red.

F-C Assay

Standards of 0.01%, 0.005%, 0.001%, and 0% TA were prepared using DMEM: F12. These standards and the collected medium samples needed to then be diluted with MilliQ water (Direct 8; Millipore; Darmstadt, Germany). This is done to prevent color saturation from occurring due to the presence of the components of the DMEM: F12

medium. For each standard and collected medium sample, 25 µL of the medium sample was combined with 75 µL of MilliQ water in a 1.5 mL micro centrifuge tube. After performing the dilution, 200 µL of a 10% Folin-Ciocalteu (F-C) reagent solution (Sigma Aldrich; St. Louis, MO) was added to each micro centrifuge tube followed by 800 µL of a 700 mM sodium carbonate solution (Fisher Scientific; Fair Lawn, NJ). All micro centrifuge tubes were then vortexed and allowed to incubate for 2 hrs at room temperature. At the end of the two hrs, the solutions were loaded in triplicate into clear bottom, black side 96 well plates (Greiner Bio One; Monroe, NC) and the absorbance of the solutions was read at 765 nm with a multi-mode micro plate reader (Synergy™ Mx; BioTek; Winooski, VT).

The absorbance readings were loaded into a Microsoft Excel worksheet, and the absorbance readings of the standards were averaged and graphed against their known concentrations. A linear trend line was fitted to the standard data points, providing an equation to model the relationship between absorbance readings and TA concentration values. This equation was then used to calculate the TA concentration of the experimental medium samples collected. The calculated TA concentrations were then averaged and graphed. Minitab, a statistics program, was then used to perform the statistical analysis on the calculated TA concentrations.

6.3 Results

Live/ Dead Assay – TA Beads

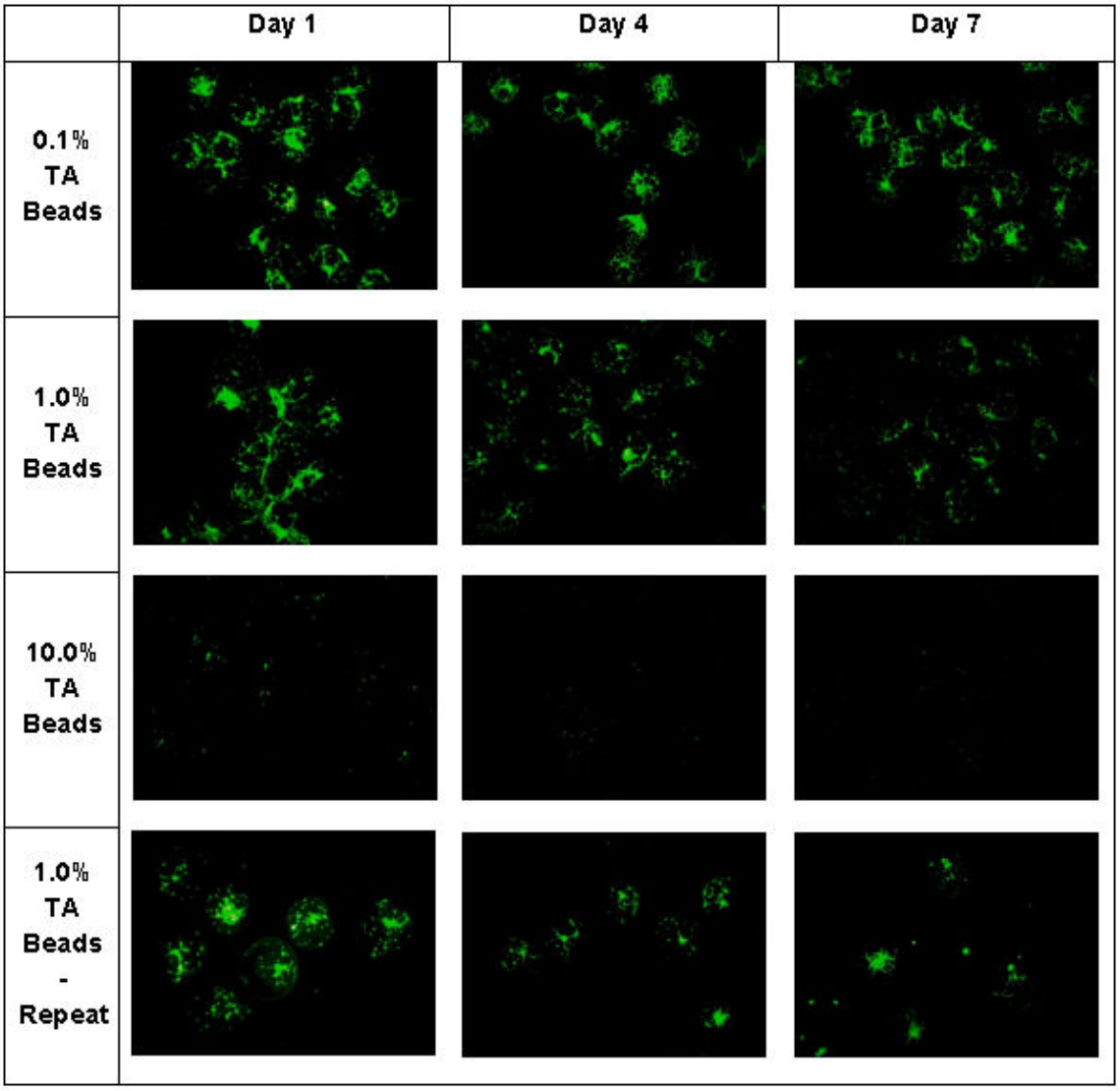

Figure 6.3: *Live/ Dead analysis on the primary cells growing on the TA cross-linked beads. Three pictures were taken of each bead type at each data collection time point. These pictures best represent the average appearance of the three pictures in each group. Bright green dots signify a live cell. All pictures were taken at a total magnification of 250x.*

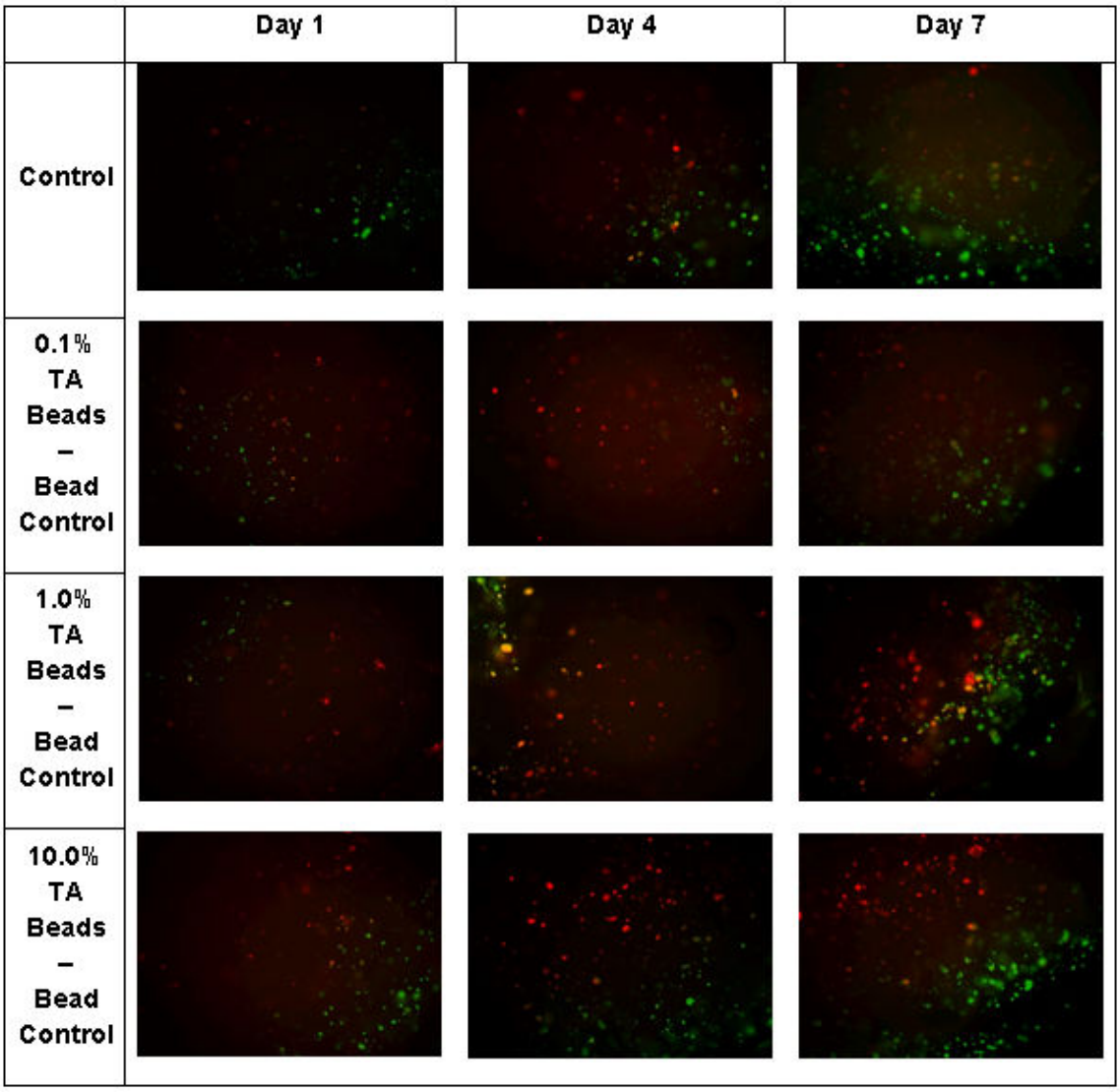

Figure 6.4: *Live/ Dead analysis on the collagen/ agarose gels in the main study that were exposed to beads that were not seeded with primary cells. Red dots signify dead MCF-7 cells, green dots signify live primary cells, and yellow dots signify live MCF-7 cells. All pictures were taken at a total magnification of 250x.*

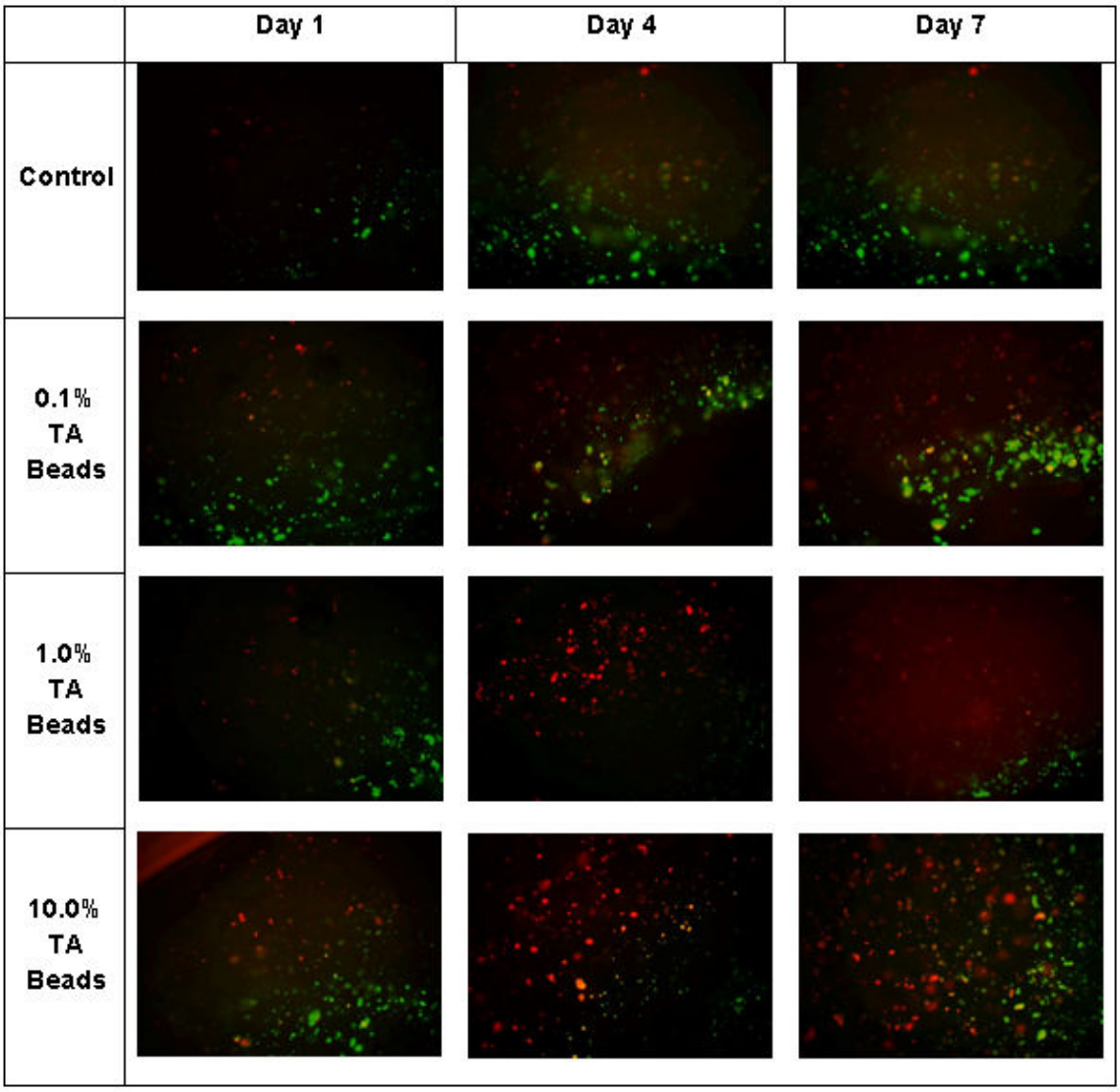

Figure 6.5: *Live/ Dead analysis on the collagen/ agarose gels in the main study that were exposed to beads that were seeded with primary cells. Red dots signify dead MCF-7 cells, green dots signify live primary cells, and yellow dots signify live MCF-7 cells. All pictures were taken at a total magnification of 250x.*

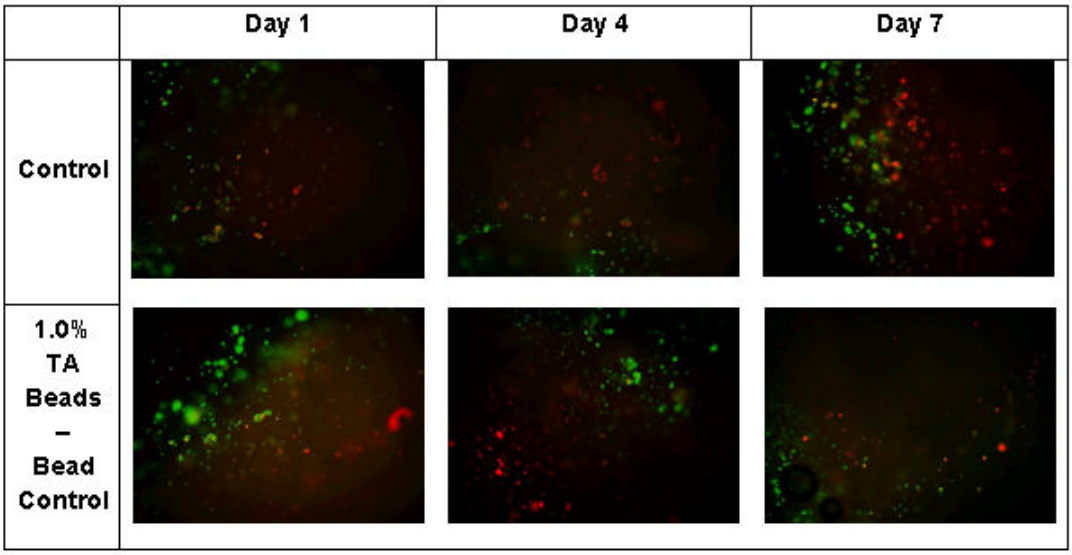

Figure 6.6: *Live/ Dead analysis on the collagen/ agarose gels in the repeat study that were exposed to beads that were not seeded with primary cells. Red dots signify dead MCF-7 cells, green dots signify live primary cells, and yellow dots signify live MCF-7 cells. All pictures were taken at a total magnification of 250x.*

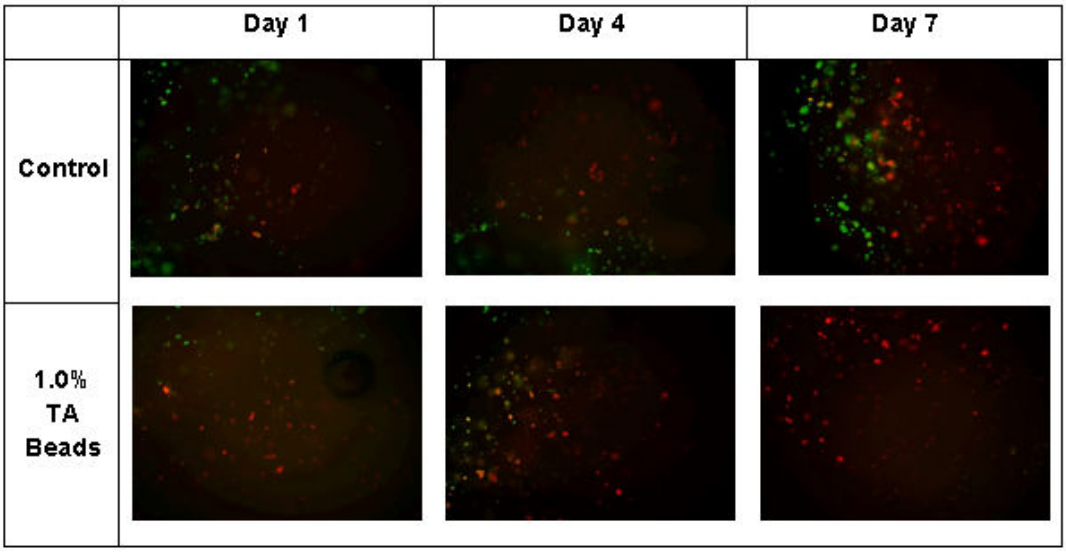

Figure 6.7: *Live/ Dead analysis on the collagen/ agarose gels in the repeat study that were exposed to beads that were seeded with primary cells. Red dots signify dead MCF-7 cells, green dots signify live primary cells, and yellow dots signify live MCF-7 cells. All pictures were taken at a total magnification of 250x.*

F-C Assay

For statistical analysis, all absorbance readings were first used to calculate all TA concentration values and then these calculated values were averaged to obtain the overall average concentration for each condition.

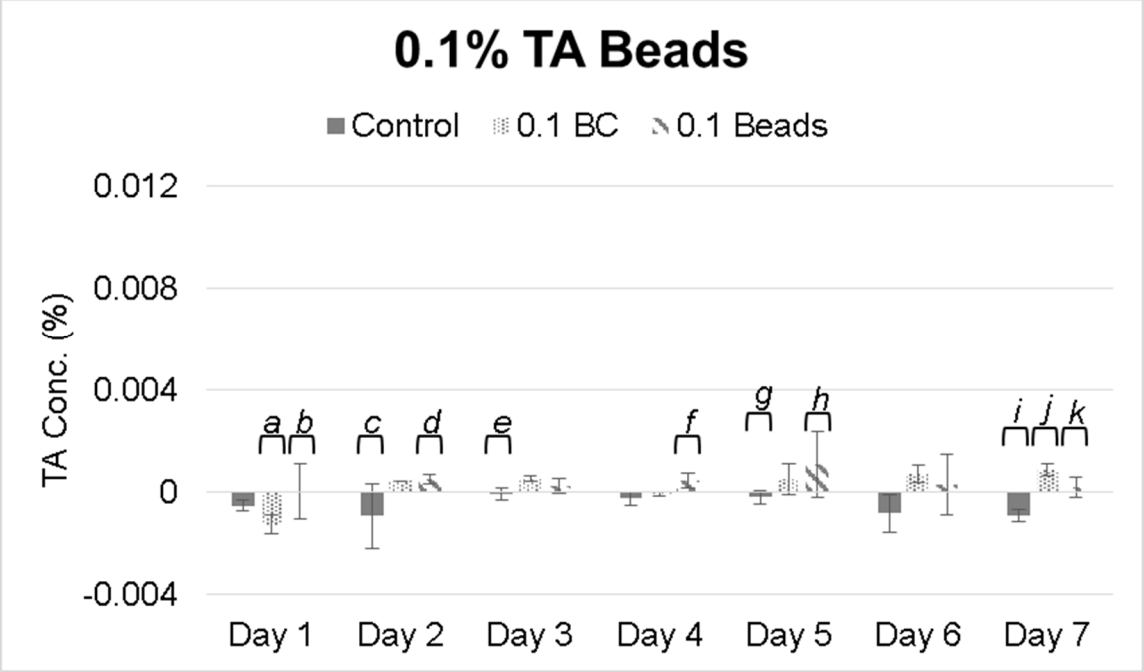

Figure 6.8: *TA concentration measurements of medium samples collected from the wells of the day 7 well plate that were exposed to 0.1% TA cross-linked beads as well as the day 7 control wells in the main study. The control group was not exposed to any TA cross-linked beads. Those marked as 0.1 BC are 0.1% TA bead control beads that were not seeded with primary cells. Those marked as 0.1 beads are 0.1% TA beads that were seeded with primary cells. Letters signify statistical significant difference (p>0.05) between the three groups within each time point. The bead control group had n=3 for each average TA concentration, all other groups had n=9.*

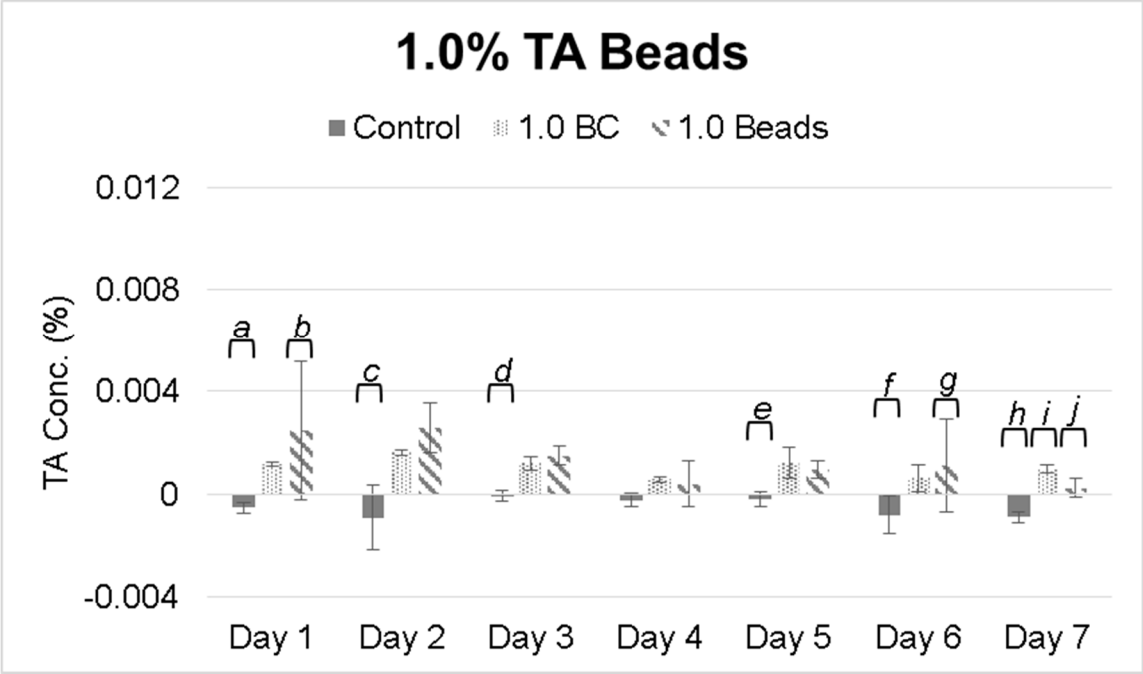

Figure 6.9: *TA concentration measurements of medium samples collected from the wells of the day 7 well plate that were exposed to 1.0% TA cross-linked beads as well as the day 7 control wells in the main study. The control group was not exposed to any TA cross-linked beads. Those marked as 1.0 BC are 1.0% TA bead control beads that were not seeded with primary cells. Those marked as 1.0 beads are 1.0% TA beads that were seeded with primary cells. Letters signify statistical significant difference (p>0.05) between the three groups within each time point. The bead control group had n=3 for each average TA concentration, all other groups had n=9.*

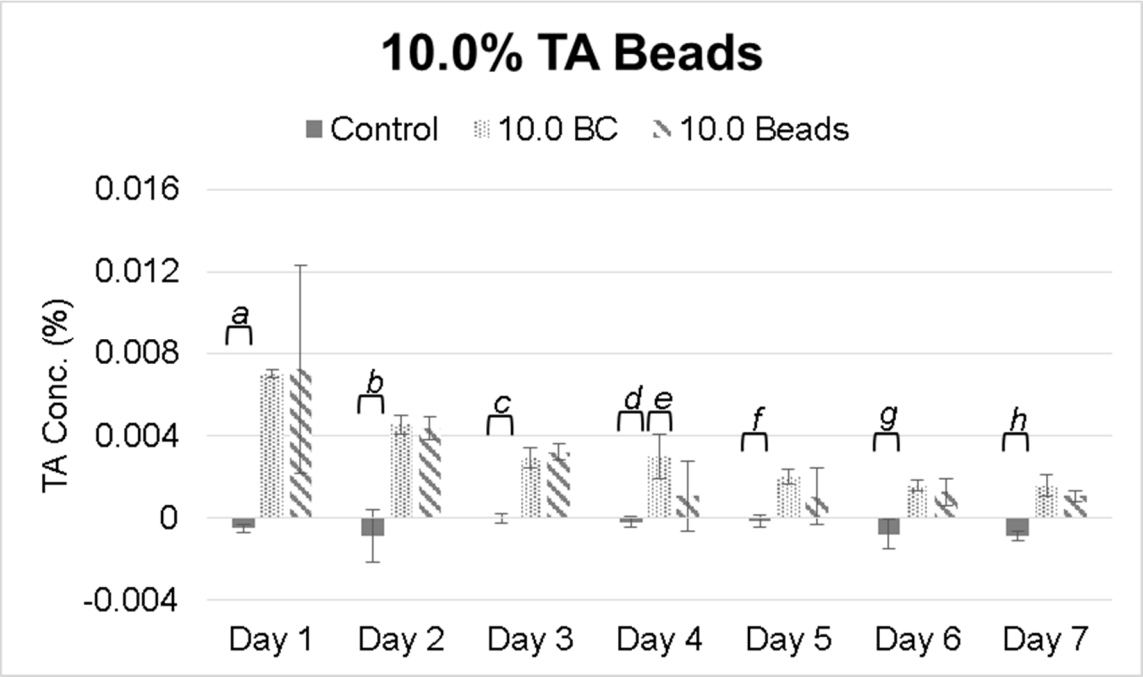

Figure 6.10: *TA concentration measurements of medium samples collected from the wells of the day 7 well plate that were exposed to 10.0% TA cross-linked beads as well as the day 7 control wells in the main study. The control group was not exposed to any TA cross-linked beads. Those marked as 10.0 BC are 10.0% TA bead control beads that were not seeded with primary cells. Those marked as 10.0 beads are 10.0% TA beads that were seeded with primary cells. Letters signify statistical significant difference (p>0.05) between the three groups within each time point. The bead control group had n=3 for each average TA concentration, all other groups had n=9.*

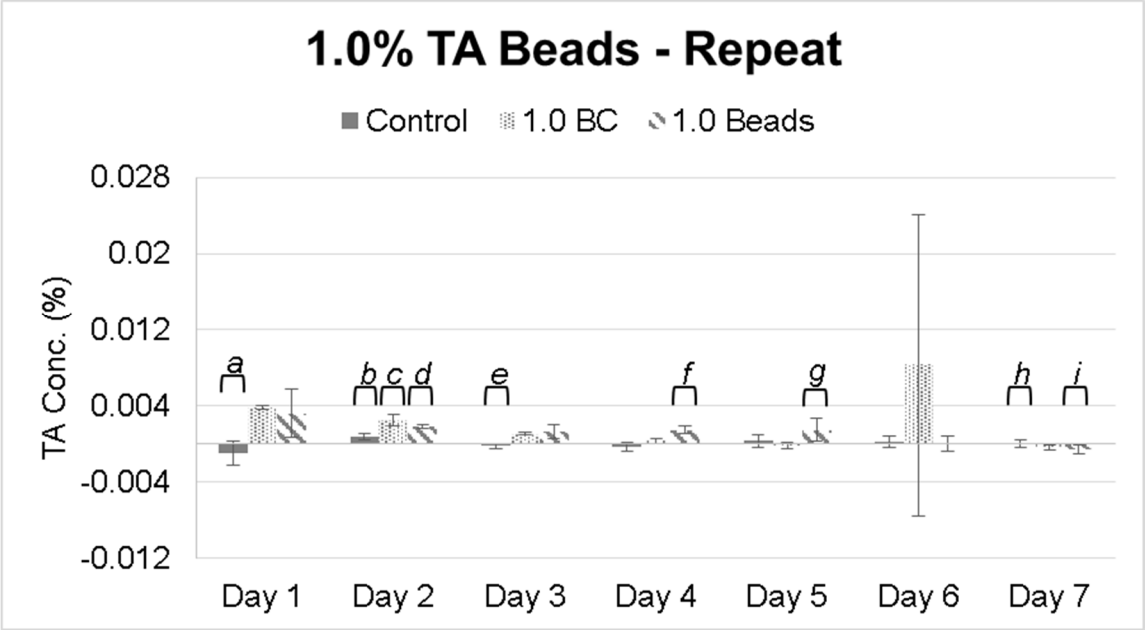

Figure 6.11: *TA concentration measurements of medium samples collected from the wells of the day 7 well plate that were exposed to 1.0% TA cross-linked beads as well as the day 7 control wells in the repeat study. The control group was not exposed to any TA cross-linked beads. Those marked as 1.0 BC are 1.0% TA bead control beads that were not seeded with primary cells. Those marked as 1.0 beads are 1.0% TA beads that were seeded with primary cells. Letters signify statistical significant difference (p>0.05) between the three groups within each time point. The bead control group had n=3 for each average TA concentration, all other groups had n=9.*

6.4 Discussion

The Live/ Dead assay performed on the different bead types show similar results to those that were seen in previous studies. For this experiment, the assay shows that both the 0.1% and 1.0% TA cross-linked collagen beads are able to initially provide a

viable scaffold for preadipocyte cells to attach and grow on. This can be seen in the day 1 results for this assay where a large number of viable cells can be seen attached to the beads. The 0.1% TA beads continued to show this characteristic through the rest of the 7 day duration for this experiment. However, by day 4, the 1.0% TA cross-linked beads are showing fewer viable cells attached to the beads and by day 7, the number of viable cells has severely decreased when compared to the initial cell count of day 1. This characteristic was seen in both the main study as well as the repeat study. The 10.0% TA cross-linked collagen beads do not show the ability to provide a viable scaffold for the preadipocyte cells to grow on. Very few viable preadipocyte cells are attached to the 10.0% TA beads on day 1 and this is seen throughout the duration of the experiment.

The live/ dead assay performed on the gels show very similar results to those seen in previous studies using SW872 cells instead of the primary preadipocytes. In this experiment the gels that were exposed to the bead controls show an increase in the amount of dead MCF-7 cells as the study progressed from day 1 to day 7. However, unlike previous studies, there is not a more pronounced effect seen as the concentration of TA used to crosslink the beads is increased. By day 7, compared to the overall control group, there is a larger amount of dead MCF-7 cells suggesting that the exposure of the gels to the bead controls has escalated the death rate of the embedded MCF-7 cells. This effect was also seen in the repeat study.

A similar effect is seen in the gels that were exposed to beads that had primary cells seeded on them. By day 4, there is a clear increase in the number of dead MCF-7 cells for all bead types when compared to the overall control group. By day 7, the 0.1% and 10.0% TA bead groups are showing slightly increased levels of dead MCF-7 cells when compared to the overall control group. The 1.0% TA beads had a significantly

higher level of dead MCF-7 cells by day 7. This was seen in both the main study as well as the repeat study. This suggests that the level of TA within the medium was able to persist longer than what was seen in the bead control group, and continue to cause apoptosis of the cancerous cells at an escalated level.

The F-C assay of the 0.1% TA cross-linked beads shows that the level of TA within the medium did not have a significant difference when compared to either of the overall control group or the bead control group for the majority if the study. The amount of TA that elute from the beads in either group did not cause a significant change in TA levels over the 7 day time period of the study.

The F-C assay of the 1.0% TA cross-linked beads shows similar levels to those seen in the 0.1% TA cross-linked beads. Levels are slightly higher for the 1.0% TA beads when compared to the 0.1% TA beads and the 1.0% TA beads that were seeded with primary cells consistently show a higher value with statistically significantly difference when compared to the overall control and bead control groups. This pattern was seen in both the main study and the repeat study.

The F-C assay of the 10.0% TA cross-linked beads show an elevated level of TA concentration for the first 3 days when compared to the other types of beads. It also consistently shows statistically similar levels of TA elution for those beads that had been seeded with primary cells and those that had not been seeded with primary cells.

6.5 Conclusions

Based on what was seen in these results, the same key conclusions that were made in previous studies can be made again about the effect of the different TA cross-linked collagen beads seeded with primary cells have on a 3D cell culture of cancerous

MCF-7 cells. As previous studies have shown, this study also confirms that the beads are able to provide a viable scaffold for the primary human preadipocyte cells when the concentration of TA used to crosslink the beads is between 0.1% and 1.0% TA. At 1.0% TA, the cells were able to attach and remain viable for the first 24 hrs but by day 4, they were showing a decrease in the count of viable cells attached.

The 0.1% TA cross-linked collagen beads, while being able to provide a viable scaffold, were not able to elicit a significant negative effect on the embedded MCF-7 cells. The reason behind this is consistent with what was stated in previous studies.

The 10.0% TA cross-linked collagen beads showed the reverse characteristics of those seen in the 0.1% TA beads. The primary human preadipocyte cells were unable to attach and remain viable on these beads due to the high concentration of TA contained within them. However, the high level of TA contained within the beads was able to cause a significant effect on the embedded MCF-7 cells by greatly increasing the level of cell death as seen by the Live/ Dead assay of the gels.

The 1.0% TA cross-linked collagen beads again showed the initial dual nature that was seen in previous studies and appeared to hold both the characteristics of providing a viable scaffold for the primary human preadipocytes to grow on as well as cause an increase in the level of cell death for the cancerous MCF-7 cells. However, by day 4, it can be seen that the number of viable cells attached to the 1.0% TA beads had decreased and by day 7, the number of viable cells was drastically reduced when compared to day 1. However, the persistence of the cells to remain viable on the 1.0% TA beads beyond day 1 and up to day 4 suggests a possible explanation as to why the level of cell death of the MCF-7 cells was higher on day 7 as compared to the other groups. With cells still growing on the 1.0% TA beads, they were able to increase the

release rate of the TA from the beads due to their remodeling activities on the beads. Therefore, the release rate of the TA from the 1.0% TA beads stayed at a more consistent rate over a longer period of time. The explanation behind this is consistent with what was previously stated in the earlier studies.

It should also be noted that the primary preadipocyte cells had another effect on the beads beyond their remodeling. It was clearly seen that as the preadipocytes were proliferating on the beads, the cells were also physically squeezing the beads to the point of causing deep folds on the surface of the beads. This type of physical interaction with the beads was not seen when the SW872 cells were used. This added manipulation of the beads could have also aided in the increased TA release from the 1.0% TA beads and contribute to the higher level of MCF-7 cell death seen on day 7.

CHAPTER 7

OVERALL CONCLUSIONS

The overall goal of this work was to evaluate the efficacy of TA cross-linked collagen beads to function as scaffolds for preadipocyte cells to attach and proliferate on as well as explore the efficacy of the beads to demonstrate anti-cancer properties to breast cancer cells. This goal was evaluated with the use of three different types of collagen beads that varied on the concentration of TA used to crosslink them during their production; 0.1% TA, 1.0% TA, and 10.0% TA beads. These same three bead types were used throughout all the studies and the results obtained during the studies were checked against a repeat study using only 1.0% TA beads.

The efficacy of the beads to function as a scaffold was consistently checked throughout all three studies. The results of all three studies show that the collagen beads cross-linked by 0.1% TA showed the best ability to allow cell attachment and proliferation. This was consistently demonstrated in both the 2D model studies as well as the 3D model studies. Both study types showed that the 0.1% TA cross-linked beads were able to provide a scaffold that cells could readily attach to and proliferate throughout the duration of the experiments, up to 7 days. This held true for both SW872 cells, a laboratory-derived cell line, and primary human preadipocytes.

The 1.0% TA beads consistently showed an initial ability to allow for proper cell attachment of the preadipocytes but as the study would progress, there would be a sharp decrease in the number of viable cells attached to the beads. Based on the consistency of these results it can be concluded that these beads do not provide a viable scaffold for preadipocyte cell growth longer than 3 days. Beyond the 3-day time period,

the attached cells are unable to withstand the effects of being in direct contact with the TA elution source and die. This effect was seen with both SW872 cells and primary human preadipocytes. It was demonstrated in the 2D model study that SW872 cells were able to survive 1.0% TA cross-linked beads when not in direct contact with them so there may be an advantage of using these beads for optimal timing when implanted. If implanted without being seeded with preadipocyte cells, the eluted TA could cause apoptosis of the cancerous cells still present around the implant site. The preadipocytes present around the implant site may survive this level of exposure and once the TA has been flushed out of the site by the body, preadipocyte cells may migrate into the scaffolds and start the regrowth of the lost tissue. The 10.0% TA beads consistently showed an inability to support preadipocyte attachment and growth. The concentration of TA is too high for the preadipocytes to withstand and subsequently die.

In the 2D and both of the 3D model studies, the 0.1% TA cross-linked beads were unable to demonstrate a significant effect on the cancerous MCF-7 cells. This is because the concentration of TA eluting from these beads does not reach a high enough concentration to cause significant apoptosis of these cancerous cells. In most cases, the results of the modified F-C assay showed that the levels of TA measured within the medium samples collected from wells exposed to the 0.1% TA cross-linked beads did not show levels significantly higher than those seen in the control wells. Also, the results of the TUNEL assay showed an inability of the 0.1% TA beads to induce apoptosis, only causing a maximum level of 26% apoptosis of the cancerous cells. These beads do not contain enough TA to provide a significant effect on the cancerous MCF-7 cells.

Both of the 1.0% and 10.0% TA beads were able to show a significant effect on cancerous cells. The TUNEL assay results of the 2D model study show a significant

level of induced apoptosis for the MCF-7 cells that were exposed to these bead types. The modified F-C assay results for both the 2D and 3D models showed an elevated level of TA in the medium when compared to the controls. This elevated level of TA present within the medium does reach a high enough concentration to cause a significant negative effect on the survival of the MCF-7 cells.

Considering these results as a whole, it is apparent that the ideal bead that can cause apoptosis of cancerous cells but also allow for preadipocyte attachment and proliferation was not found in this study. The 1.0% TA cross-linked beads showed the closest characteristics to this ideal but the preadipocytes were not able to survive for a long duration when growing in direct contact with the beads. Therefore, the ideal bead TA cross-linking concentration is between the range of 0.1% and 1.0% TA.

Another commonality that was seen between all the studies and worthy of mention is the release rate of the TA from the different bead types. Based on the results of the F-C assays performed during these studies, the majority of the TA released from all bead types occurs within the first 48 to 72 hrs of incubation at 37°C. If these beads were to be implanted within the body, this type of bolus release of TA may be too quick to provide the anti-cancer properties that were seen in the lab due to the body metabolism and general circulation removing the released TA from the implant site.

Lastly, the efficacy of the developed F-C assay during the evaluation of the studies provide a confirmation of the effectiveness of the modified procedure. The results of this assay were consistent and provided results that were consistent with what was being observed in the results of other established assays.

CHAPTER 8

RECOMMENDATIONS FOR FUTURE WORK

1. Mechanical testing to determine the stiffness of the beads was attempted but was not able to be concluded. Atomic force microscopy proved difficult due to the hydrogel nature of the beads and their delicate nature. The use of an Instron machine to perform compressive tests on the beads was promising but the available load cells were too high to provide the needed measurements. It is recommended that an Instron with a maximum load cell of 5 N be used for these measurements to accommodate for the delicate nature of the beads and allow for viable measurement values.

2. Further exploration of collagen beads cross-linked with TA at a concentration between 0.1% and 1.0% is needed. As stated before, the results of these studies demonstrate that the ideal bead cross-linking concentration of TA in which preadipocytes can grow on the bead as well as have the bead elute enough TA to cause apoptosis of cancerous cells is within that range.

3. The development of the beads to be an injectable scaffold must be further modified. Currently, the beads used measure a diameter of 1.5 mm on average. In order to manufacture injectable beads, methods of decreasing their diameter need to be explored, perhaps the use of a smaller gauge needle will provide the solution.

4. A delivery system for these beads must be explored in which either the elution rate of the TA into the surrounding medium will be reduced to prevent the bolus effect seen in these studies or the TA is protected from the effects of the body attempting to flush it from the implant site. This would ensure that the TA has the needed time to perform its desired anti-cancer properties.

5. These studies only focused on the effects the beads have on one type of cancer cell line. It is well known that there are many different breast cancer cell types and further exploration of the efficacy of these beads on these other cancer cell types is needed.

6. These studies were primarily focused on the functionality of the scaffolds and did not delve in depth into the effect the scaffold has on the cells growing on it. Further studies must be performed to evaluate the phenotypic effect the scaffold has on the cells that are growing on it to ensure that the preadipocyte cells are still functioning normally and still showing potential to differentiate into mature adipocytes.

7. The amount of MCF-7 cell death seen in the gel studies needs to be quantified. This should be done to better account for the effect of the different bead types on the embedded MCF-7 cells instead of using qualitative analysis alone. This could be done by simply counting the total number of MCF-7 cells from the red fluorescent image as well as the total number of dead MCF-7 cells in the overlaid image. These values could then be used to calculate the percent survival of the embedded MCF-7 cells.

8. The methodology used to quantify the amount of Tannic Acid contained within the beads after being processed needs to be further refined. Using a method in which the dilutions of the different samples and standards was consistent would be preferred in order to provide a more accurate result. Also, tannic acid that may have eluted out during the subsequent washes after the TA cross-linking solution were not taken into account. This should also be done to better represent what the final concentration of tannic acid is within the different bead types.

APPENDICES

Appendix A

Use of Electrostatic Syringe Pump for the Development of TA Cross-linked Collagen Beads

MATERIALS:

1.4% m/v Alginate Solution w/ MiliQ Water
3.1 mg/mL Bovine Collagen Solution
Fetal Bovine Serum (FBS)
10x Phosphate Buffered Saline Solution (PBS)
Dulbecco's Modified Eagle Medium (DMEM) – Serum Free
1N NaOH Solution w/ MiliQ Water
1.5% m/v $CaCl_2$ Solution w/ MiliQ Water
100 mL Tannic Acid (TA) Cross-linking Solution w/ MiliQ Water

- 1.0g Tannic Acid (Can be altered to increase or decrease TA levels)
- 1.10g $CaCl_2$
- 1.10g CHES Buffer
- 0.78g NaCl

100 mL 50 mM Sodium Citrate Solution w/ MiliQ Water
Phosphate Buffered Saline (PBS) Solution

EQUIPMENT AND SUPPLIES:

Biological Safety Cabinet
Weigh Scale
Stir Plate
Electrostatic Bead Generator Box w/ Glassware, Needle, Tubing, Probe, and Stir Bar
Syringe Pump
Syringe (10 or 20cc)
1.5" 16G Syringe Needle
Metal Strainer
Metal Forceps
Metal Surgical Spatula

PROCEDURE:

1. Prepare a 1.4% m/v alginate solution using a stir plate with the heat level set between 1 and 2.
   * If preparing sterile beads, filter the alginate through a 50 mL centrifuge tube Nalgene filter overnight

2. Prepare 200 mL of a 1.5% m/v $CaCl_2$ solution using MiliQ Water

3. Prepare 6 mL of a 1 mg/mL Bovine collagen solution within a Biological Safety Hood
   a. 3.178 mL DMEM – Serum Free
   b. 0.222 mL 10x PBS
   c. 0.600 mL FBS
   d. 2.00 mL 3.1 mg/mL Bovine Collagen
   e. Enough 1N NaOH to neutralize the solution turning it a slight pink color (~ 20 µL)

4. Mix 4 mL of 1.4% m/v Alginate with the prepared 6 mL collagen solution

5. Assemble the pieces to the electrostatic bead generator box as pictured below
   * If making sterile beads, autoclave the pieces of the electrostatic bead generator box and wipe down the electrostatic box and syringe pump with 70% ethanol before placing them in a biological safety hood.

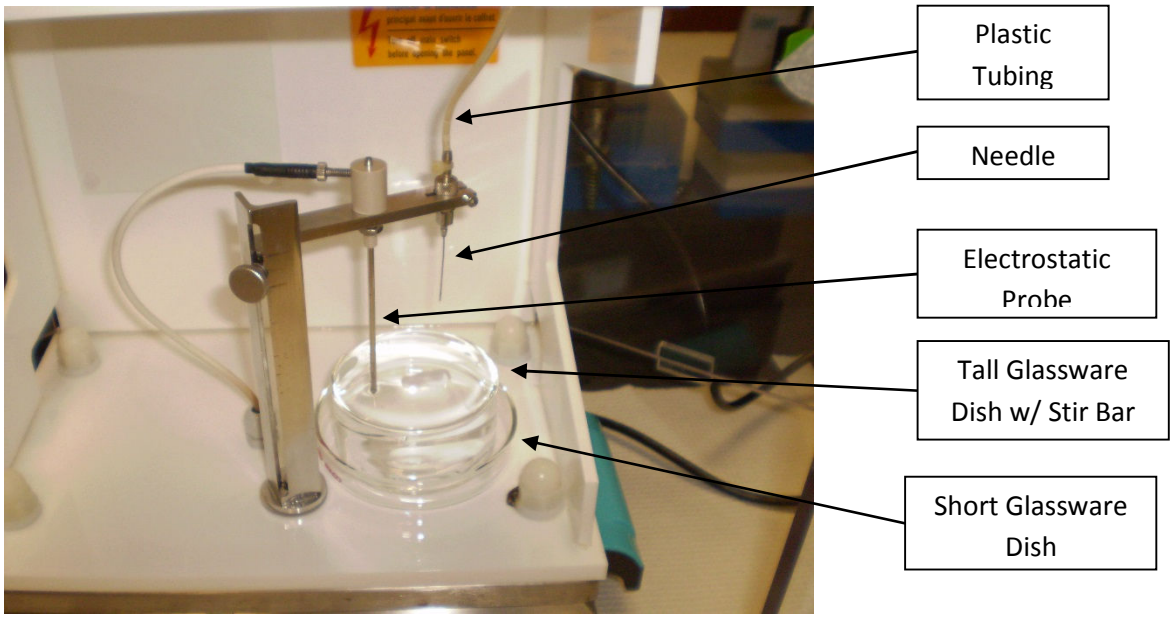

Figure A.1: *Schematic of electrostatic box setup*

6. Add the prepared 1.5% m/v $CaCl_2$ to the tall glassware dish with the stir bar till just after it overflows into the short glassware dish. Ensure that the stir bar is able to stir freely by adjusting the position of the glassware dishes.

7. Adjust the electrostatic probe within the plastic holder till approximately a quarter inch of the probe is above the plastic holder. Lower the arm assembly till the electrostatic probe is slightly immersed into the $CaCl_2$ solution.

8. Connect the needle to the plastic tubing and place the assembly in the holder with the open end of the tubing going through the slot in the roof of the electrostatic box.

9. Close the doors to the electrostatic box, right side first. Check the settings on the dials for the box:
    a. %Pump = 0%
    b. Agitator = ~15%
    c. Check the voltage by pressing the green "on" button and adjusting the voltage dial till the digital read out says 6.00. Afterwards, turn the box off by pressing the red "off" button

10. Place the syringe pump on top of the electrostatic box.

11. Attach the 16G needle to the syringe and load the syringe with the collagen/ alginate solution while attempting to minimize the number of bubbles in the syringe. Once the solution is loaded, turn the syringe so the needle points upwards and flick the syringe so all the accumulated bubbles within the solution will rise to the top. Carefully cover the needle with gauze and depress the syringe plunger till the air bubbles are removed. Carefully remove the needle and dispose of it in the red sharps container. Attach the loaded syringe to the open end of the plastic tubing and place the syringe in the syringe pump.

12. Turn on the syringe pump and press the menu button. Use the arrow buttons to select the Table option and select the appropriate syringe material and size. Set the volume to 10.0 mL and the rate to 10.0 mL/h.

13. Press the start button on the syringe pump and observe the solution flowing from the syringe through the tubing. Once the solution reaches the needle, press the green "on" button on the electrostatic box. Observe the flow from the needle to ensure that there are no clogs or obstructions that are altering the flow. Once everything is confirmed to be operating correctly, allow the solution to drop for an hour.
    * If preparing sterile beads, autoclave the metal forceps, metal strainer, and metal surgical spatula, and sterile filter the TA cross-linking solution through a 150 mL Nalgene filter bottle.

    ** It is important that the needle and tubing are cleaned after every use to prevent the formation of clogs. These can be cleaned by forcing DI water through both the tubing and the needle with a syringe followed by forcing air through both.

14. After the solution has dropped, turn off both the syringe pump and the electrostatic box. Use metal forceps to remove the stir bar from the tall glassware dish. Strain the formed beads from the 1.5% $CaCl_2$ solution using the metal strainer and transfer the beads to the TA cross-linking solution.

15. Place the bottle with the beads and TA cross-linking solution on the shaker plate, set to 150 rpm, overnight.
    * If making sterile beads, autoclave the metal strainer and the metal surgical spatula again after transferring the beads to the TA cross-linking solution, and sterile filter the 50 mM sodium citrate solution through a 150 mL Nalgene filter bottle.

16. Strain the beads from the TA cross-linking solution using the metal strainer. They should have an opaque white-brown color. Use the metal surgical spatula to transfer the beads to the 50 mM sodium citrate solution, and place the bottle with the beads and sodium citrate solution on the shaker plate, set to 150 rpm, for 3 hrs.
    * If making sterile beads, autoclave the metal strainer and metal surgical spatula again after transferring the beads to the sodium citrate solution.

17. Strain the beads from the sodium citrate solution. While they are held within the strainer, rinse the beads with 20 mL of sterile PBS twice. Gently transfer the beads from the strainer to 50 mL centrifuge tube and add an additional 20 mL of sterile PBS.

18. Store the generated beads in the centrifuge tube with the PBS in the refrigerator. It is recommended to use the beads within two weeks of them being made to minimize TA loss while in storage.

TROUBLESHOOTING:

- If the needle becomes clogged, place the needle in a crucible set to 300 °F for one hour. Check that the clog has been removed by forcing water through the needle with a syringe. If making sterile beads, autoclave the needle after it has been in the crucible.

Appendix B

Preparation of Sterile Agarose Using Medium

EQUIPMENT AND SUPPLIES:
Agarose, Type VII-A, Sigma-Aldrich (A0701-25G)
Autoclave
Biological Safety Cabinet
70% Ethanol Spray
Waterbath warmed to 37°C
Waterbath warmed to 65°C

PROCEDURE:

Note: All work is performed using aseptic technique in the Biological Safety Cabinet.

Agarose Solution Preparation (Cell Culture Medium)

1. Weigh the appropriate mass of Agarose powder and autoclave in a glass vial at 121°C for 45 minutes. Do not autoclave at 134°C, as this may significantly degrade the molecular weight of the Agarose, resulting in reduced mechanical properties.

2. Add cell culture medium to Agarose to a concentration of 0.5 to 3.0 g/100 mL. The concentration will be dependent upon the desired stiffness of the gel.

3. Warm Agarose & cell culture medium solution in waterbath, heated to 65°C until Agarose is dissolved (will be transparent and fluid). Do not microwave, as this may destroy proteins in the medium serum.

4. Use solution now, or store in refrigerator.

5. If solution has solidified, melt solution (lid on to keep sterile) by waterbath at 65°C. Do not microwave, as this may destroy proteins in the medium serum.

6. If cells are to be added, place melted solution in 37°C waterbath to equilibrate solution and prevent heat shock to cells (for at least 15 minutes).

Appendix C

Digestion of Human Fat Tissue

Reagents and Medium:

- **Collagenase Medium (DMEM-Incomplete)**
  500ml Dulbecco's Modified Eagle Medium (DMEM) + 5mL AA + 1mL fungizone
- **Fat Growth Medium (DMEM-Fat)**
  500mL DMEM: F12 + 50mL FBS + 5mL AA + 1mL fungizone

- **Red Blood Cell (RBC) Lysis Buffer**
  Stock Solutions:
  1M NH4Cl (FW=53.49) 26.75g to 500mL ddH2O
  100mM KHCO3 (FW=100.1) 5.0g to 500mL ddH2O
  10mM EDTA
  Working Solution (500mL):
  77mL 1M NH4Cl + 50mL 100mM KHCO3 + 5mL 10mM EDTA + 368mLddH2O

Tissue Retrieval Preparation:

1. Autoclave all needed instruments including scissors, forceps, metal strainers

Collection and Isolation of Fat Cells:

1. Warm all media and PBS to 37°C in the water bath.

2. Open the tissue sample in the sterile hood. Place the fat tissue on a sterile disposable Petri dish and rinse with fresh PBS. Rinse 1-2 more times to rinse away excess blood from the tissue.

3. Mince the tissue finely using scissors and forceps, carefully removing excess connective tissue and blood vessels.

4. Place ~5 grams of tissue into a sterile 50mL-centrifuge tube. Add filter sterilized collagenase solution to each tube 4mL/gram tissue.

   Prepare as much collagenase solution as needed for a given day immediately before use. Filter sterilize before use.
   To prepare the collagenase solution, add:

   DMEM-Incomplete + 2mg/mL Type I collagenase + 2mg/mL Type II collagenase (both from Worthington Biochemical) + 2% BSA (Sigma)

5. Incubate the tubes containing the tissue at 37°C for 45 minutes.

6. Shake the centrifuge tubes to break up any remaining large pieces. Filter the digested material using the metal strainer into another sterile 50ml centrifuge tube to remove remaining tissue fragments. Dilute the filtrate with DMEM-Fat to minimize collagenase activity.

7. Spin the tubes for 10 minutes at 1000rpm. At the top will be an oily layer with a fatty layer beneath. The middle is aqueous layer and the sediment is preadipocytes and endothelial cells. Aspirate the fatty layer and liquid layer from the tube.

8. Resuspend the cell pellet in 20mL of RBC Lysis Buffer for 10 minutes. Filter the lysate with 100µm cell strainer into a new tube and spin for 5 minutes at 1000rpm.

9. Aspirate the top layer and aqueous layer in the tube. Resuspend the final pellet in DMEM-Fat and seed in T-25 culture flasks with 5ml of DMEM-Fat medium. If there appears to be a large number of cells, perform a cell count and seed cells in T-75 flask with 10ml fresh medium. Check cells after 24 hours to ensure no contamination.

10. Change medium after 48hours to remove cellular debris and unattached cells. Aspirate medium, rinse with sterile PBS, aspirate PBS, and replace culture medium.

LITERATURE CITED

1. *U.S. Breast Cancer Statistics.* 2014 09-20 [cited 2014 11-24]; Available from: http://www.breastcancer.org.

2. *Understanding Breast Cancer Guide.* 2011 01-28 [cited 2011 4-19]; Available from: http://ww5.komen.com.

3. *What You Need To Know About Breast Cancer.* 2009 10-15 [cited 2011 4-14]; Available from: http://www.cancer.gov.

4. *Lymph System*. 2010 11-15 [cited 2012 6-14]; Available from: http://www.nlm.nih.gov/medlineplus/ency/article/002247.htm.

5. Patrick, C. W. (2004). Breast tissue engineering. *Annual Review of Biomedical Engineering*, *6*, 109-30.

6. *Anatomy of the Breast.* [cited 2011 6-24]; Available from: http://mammary.nih.gov.

7. *Breast Cancer.* 2011 06-15 [cited 2011 6-24]; Available from: http://www.wikipedia.org.

8. *What are the Causes of Breast Cancer*. 2010 11-22 [cited 2011 06-24]; Available from: http://www.medicinenet.com.

9. Ginsburg, O. M., Martin, L. J., & Boyd, N. F. (2008). Mammographic density, lobular involution, and risk of breast cancer. *British Journal of Cancer*, *99*(9), 1369-1374.

10. Martin, L. J., & Boyd, N. F. (2008). Mammographic density. Potential mechanisms of breast cancer risk associated with mammographic density: hypotheses based on epidemiological evidence. *Breast Cancer Research*, *10*(1), 201.

11. Harvey, J. (2004). Quantitative Assessment of Mammographic Breast Density: Relationship with Breast Cancer Risk. *Radiology*, *230*(1), 29-41.

12. Vachon, C. M., Kushi, L. H., Cerhan, J. R., Kuni, C. C., & Sellers, T. A. (2000). Association of Diet and Mammographic Breast Density in the Minnesota Breast Cancer Family Cohort. *Cancer Epidemiology, Biomarkers & Prevention*, *9*, 151-160.

13. Cil, T., Fishell, E., Hanna, W., Sun, P., Rawlinson, E., Narod, S. A., & McCready, D. R. (2009). Mammographic density and the risk of breast cancer recurrence after breast-conserving surgery. *Cancer*, *115*(24), 5780-5787.

14. Jeffreys, M., Warren, R., Highnam, R., & Davey Smith, G. (2008). Breast cancer risk factors and a novel measure of volumetric breast density: cross-sectional study. *British Journal of Cancer*, *98*(1), 210-216.

15. Gram, I. T., Funkhouser, E., & Tabar, L. (1997). Anthropometric indices in relation to mammographic patterns among peri-menopausal women. *International Journal of Cancer*, *73*(3), 323-326.

16. El-Bastawissi, A. Y., White, E., Mandelson, M. T., & Taplin, S. H. (2000). Reproductive and hormonal factors associated with mammographic breast density by age (United States). *Cancer Causes & Control*, *11*(10), 955-963.

17. Livingston, E. (2001). Body Surface Area Prediction in Normal-Weight and Obese Patients. *American Journal of Physiology*, *281*, E586 - E591.

18. Sawyer, M., & Ratain, M. J. (2001). Body surface area as a determinant of pharmacokinetics and drug dosing. *Investigational New Drugs*, *19*(2), 171-177.

19. Verbraecken, J., Van de Heyning, P., De Backer, W., & Van Gaal, L. (2006). Body Surface Area in Normal-Weight, Overweight, and Obese Adults. A Comparison Study. *Metabolism: Clinical and Experimental*, *55*(4), 515-524.

20. *Hormone Replacement Therapy (menopause)*. 2011 06-11 [cited 2011 7-7]; available from: http://www.wikipedia.org.

21. Vachon, C. M., Kuni, C. C., Anderson, K., Anderson, V. E., & Sellers, T. A. (2000). Association of mammographically defined percent breast density with epidemiologic risk factors for breast cancer (United States). *Cancer Causes & Control*, 11(7), 653-662.

22. Kumle, M., Weiderpass, E., Braaten, T., & Persson, I. (2002). Use of Oral Contraceptives and Breast Cancer Risk: The Norwegian-Swedish Women's Lifestyle and Health Cohort Study. *Cancer Epidemiology*, *11*(11), 1375-1381.

23. Rosenberg, L., Zhang, Y., Coogan, P. F., Strom, B. L., & Palmer, J. R. (2009). A case-control study of oral contraceptive use and incident breast cancer. *American Journal of Epidemiology*, *169*(4), 473-479.

24. Hunter, D. J., Colditz, G. A, Hankinson, S. E., Malspeis, S., Spiegelman, D., Chen, W., Stampfer, M. J., & Wilett, W. C. (2010). Oral contraceptive use and breast cancer: a prospective study of young women. *Cancer Epidemiology, Biomarkers & Prevention*, *19*(10), 2496-2502.

25. Spicer, D., & Pike, M. C. (1995). Hormonal Manipulation to Prevent Breast Cancer. *Science & Medicine*, *2*(4), 58-67.

26. Eifel, P., Axelson, J. A, Costa, J., Crowley, J., Curran, W. J., Deshler, A, Fulton, S., Hendricks, C. B., Kemeny, M., Kornblith, A. B., Louis, T. A., Markman, M., Mayer, R., & Roter, D. (2001). National Institutes of Health Consensus Development Conference Statement: adjuvant therapy for breast cancer, November 1-3, 2000. *Journal of the National Cancer Institute*, *93*(13), 979-989.

27. Shalaby, W. S. W. (2010). Chemotherapy in Gynecologic Malignancies. *Manual of Gynecologic Oncology* (pp. 1-36).

28. Fang, L., Barekati, Z., Zhang, B., Liu, Z., & Zhong, X. Y. (2011). Targeted therapy in breast cancer: what's new? *Swiss Medical Weekly*, *141*(June).

29. Eberline, T. J., & Tsangaris, T. N. (1995). Breast cancer surgery. *Atlas of Breast Cancer* (pp. 6.1-6.19).

30. Malata, C. M., McIntosh, S. A, & Purushotham, A. D. (2000). Immediate breast reconstruction after mastectomy for cancer. *The British Journal of Surgery*, *87*(11), 1455-1472.

31. Al-Ghazal, S. K., Sully, L., Fallowfield, L., & Blamey, R. W. (2000). The Psychological Impact of Immediate Rather than Delayed Breast Reconstruction. *European Journal of Surgical Oncology*, *26*(1), 17-19.

32. Burg, K., Halberstadt, C., & Holder, W. (2001). Absorbable Tissue Expander. *US Patent 6,206,930*.

33. Robb, G.L. (2001). Reconstructive Surgery. *Breast Cancer* (pp. 223 – 253).

34. Chevray, P. M., & Robb, G. L. (2008). Breast Reconstruction. *Breast Cancer: 2nd Edition* (pp. 235-269).

35. *Tissue Engineering*. 2011 11-25 [cited 2011 12-1]; available from: http://en.wikipedia.org/wiki/Tissue_engineering.

36. Gomillion, C. T., & Burg, K. J. L. (2006). Stem cells and adipose tissue engineering. *Biomaterials*, *27*(36), 6052-6063.

37. Brey, E., & Patrick, C. W. (2000). Tissue engineering applied to reconstructive surgery. *Engineering in Medicine and Biology Magazine*, *19*(5), 122-125.

38. Patrick, C. W., Zheng, B., Johnston, C., & Reece, G. P. (2002). Long-term implantation of preadipocyte-seeded PLGA scaffolds. *Tissue Engineering*, *8*(2), 283-293.

39. Patrick, C. W. (2001). Tissue Engineering Strategies for Adipose Tissue Repair. *The Anatomical Record*, *263*, 361-366.

40. Kimura, Y., Ozeki, M., Inamoto, T., & Tabata, Y. (2003). Adipose tissue engineering based on human preadipocytes combined with gelatin microspheres containing basic fibroblast growth factor. *Biomaterials*, *24*(14), 2513-2521.

41. Choi, J. H., Gimble, J. M., Lee, K., Marra, K. G., Rubin, J. P., Yoo, J. J., Vunjak-Novakovic, G., & Kaplan, D.L. (2010). Adipose Tissue Engineering for Soft Tissue Regeneration. *Tissue Engineering*, *16*(4) 413-426.

42. Vats, a, Tolley, N. S., Polak, J. M., & Buttery, L. D. K. (2002). Stem cells: sources and applications. *Clinical Otolaryngology and Allied Sciences*, *27*(4), 227-232.

43. Young, H. E., & Black, A. C. (2004). Adult stem cells. *The Anatomical Record. Part A*, *276*(1), 75-102.

44. Barry, F. P., & Murphy, J. M. (2004). Mesenchymal stem cells: clinical applications and biological characterization. *The International Journal of Biochemistry & Cell Biology*, *36*(4), 568-584.

45. Jiang, Y., Jahagirdar, B. N., Reinhardt, R. L., Schwartz, R. E., Keenek, C. D., Ortiz-gonzalezk, X. R., Reyes, M., Lenvik, T., Lund, T., Blackstad, M., Du, J., Aldrich, S., Lisberg, A., Low, W. C., Largaespada, D. A., & Verfaillie, C. M. (2002). Pluripotency of mesenchymal stem cells derived from adult marrow. *Nature*, *418*, 41-49.

46. Gronthos, S., Zannettino, A. C. W., Hay, S. J., Shi, S., Graves, S. E., Kortesidis, A., & Simmons, P. J. (2003). Molecular and cellular characterisation of highly purified stromal stem cells derived from human bone marrow. *Journal of Cell Science*, *116*(9), 1827-1835.

47. Zuk, P., Zhu, M., Ashjian, P., De Ugarte, D. A., Huang, J. I., Mizuno, H., Alfonso, Z. C., Fraser, J. K., Benhaim, P., & Hedrick, M. H. (2002). Human adipose tissue is a source of multipotent stem cells. *Molecular Biology of the Cell*, *13*, 4279-4295.

48. Zuk, P. A., Zhu, M., Mizuno, H., Huang, J., Futrell, J. W., Katz, A. J., Benhaim, P., Lorenz, H. P., & Hedrick, M. H. (2001). Multilineage cells from human adipose tissue: implications for cell-based therapies. *Tissue Engineering*, *7*(2), 211-228.

49. Guilak, F., Lott, K. E., Awad, H. A., Cao, Q., Hicok, K. C., Fermor, B., & Gimble, J. M. (2006). Clonal analysis of the differentiation potential of human adipose-derived adult stem cells. *Journal of Cellular Physiology*, *206*(1), 229-237.

50. Gronthos, S., Franklin, D. M., Leddy, H. A., Robey, P. G., Storms, R. W., & Gimble, J. M. (2001). Surface protein characterization of human adipose tissue-derived stromal cells. *Journal of Cellular Physiology*, *189*(1), 54-63.

51. Vashi, A. V., Keramidaris, E., Abberton, K. M., Morrison, W. A., Wilson, J. L., O'Connor, A. J., Cooper-White, J. J., & Thompson, E.W. (2008). Adipose differentiation of bone marrow-derived mesenchymal stem cells using Pluronic F-127 hydrogel in vitro. *Biomaterials*, *29*(5), 573-579.

52. Bunnell, B. A., Flaat, M., Gagliardi, C., Patel, B., & Ripoll, C. (2008). Adipose-derived stem cells: isolation, expansion and differentiation. *Methods*, *45*(2), 115-120.

53. Gimble, J. M., Katz, A. J., & Bunnell, B. A. (2007). Adipose-derived stem cells for regenerative medicine. *Circulation Research*, *100*(9), 1249-1260.

54. Aust, L., Devlin, B., Foster, S. J., Halvorsen, Y. D. C., Hicok, K., du Laney, T., Sen, A., Willingmyre, G. D., & Gimble, J. M. (2004). Yield of human adipose-derived adult stem cells from liposuction aspirates. *Cytotherapy*, *6*(1), 7-14.

55. Atala, A. (2004). Tissue engineering and regenerative medicine: concepts for clinical application. *Rejuvenation research*, *7*(1), 15-31.

56. Brey, E. M., Uriel, S., Greisler, H. P., Patrick, C. W., & McIntire, L. V. (2005). Therapeutic neovascularization: Contributions from bioengineering. *Tissue Engineering*, *11*(3-4), 567-584.

57. Hannan, N. R. F., & Wolvetang, E. J. (2009). Adipocyte differentiation in human embryonic stem cells transduced with Oct4 shRNA lentivirus. *Stem Cells and Development*, *18*(4), 653-660.

58. Cukierman, E., Pankov, R., & Yamada, K. M. (2002). Cell interactions with three-dimensional matrices. *Current Opinion in Cell Biology*, *14*(5), 633-639.

59. Mauney, J. R., Nguyen, T., Gillen, K., Kirker-Head, C., Gimble, J. M., & Kaplan, D. L. (2007). Engineering adipose-like tissue in vitro and in vivo utilizing human bone marrow and adipose-derived mesenchymal stem cells with silk fibroin 3D scaffolds. *Biomaterials*, *28*(35), 5280-5290.

60. Flynn, L., Prestwich, G. D., Semple, J. L., & Woodhouse, K. A. (2007). Adipose tissue engineering with naturally derived scaffolds and adipose-derived stem cells. *Biomaterials*, *28*(26), 3834-3842.

61. Stacey, D. H., Hanson, S. E., Lahvis, G., Gutowski, K. A., & Masters, K. S. (2009). *In vitro* adipogenic differentiation of preadipocytes varies with differentiation stimulus, culture dimensionality, and scaffold composition. *Tissue Engineering. Part A*, *15*(11), 3389-3399.

62. Inanc, B., Elcin, A., & Elcin, Y. (2006). Osteogenic induction of human periodontal ligament fibroblasts under two-and three-dimensional culture conditions. *Tissue Engineering*, *12*(2), 257-266.

63. Huss, F. R., & Kratz, G. (2001). Mammary epithelial cell and adipocyte co-culture in a 3-D matrix: the first step towards tissue-engineered human breast tissue. *Cells, Tissues, Organs*, *169*(4), 361-367.

64. Patrick, C. W., Chauvin, P. B., Hobley, J., & Reece, G. P. (1999). Preadipocyte seeded PLGA scaffolds for adipose tissue engineering. *Tissue Engineering*, *5*(2), 139-151.

65. Mann, B. K., Gobin, A. S., Tsai, A. T., Schmedlen, R. H., & West, J. L. (2001). Smooth muscle cell growth in photopolymerized hydrogels with cell adhesive and proteolytically degradable domains: synthetic ECM analogs for tissue engineering. *Biomaterials*, *22*(22), 3045-3051.

66. Mann, B., Tsai, A., & Scott-Burden, T. (1999). Modification of surfaces with cell adhesion peptides alters extracellular matrix deposition. *Biomaterials*, *20*, 2281-2286.

67. Gobin, A. S., & West, J. L. (2002). Cell migration through defined, synthetic ECM analogs. *The FASEB Journal*, *16*(7), 751-753.

68. Eiselt, P., Yeh, J., Latvala, R. K., Shea, L. D., & Mooney, D. J. (2000). Porous carriers for biomedical applications based on alginate hydrogels. *Biomaterials*, *21*(19), 1921-1927.

69. Lin, S.D., Wang, K.H., & Kao, A.P. (2008). Engineered adipose tissue of predefined shape and dimensions from human adipose-derived mesenchymal stem cells. *Tissue Engineering. Part A*, *14*(5), 571-581.

70. Shi, H., Han, C., Mao, Z., Ma, L., & Gao, C. (2008). Enhanced angiogenesis in porous collagen-chitosan scaffolds loaded with angiogenin. *Tissue Engineering. Part A*, *14*(11), 1775-1785.

71. Lee, J. E., Kim, K. E., Kwon, I. C., Ahn, H. J., Lee, S. H., Cho, H., Kim, H. J., Seong, S.C., & Lee, M. C. (2004). Effects of the controlled-released TGF-beta 1 from chitosan microspheres on chondrocytes cultured in a collagen/chitosan/glycosaminoglycan scaffold. *Biomaterials*, *25*(18), 4163-4173.

72. Gupta, V., Mun, G.H., Choi, B., Aseh, A., Mildred, L., Patel, A., Zhang, Q., Price, J. E., Chang, D., Robb, G., & Mathur, A. B. (2011). Repair and reconstruction of a resected tumor defect using a composite of tissue flap-nanotherapeutic-silk fibroin and chitosan scaffold. *Annals of Biomedical Engineering*, *39*(9), 2374-2387.

73. Patrick, C. W., Uthamanthil, R., Beahm, E., & Frye, C. (2008). Animal models for adipose tissue engineering. *Tissue Engineering. Part B, Reviews*, *14*(2), 167-178.

74. *The Jackson Laboratory: Mouse strain information.* [cited 2012 7-05]; Available from: http://www.jax.org.

75. Rangarajan, A., & Weinberg, R. a. (2003). Opinion: Comparative biology of mouse versus human cells: modelling human cancer in mice. *Nature reviews. Cancer*, *3*(12), 952-959.

76. Vodicka, P., Smetana, K., Dvoránková, B., Emerick, T., Xu, Y. Z., Ourednik, J., Ourednik, V., & Motlik, J. (2005). The miniature pig as an animal model in biomedical research. *Annals of the New York Academy of Sciences*, *1049*, 161-171.

77. Hemmrich, K., Van de Sijpe, K., Rhodes, N. P., Hunt, J. A, Di Bartolo, C., Pallua, N., Blondeel, P., & von Heimburg, D. (2008). Autologous in vivo adipose tissue engineering in hyaluronan-based gels--a pilot study. *The Journal of Surgical Research*, *144*(1), 82-88.

78. Halberstadt, C., Austin, C., Rowley, J., Culberson, C., Loebsack, A., Wyatt, S., Coleman, S., Blacksten, L., Burg, K., Mooney, D., & Holder Jr, W. (2002). A hydrogel material for plastic and reconstructive applications injected into the subcutaneous space of a sheep. *Tissue engineering*, *8*(2), 309-319.

79. Rowson, A. R., Daniels, K. M., Ellis, S. E., & Hovey, R. C. (2012). Growth and development of the mammary glands of livestock: A veritable barnyard of opportunities. *Seminars in Cell & Developmental Biology*. *In Press*.

80. Horigan, K. C., Trott, J. F., Barndollar, A. S., Scudder, J. M., Blauwiekel, R. M., & Hovey, R. C. (2009). Hormone interactions confer specific proliferative and histomorphogenic responses in the porcine mammary gland. *Domestic Animal Endocrinology*, *37*(2), 124-138.

81. Roberts, R. M., Smith, G. W., Bazer, F. W., Cibelli, J., Seidel, G. E., Bauman, D. E., Reynolds, L. P., & Ireland, J. J. (2009). Farm Animal Research in Crisis. *Science*, *324*, 468-469.

82. Chung, K. T., Wong, T. Y., Wei, C. I., Huang, Y. W., & Lin, Y. (1998). Tannins and human health: a review. *Critical Reviews in Food Science and Nutrition*, *38*(6), 421-464.

83. Isenburg, J. C., Simionescu, D. T., & Vyavahare, N. R. (2005). Tannic acid treatment enhances biostability and reduces calcification of glutaraldehyde fixed aortic wall. *Biomaterials*, *26*(11), 1237-1245.

84. Gülçin, I., Huyut, Z., Elmastaş, M., & Aboul-Enein, H. Y. (2010). Radical scavenging and antioxidant activity of tannic acid. *Arabian Journal of Chemistry*, *3*(1), 43-53.

85. Mueller-Harvey, I. (2001). Analysis of hydrolysable tannins. *Animal Feed Science and Technology*, *91*(1-2), 3-20.

86. Schofield, P., Mbugua, D., & Pell, A. (2001). Analysis of condensed tannins: a review. *Animal Feed Science and Technology*, *91*(1-2), 21–40.

87. Hupkens, P., Boxma, H., & Dokter, J. (1995). Tannic acid as a topical agent in burns: historical considerations and implications for new developments. *Burns*, *21*(1), 57-61.

88. Lindsay, J. C. (1927). Tannic Acid Treatment of Burns. *Canadian Medical Association Journal*, *17*(1), 86.

89. Lucke, H., & Hodge, K. (1963). Fatal liver damage after barium enemas containing tannic acid. *Canadian Medical Association*, *89*(22), 1111-1114.

90. Halkes, S. B., van den Berg, A. J., Hoekstra, M. J., du Pont, J. S., & Kreis, R. W. (2001). Treatment of burns: new perspectives for highly purified tannic acid? *Burns*, *27*(3), 299-300.

91. Jayakrishnan, A., & Jameela, S. R. (1996). Glutaraldehyde as a fixative in bioprostheses and drug delivery matrices. *Biomaterials*, *17*(5), 471-484.

92. Isenburg, J. C., Simionescu, D. T., & Vyavahare, N. R. (2005). Tannic acid treatment enhances biostability and reduces calcification of glutaraldehyde fixed aortic wall. *Biomaterials*, *26*(11), 1237-1245.

93. Heijmen, F., Du Pont, J., Middelkoop, E., Kreis, R., & Hoekstra, M. (1997). Cross-linking of dermal sheep collagen with tannic acid. *Biomaterials*, *18*(10), 749–754.

94. Van Buren, J. P., & Robinson, W. B. (1969). Formation of complexes between protein and tannic acid. *Journal of Agricultural and Food Chemistry*, *17*(4), 772-777.

95. Nam, S., Smith, D. M., & Dou, Q. P. (2001). Tannic acid potently inhibits tumor cell proteasome activity, increases p27 and Bax expression, and induces G1 arrest and apoptosis. *Cancer Epidemiology, Biomarkers & Prevention*, *10*(10), 1083-1088.

96. Chen, X., Beutler, J. A., McCloud, T. G., Loehfelm, A., Yang, L., Dong, H. F., Chertov, O. Y., Salcedo, R., Oppenheim, J. J., & Howard, O. M. Z. (2003). Tannic acid is an inhibitor of CXCL12 (SDF-1α)/CXCR4 with antiangiogenic activity. *Clinical Cancer Research*, *9*(8), 3115–3123.

97. Tikoo, K., Sane, M. S., & Gupta, C. (2011). Tannic acid ameliorates doxorubicin-induced cardiotoxicity and potentiates its anti-cancer activity: potential role of tannins in cancer chemotherapy. *Toxicology and Applied Pharmacology*, *251*(3), 191-200.

98. Cosan, D. T., Bayram, B., Soyocak, A., Basaran, A., Gunes, H. V., Degirmenci, I., & Musmul, A. (2010). Role of phenolic compounds in nitric oxide synthase activity in colon and breast adenocarcinoma. *Cancer Biotherapy & Radiopharmaceuticals*, *25*(5), 577-580.

99. Liu, X., Kim, J. K., Li, Y., Li, J., Liu, F., & Chen, X. (2005). Tannic acid stimulates glucose transport and inhibits adipocyte differentiation in 3T3-L1 cells. *The Journal of Nutrition*, *135*(2), 165.

100. Muthusamy, V. S., Anand, S., Sangeetha, K. N., Sujatha, S., Arun, B., & Lakshmi, B. S. (2008). Tannins present in Cichorium intybus enhance glucose uptake and inhibit adipogenesis in 3T3-L1 adipocytes through PTP1B inhibition. *Chemico-Biological Interactions*, *174*(1), 69-78.

101. Cass, C. A. P., & Burg, K. J. L. (2012). Tannic acid cross-linked collagen scaffolds and their anti-cancer potential in a tissue engineered breast implant. *Journal of Biomaterials Science. Polymer Edition*, *23*, 281-298.

102. Tebb, T. A., Tsai, S., Glattaur, V., White, J. F., Ramshaw, J. A. M., & Werkmeister, J. A. (2006). Development of porous collagen beads for chondrocyte culture. *Cytotechnology*, *52*(2), 99-106.

103. Vernon, R. B., Gooden, M. D., Lara, S. L., & Wight, T. N. (2005). Microgrooved fibrillar collagen membranes as scaffolds for cell cupport and alignment. *Biomaterials*, *26*, 3131-3140.

104. E. A. Ainsworth, K. M. Gillespie, Estimation of total phenolic content and other oxidation substrates in plant tissues using Folin-Ciocalteu reagent, Nature Protocols. 2, (2007) 875–7.